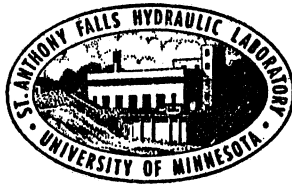


UNIVERSITY OF MINNESOTA
ST. ANTHONY FALLS HYDRAULIC LABORATORY

Project Report No. 121

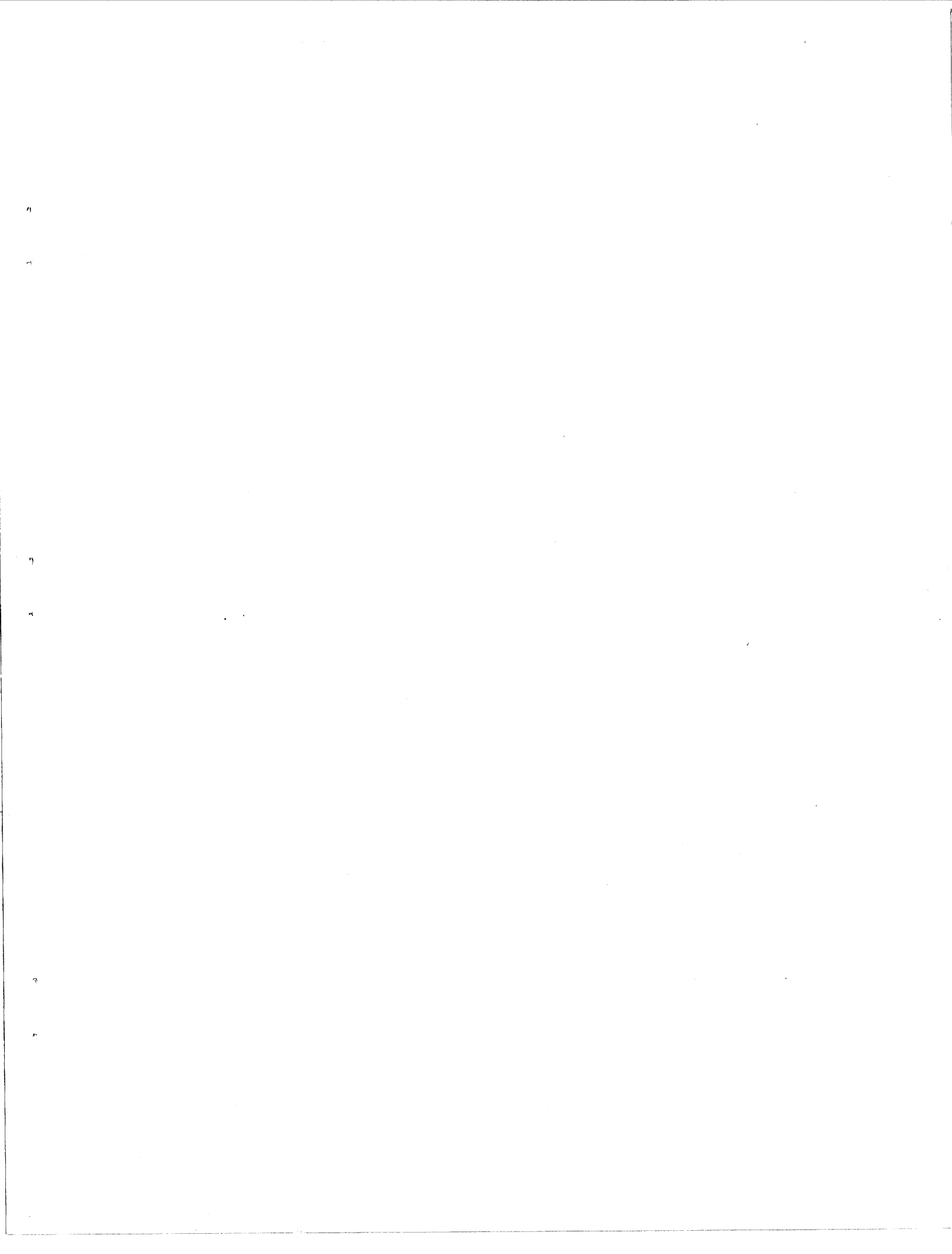
FURTHER STUDIES OF FRICTION FACTORS FOR
CORRUGATED ALUMINUM PIPES FLOWING FULL

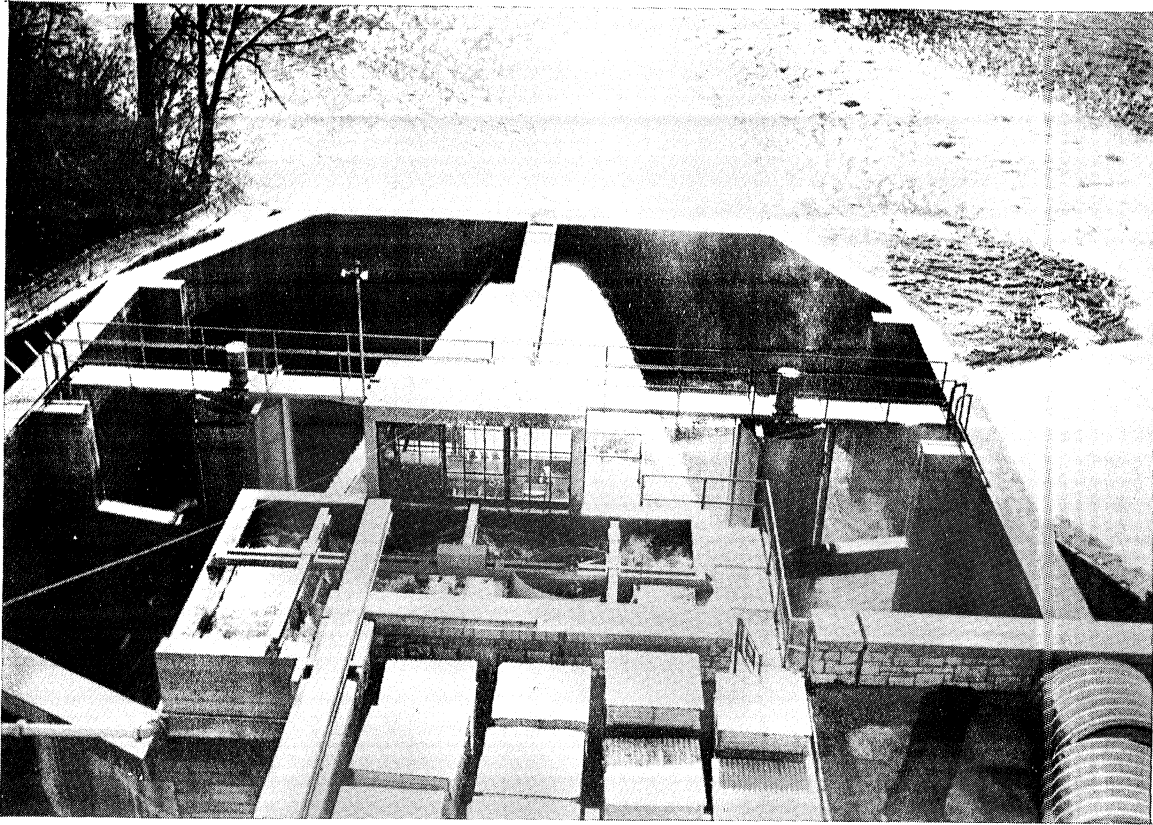
by
Edward Silberman
and
Warren Q. Dahlin



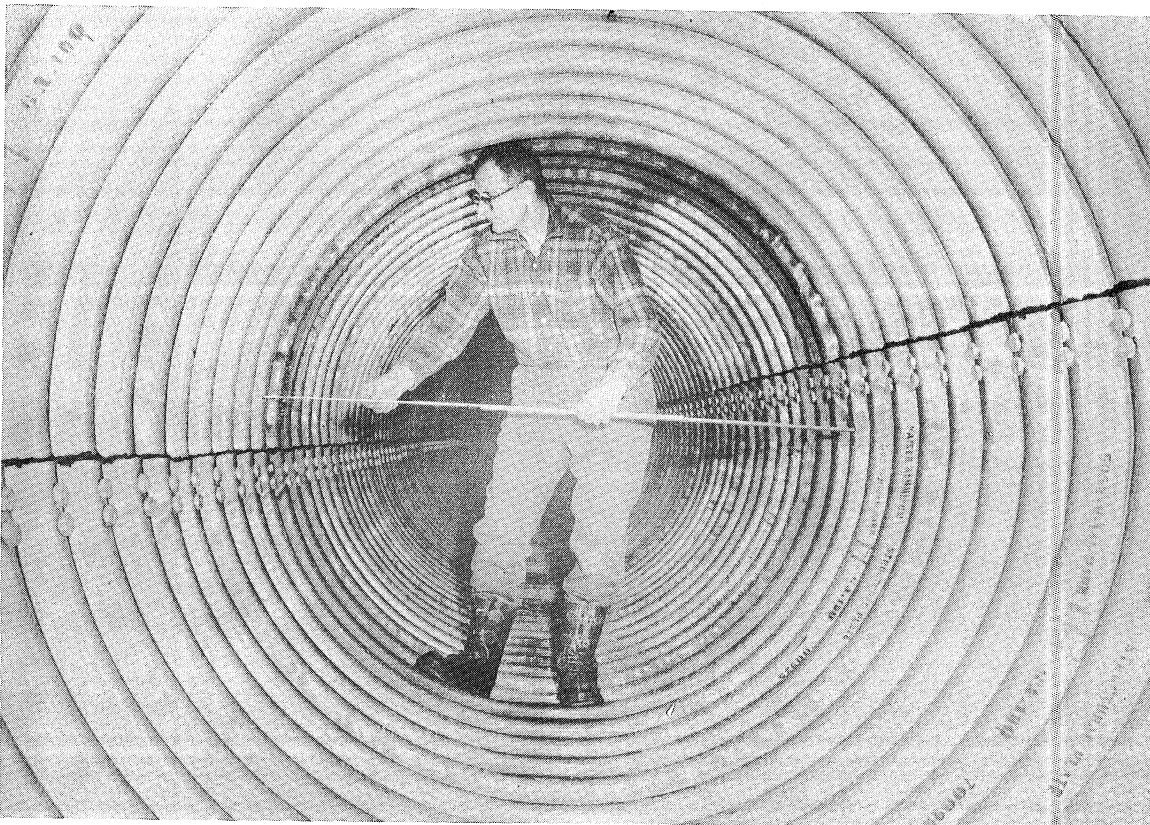
Prepared for
Department of Public Works
CITY OF LA SALLE, ILLINOIS
and
CHAMLIN AND ASSOCIATES, INC.
Peru, Illinois

April 1971
Minneapolis, Minnesota





Measuring a 300 cfs flow in the Volumetric Tanks



Inside View of the 66 in. Annular Bolted Pipe

CONTENTS

	Page
FRONTISPIECE -	
<u>Top</u> - Measuring a 300 cfs flow in the Volumetric Tanks	
<u>Bottom</u> - Inside View of the 66 in. Annular Bolted Pipe	
List of Tables	iv
List of Illustrations	v
List of Symbols	ix
I. PIPE CHARACTERISTICS	1
II. TEST PREPARATIONS AND PROCEDURES	2
III. FRICTION FACTORS	6
IV. DISCUSSION OF FRICTION FACTOR RESULTS	9
V. CONCLUSIONS	13
List of References	15
Tables I thru VIII	17
Figures 1 thru 31	29
Appendix A - POSITION OF HYDRAULIC GRADE LINE AT THE PIPE OUTLET	A-1
Table A-1	A-2
Figures A-1 thru A-8	A-5
Appendix B - VELOCITY PROFILES	B-1
Tables B-1 thru B-3	B-3
Figures B-1 thru B-6	B-7

LIST OF TABLES

		Page
Table I.	SUMMARY OF FRICTION MEASUREMENTS FOR 66-INCH ANNULAR RIVETED PIPE WITH 6-INCH BY 1-INCH CORRUGATIONS	18
Table II.	SUMMARY OF FRICTION MEASUREMENTS FOR 66-INCH ANNULAR BOLTED PIPE WITH 9-INCH BY 2-1/2-INCH CORRUGATIONS	19
Table III.	SUMMARY OF FRICTION MEASUREMENTS FOR 48-INCH ANNULAR RIVETED PIPE WITH 6-INCH BY 1-INCH CORRUGATIONS	20
Table IV.	SUMMARY OF FRICTION MEASUREMENTS FOR 48-INCH HELICAL PIPE WITH 2-INCH BY 1/2-INCH CORRUGATIONS	21
Table V.	SUMMARY OF FRICTION MEASUREMENTS FOR 48-INCH HELICAL PIPE WITH 2-2/3-INCH BY 1/2-INCH CORRUGATIONS	22
Table VI.	SUMMARY OF FRICTION MEASUREMENTS FOR 24-INCH HELICAL PIPE WITH 2-2/3-INCH BY 1/2-INCH CORRUGATIONS	23
Table VII.	SUMMARY OF FRICTION MEASUREMENTS FOR 12-INCH HELICAL PIPE WITH 2-2/3-INCH BY 1/2-INCH CORRUGATIONS	24
Table VIII.	FRICTION FACTORS AT HIGH REYNOLDS NUMBERS AND OTHER DATA	26
Table A-1.	POSITION OF HYDRAULIC GRADE LINE AT THE PIPE OUTLET	A-2
Table B-1.	VELOCITY PROFILE DATA FOR 24 IN. PIPE - 2-2/3 in. by 1/2 in. Corrugations	B-3
Table B-2.	VELOCITY PROFILE DATA FOR 12 IN. PIPE - RUN 1 - 2-2/3 in. by 1/2 in. Corrugations	B-4
Table B-3.	VELOCITY PROFILE DATA FOR 12 IN. PIPE - RUN 2 - 2-2/3 in. by 1/2 in. Corrugations	B-5

LIST OF ILLUSTRATIONS

Page

FRONTISPIECE -

Top (Ser. No. 200-55) Measuring a 300 cfs flow in the Volumetric Tanks
Bottom (Ser. No. 200-62) Inside View of the 66 in. Annular Bolted Pipe

Fig. 1	Pipe Details	30
Fig. 2	(Ser. No. 200-1) Unloading the 48 in. Pipe	31
Fig. 3	(Ser. No. 200-59) Assembly of the 66 in. Bolted Pipe	31
Fig. 4	(Ser. No. 200-14) A Typical Leak in a Riveted Joint of the 48 in. Annular Pipe (Dye colors the leaking water)	32
Fig. 5	(Ser. No. 200-66) Joint Detail inside the 66 in. Bolted Pipe	32
Fig. 6	Test Arrangement in Main Test Channel for 48 in. and 66 in. Pipe	33
Fig. 7	Test Arrangement for 24 in. and 12 in. Pipe	34
Fig. 8	(Ser. No. 200-47) The 66 in. Annular Riveted Pipe Installed in the Main Channel with 24 in. Helical Pipe along the Side	35
Fig. 9	(Ser. No. 200-72) Flow at the Exit of the 66 in. Bolted Pipe (240 cfs)	35
Fig. 10	(Ser. No. 200-78) Flow at the Exit of the 24 in. Helical Pipe (38 cfs); 66 in. Bolted Pipe Installed in Main Channel along Side	36
Fig. 11	(Ser. No. 200-26) Piezometer Tap Arrangement (48 in. Helical Pipe)	36
Fig. 12	(Ser. No. 200-5) The Inlet for the 48 in. Pipes	37
Fig. 13	(Ser. No. 200-37) The Inlet for the 66 in. Pipes	37
Fig. 14	Typical Hydraulic Grade Lines for 66 in. Annular Riveted Pipe with 6 in. by 1 in. Corrugations	38
Fig. 15	Typical Hydraulic Grade Lines for 66 in. Annular Bolted Pipe with 9 in. by 2-1/2 in. Corrugations	39
Fig. 16	Typical Hydraulic Grade Lines for 48 in. Annular Riveted Pipe with 6 in. by 1 in. Corrugations	40
Fig. 17	Typical Hydraulic Grade Lines for 48 in. Helical Lock Seam Pipe with 2 in. by 1/2 in. Corrugations	41

Fig. 18	Typical Hydraulic Grade Lines for 48 in. Helical Lock Seam Pipe with 2-2/3 in. by 1/2 in. Corrugations	42
Fig. 19	Typical Hydraulic Grade Lines for 24 in. Helical Lock Seam Pipe with 2-2/3 in. by 1/2 in. Corrugations	43
Fig. 20	Typical Hydraulic Grade Lines for 12 in. Helical Lock Seam Pipe with 2-2/3 in. by 1/2 in. Corrugations	44
Fig. 21	Variation of Darcy Friction Factor f with Reynolds Number - 66 Inch Corrugated Pipe	45
Fig. 22	Variation of Darcy Friction Factor f with Reynolds Number - 48 Inch Corrugated Pipe	46
Fig. 23	Variation of Darcy Friction Factor f with Reynolds Number - 12 Inch and 24 Inch Corrugated Pipe	47
Fig. 24	Variation of Manning n with Reynolds Number - 66 Inch Corrugated Pipe	48
Fig. 25	Variation of Manning n with Reynolds Number - 48 Inch Corrugated Pipe	49
Fig. 26	Variation of Manning n with Reynolds Number - 12 Inch and 24 Inch Corrugated Pipe	50
Fig. 27	Variation of Darcy Friction Factor f with Wall Reynolds Number - Annular Corrugated Pipe	51
Fig. 28	Darcy Friction Factor f as a Function of Pipe Diameter at High Reynolds Numbers	52
Fig. 29	Manning Roughness Coefficient n as a Function of Pipe Diameter at High Reynolds Numbers	53
Fig. 30	Friction Factor as a Function of Helix Angle at High Reynolds Numbers	54
Fig. 31	Friction Factor as a Function of Relative Roughness for Helical Pipes at High Reynolds Numbers	55
Fig. A-1	Typical Hydraulic Grade Lines without Tailwater for 66 in. Annular Riveted Pipe with 6 in. by 1 in. Corrugations	A-6
Fig. A-2	Typical Hydraulic Grade Lines without Tailwater for 66 in. Annular Bolted Pipe with 9 in. by 2-1/2 in. Corrugations .	A-7
Fig. A-3	Typical Hydraulic Grade Lines without Tailwater for 48 in. Annular Riveted Pipe with 6 in. by 1 in. Corrugations	A-8
Fig. A-4	Typical Hydraulic Grade Lines without Tailwater for 48 in. Helical Lock Seam Pipe with 2 in. by 1/2 in. Corrugations	A-9

Fig. A-5 Typical Hydraulic Grade Lines without Tailwater for 48 in. Helical Lock Seam Pipe with 2-2/3 in. by 1/2 in. Corrugations A-10

Fig. A-6 Typical Hydraulic Grade Lines without Downstream Valve for 24 in. Helical Lock Seam Pipe with 2-2/3 in. by 1/2 in. Corrugations A-11

Fig. A-7 Typical Hydraulic Grade Lines without Downstream Valve for 12 in. Helical Lock Seam Pipe with 2-2/3 in. by 1/2 in. Corrugations A-12

Fig. A-8 Position of Hydraulic Grade Line at the Pipe Outlet A-13

Fig. B-1 Velocity Distribution in 24 In. Helical Lock Seam Pipe with 2-2/3 in. by 1/2 in. Corrugations B-8

Fig. B-2 Velocity Distribution in 12 In. Helical Lock Seam Pipe with 2-2/3 in. by 1/2 in. Corrugations B-9

Fig. B-3 Velocity Vectors, Top Halves of Pipes for 24 in. and 12 in. Helical Lock Seam Pipe with 2-2/3 in. by 1/2 in. Corrugations B-10

Fig. B-4 Flow Direction at 48 in. Pipe Outlets
 a. (Ser. No. 200-18) Annular Pipe, 6 in. by 1 in. Corrugations B-11
 b. (Ser. No. 200-32) Helical Pipe, 2-2/3 in. by 1/2 in. Corrugations B-11

Fig. B-5 Velocity Profiles in Defect-Law Form B-12

Fig. B-6 Velocity Profiles in Law-of-the-Wall Form B-13

1. The first part of the document discusses the importance of maintaining accurate records of all transactions and activities. It emphasizes that this is crucial for ensuring transparency and accountability in the organization's operations.

2. The second part of the document outlines the various methods and tools used to collect and analyze data. It highlights the need for consistent data collection procedures and the use of advanced analytical techniques to derive meaningful insights from the data.

3. The third part of the document focuses on the role of technology in data management and analysis. It discusses how modern software solutions can streamline data collection, storage, and processing, thereby improving efficiency and accuracy.

4. The fourth part of the document addresses the challenges associated with data management, such as data quality, security, and privacy. It provides strategies to mitigate these risks and ensure that the data remains reliable and secure throughout its lifecycle.

5. The fifth part of the document discusses the importance of data governance and the role of a data governance committee. It outlines the key principles of data governance, including data ownership, access control, and data retention policies.

6. The sixth part of the document focuses on the integration of data from various sources and systems. It discusses the importance of data integration in providing a comprehensive view of the organization's operations and enabling data-driven decision-making.

7. The seventh part of the document discusses the role of data in strategic planning and performance management. It highlights how data can be used to identify trends, opportunities, and risks, and to set realistic goals and metrics for the organization.

8. The eighth part of the document focuses on the importance of data literacy and training. It discusses how providing training and resources to employees can help them understand the value of data and use it effectively in their work.

9. The ninth part of the document discusses the role of data in innovation and new product development. It highlights how data can be used to identify customer needs, test new ideas, and optimize product design and development processes.

10. The tenth part of the document discusses the importance of data in risk management and compliance. It highlights how data can be used to identify potential risks, assess their impact, and implement effective risk mitigation strategies.

11. The eleventh part of the document discusses the role of data in sustainability and social responsibility. It highlights how data can be used to track and report on environmental, social, and governance (ESG) metrics, and to identify areas for improvement.

12. The twelfth part of the document discusses the importance of data in customer experience and retention. It highlights how data can be used to understand customer behavior, identify pain points, and develop targeted marketing and service strategies.

13. The thirteenth part of the document discusses the role of data in talent management and workforce development. It highlights how data can be used to identify high-potential employees, track their performance, and provide targeted training and development opportunities.

14. The fourteenth part of the document discusses the importance of data in financial management and reporting. It highlights how data can be used to track financial performance, identify trends, and provide accurate and timely financial reports to stakeholders.

LIST OF SYMBOLS

- A = area, ft^2
 d = corrugation depth, ft
 D = inside diameter of test pipe, ft
 f = Darcy friction factor
 g = acceleration due to gravity, ft/sec^2
 h = head loss in pipe, ft
 L = length of pipe, ft
 n = Manning roughness coefficient
 p = corrugation pitch, in.
 P = perimeter, ft
 Q = discharge, cfs
 R_h = hydraulic radius = A/P , ft
 R = radius, ft
 Re = Reynolds number = $\bar{V}D/\nu$
 Re_w = Wall Reynolds number = $Re \frac{d}{D} \sqrt{\frac{f}{8}}$
 S = slope of hydraulic grade line = h/L
 t = pipe wall thickness, in.
 U = local velocity component parallel to axis of pipe = $V \cos \alpha$, fps
 U_{\max} = maximum local velocity component parallel to axis of pipe, fps
 V = magnitude of local velocity, fps
 \bar{V} = average axial velocity = Q/A , fps
 V_* = shear velocity = $\sqrt{\tau_o/\rho} = \bar{V}\sqrt{f/8}$, fps
 Y = vertical distance from pipe invert to hydraulic grade line at exit, ft
 y = vertical distance from wall of pipe, ft
 α = angle between velocity vector and axis of pipe, deg
 θ = helix angle of corrugation measured from axial direction, deg
 ϵ = kinematic eddy viscosity, ft^2/sec
 ν = kinematic viscosity, ft^2/sec
 ρ = density, $\text{lb sec}^2/\text{ft}^4$
 τ_o = shear stress, lb/ft^2

FURTHER STUDIES OF FRICTION FACTORS FOR CORRUGATED ALUMINUM PIPES FLOWING FULL

I. PIPE CHARACTERISTICS

The St. Anthony Falls Hydraulic Laboratory was engaged by Chamlin and Associates, Inc., of Peru, Illinois, to determine the friction factors for fully developed flow in several sizes of annular and helical corrugated pipes flowing full and to make qualitative observations of the pipe joint characteristics. The pipes, which ranged in diameter from 12 to 66 inches, are being considered for use in a demonstration storm sewer project located in La Salle, Illinois, which is being supported in part by the Office of Water Quality of the U.S. Environmental Protection Agency. The pipe characteristics are given in Fig. 1.

Pipe for the tests was provided by two suppliers, Kaiser Aluminum and Chemical Sales, Inc., and the Reynolds Metals Company. Except for the 66 in. bolted pipe, the pipes were shipped to the laboratory in mostly 40 ft (a few 20 ft) lengths (Fig. 2) to provide a test pipe about 220 ft in length for the 66 in. and 48 in. sizes and about 100 ft in length for the 24 in. and 12 in. sizes. The 66 in. bolted pipe was shipped in 4.5 ft wide semi-circular pieces and assembled into a 220 ft length in the Laboratory's main test channel (Fig. 3). The pipes were inspected upon receipt to insure against leakage and to get accurate measurements for use in reducing test results. The seams of the factory-assembled pipes had been sealed with sealing compound during fabrication according to standard factory methods.

In some of the helical pipes, considerable sealant had been forced inside the pipe and would have affected the friction factor measurements. The 48 in. and 24 in. helical pipes were thoroughly scraped on the inside by Laboratory personnel. Since it was impossible for a man to enter the 12 in. pipe to scrape it, the first shipment of that size could not be used. It was replaced by a second shipment in which greater care had been taken during manufacture to prevent the sealant from getting inside the pipe.

The helical pipe seams did not leak during the experiments, but some leakage occurred from the annular riveted pipes and considerable leakage occurred from the bolted pipe. Leakage from the 48 in. annular riveted pipes,

illustrated in Fig. 4, was easily stopped by application of silicone cement from outside the pipe. There was more leakage from the 66 in. annular riveted pipe, especially where the transverse and longitudinal seams met, but this was also sealed with silicone cement.

The greatest seam leakage problems occurred with the bolted pipe. The assembly materials included strips of 3M joint sealant tape which were applied over every row of bolt holes, both longitudinally and transversely. Notwithstanding this tape, leakage was severe until it was finally reduced to manageable proportions by inserting a black permagum sealer with a putty knife into all joints from the inside of the pipe. The sealed joints can be seen in the lower photograph of the frontispiece and in Fig. 5. Figure 5 also shows, incidentally, the roughness of the interior of the bolted pipe. It should be understood that this pipe, like all the pipes under test, was unsupported on the outside; with compacted earth fill around the pipe, the leakage would have been much less.

The inside pipe diameter is an important parameter in determining the friction factor, and it was measured carefully. Personnel entered all pipes 24 inches in diameter or larger and measured the actual inside diameters with two sliding bars equipped with verniers (frontispiece). The inside diameter of each pipe was measured every 2 ft (every 1-1/2 ft for the bolted pipe) through the test section in both vertical and horizontal directions. Corrugation depths were measured with a depth gage about every 4 ft, four readings being made at each section. For the 12 in. pipe, the outside diameter and corrugation depths were measured and the inside diameter computed. The average measured values of inside diameter, standard deviation, and corrugation depth are reported in Fig. 1 over the length of pipe used for determining hydraulic grade lines. The helix angle was also measured and is given in Fig. 1; it agreed closely with factory specifications.

II. TEST PREPARATIONS AND PROCEDURES

The pipes were installed in the laboratory flow system in two separate experimental set-ups as indicated in Figs. 6 and 7 and shown in the photographs of Figs. 8 through 10. Figure 6 shows the test arrangement for the 66 in. and 48 in. pipes in the 9-ft-wide-by-6-ft-deep-by-225-ft-long main test channel. Water from the Mississippi River enters the facility through a traveling

mechanical screen, drops vertically down a dropshaft about 20 ft to the level of the main channel, and passes through a flow control baffle and under a sluice gate into the main channel. A head gate at the upstream end controls the inflow and a tailgate at the downstream end controls the tailwater level. The flow passes over the tailgate and out to the Laboratory's twin volumetric tanks (frontispiece). These tanks have a flow rate capacity up to 300 cfs and are calibrated to produce measurements which have an accuracy of 0.5 per cent.

Figure 7 shows the test arrangement for the 24 in. and 12 in. helical pipes, which is similar to the set-up used in earlier tests on helical pipe [1]*. Water for this facility is taken from the Mississippi River via a laboratory supply channel and drops about 18 ft through a 24 in. pipe. Water passes through a shut-off valve and three right-angled guide vane bends and enters the test pipe. A plate with a 12 in. hole was centered over the outlet of the 24 in. supply pipe to provide an entrance for the 12 in. pipe. At the downstream end a butterfly control valve of 24 in. or 12 in. size, as appropriate, was installed to control the discharge. The test pipe discharges into a channel from which the flow can be diverted to the laboratory volumetric tanks mentioned earlier or to the laboratory weighing tanks, which have a flow rate capacity up to 15 cfs with an accuracy of measurements of 0.1 per cent.

To measure the hydraulic grade lines, the downstream sections of all pipes were provided with 11 pairs of interconnected flush-mounted wall taps (Figs. 6, 7, and 11) spaced about 10 ft apart for the 66 in. and 48 in. pipes and 5 ft apart for the 24 in. and 12 in. pipes. This provided test section lengths of 100 ft and 50 ft, respectively, with the downstream tap 7.5 ft from the end of the pipe. These dimensions varied slightly depending on the type of pipe. The entry length was thus over 110 ft for the larger pipes and 40 ft for the smaller pipes. Hydraulic grade line measurements indicated that these were adequate to produce fully developed flow.

The flush-mounted wall taps were carefully located at the crests of the corrugations (as seen from inside) with a dial indicator. A 1/8 in. hole was drilled through the pipe wall and a rod was inserted in the hole. A mold was centered around the rod and plastic filler material was cast in the mold, and after it had set the rod was withdrawn. Pipe connectors were threaded into

*Numbers in brackets refer to references listed on page 15.

the holes to provide a means of connecting the piezometer lines to the pipe as shown in Fig. 11. The 11 piezometers were connected to a central manometer board. In the earlier study [1] a second piezometric system consisting of static tubes inserted 2-1/4 inches into the 24 in. pipe was used. The pressure drop recorded in the interior of the pipe by these tubes was nearly the same as the pressure drop measured by the wall taps. It was concluded in the earlier study that since the flow was fully developed, the wall taps would give reliable results; therefore, only the wall taps were used in the current study.

Since the main channel entrance is rectangular in cross-sectional shape, special transitions had to be made for the pipes. For the 48 in. pipes a bulkhead was installed under the sluice gate with an opening 48 inches high. A 20 ft section of 48 in. annular corrugated pipe was cemented into the bulkhead as shown in Fig. 12 and served as the inlet for all 48 in. pipes. For the 66 in. pipes, the end of a 20 ft section of 66 in. annular riveted pipe was compressed to 48 in., forced into the bulkhead, and cemented in place (Fig. 13). This provided a gradual transition from an elliptical inlet to the circular 66 in. pipe.

During the laying of the pipe, care was taken at the joints so that no unnecessary roughness would be introduced. The corrugations and crimps were carefully aligned and the joint taped with a fiber tape to prevent the intrusion of joint-sealing material. The joints were sealed using a heat-shrinkable coupler consisting of a thermoplastic sealant or asphalt-like material on a polyolefin sheet backing, applied with heat. While the coupler was still warm, a metal collar was placed over it to insure against leakage.

Without the metal collars, the heat-shrinkable couplings tended to start leaking during the tests. The 15 to 20 ft of head on the pipe, the cold water flowing through the pipe, vibrations, and the pipe's not being buried in the ground as it would be in a field installation to give it support probably contributed to this leakage problem at the joints. When a metal collar with corrugations to match the pipe corrugations was installed over the heat-shrinkable coupling, practically no leakage occurred. Non-corrugated collars were used on some pipe joints and were not as effective in preventing leakage.

In the main channel installations, the pipes were laid directly on the channel floor at an approximate slope of 0.00133 ft/ft. No attempts were made to adjust the slope of the large pipes, as the variation in pipe diameter was far

greater than the irregularities in the channel floor. The pipe was aligned and horizontal braces to the channel sides were placed every 20 ft; in addition, several cables were placed over the pipe and anchored to the floor. A watertight bulkhead was installed near the downstream ends of the pipes. Before tests were run, the joints, taps, and alignment were checked inside the pipe. The 24 in. and 12 in. pipes were laid on wooden sleepers placed about every 5 ft with horizontal side braces placed about every 10 ft. These smaller pipes were set to a grade of 0.002 ft/ft with the pipe filled with water. Levels were recorded for all pipes, both filled with water and empty, and the measurements showed that the pipes flattened out slightly when filled (on the order of 1/64 in. for the 12 in. pipe and 1-1/4 in. for the 66 in. riveted pipe).

Provisions were also made for installation of a 3/8-inch-diameter pitot cylinder in the 24 in. and 12 in. pipes (Fig. 7) to measure velocity direction and magnitude [2]. Glands similar to those used for pressure taps were cast on the top and bottom of the pipe through which the pitot cylinder was inserted to measure the total head along a vertical diameter. In the same section, on the side of the pipe, a special gland was cast for the insertion of a static tube to measure the static pressure for use with the total head readings from the pitot cylinder.

A test run involved establishing a given discharge through the test pipe, measuring the discharge and water temperature, and reading the wall tap pressures on the manometer board. The discharge was regulated for the smaller pipes by the downstream valve; in the main channel the flow was regulated using the tailgate and a head loss baffle in the channel entrance structure. All discharges from the main channel and those above 15 cfs for the smaller pipes were measured in the volumetric tanks; flows up to 15 cfs were measured in the weighing tanks. The usual procedure was to make two discharge measurements during the reading of the manometer board. As some manometer tubes fluctuated considerably for some runs, each tube was observed for a period of time and a visual average was determined. It took from 30 to 45 minutes to make a run in the smaller pipes and about twice as long in the larger pipes. A number of runs were made for each pipe to establish the friction-factor-versus-Reynolds-number curve. Most runs for the 12 and 24 in. pipes were made with the downstream valve in place. For the larger pipes, the tailwater was raised to the top of the pipe for most tests. To obtain maximum

discharge, however, several runs for each pipe were made with the downstream valve removed or with no tailwater. These latter results were also used to determine the tailwater depth at exit. In addition, velocity profiles were measured for one discharge in the 24 in. pipe and one in the 12 in. pipe.

The remainder of the body of this paper is devoted to a report on the friction factor measurements. The measurements of tailwater depth at exit are discussed in Appendix A and the velocity measurements in Appendix B.

III. FRICTION FACTORS

The Darcy friction factor f , the Manning roughness coefficient n , and the Reynolds number Re were computed from the test data for each run. The Darcy friction factor f was determined from

$$f = \frac{2gDS}{\bar{V}^2} \quad (1)$$

with $S = h/L$ where h is the head loss over the length of pipe L , both in feet, and g is the acceleration of gravity in ft/sec^2 . The Manning roughness coefficient n was determined from

$$\bar{V} = \frac{1.486}{n} R_h^{2/3} S^{1/2} \quad \text{or} \quad n = \frac{1.486 R_h^{2/3} S^{1/2}}{\bar{V}} \quad (2)$$

where R_h is the hydraulic radius of the cross section, area divided by the wetted perimeter, both based on measured inside diameter. The Reynolds number Re was computed from

$$Re = \frac{\bar{V}D}{\nu} \quad (3)$$

In all the equations the mean velocity \bar{V} was computed from $\bar{V} = Q/A$, where Q is the measured discharge and A is the area based on the average measured inside diameter D . Kinematic viscosity ν was obtained from standard tables using the measured water temperature.

Typical hydraulic grade lines observed on the manometer board for the seven pipes tested are plotted in Figs. 14 through 20. For convenience, the hydraulic grade lines for each pipe are shown together on one plot and to the

same vertical scale. Individual plots were made for determining the slope S from the hydraulic grade lines, and for lower discharges the vertical scale was expanded to obtain more accuracy in the results.

Most of the grade lines plotted as straight lines, indicating that the flow was fully developed through the test section, although deviations occurred for some pipes. Particularly noticeable are the variations for the 48 in. helical pipe with 2 in. by 1/2 in. corrugations (Fig. 17) from stations 120 through 170 (taps 1 through 7). Investigation showed an almost perfect correlation between these pressure variations and variations in the measured inside diameter of the pipe. The last 40 ft of the pipe had a fairly uniform inside diameter, the average being 48.47 in. with a standard deviation of 0.2042 in. based on measurements every 2 ft; this is the length for which the data are shown in Fig. 1 and on which the slope measurement was based. Measurements at taps 5 (station 151.6 ft) and 6 (station 161.5 ft) indicated the inside diameters to be 50.46 in. and 49.82 in., respectively. The inside diameter at tap 3 (station 131.4 ft) was found to be 48.3 in. The standard deviation from taps 1 through 11 was 0.7655 in., and this is why the hydraulic grade line was not drawn through all points. When the individual pressure readings were corrected for the change in velocity head caused by the variations in diameter, the points were found to plot considerably closer to the grade lines shown in Fig. 17.

Some variations in hydraulic grade lines are thus attributed to variations in the inside diameter of the pipe; another factor which could have affected the readings is the closeness to one of the wall taps of a helical lock seam on the helical pipe or an overlapping seam on the annular pipe.

Summaries of the friction measurements for the seven pipes tested are presented in Tables I through VII. The variations of Darcy friction factor f with Reynolds number Re are shown in Fig. 21 for the 66 in. pipes, Fig. 22 for the 48 in. pipes, and Fig. 23 for the 24 in. and 12 in. pipes. The variations of the Manning roughness coefficient n with Reynolds number are shown in Fig. 24 for the 66 in. pipes, Fig. 25 for the 48 in. pipes, and Fig. 26 for the 24 in. and 12 in. pipes. The data appear to plot in a reasonably consistent manner.

For the annular pipe, the wall Reynolds number defined by

$$Re_w = \frac{dV_*}{\nu} = Re \frac{d}{D} \sqrt{\frac{f}{8}} \quad (4)$$

where d is the corrugation depth and V_* the friction velocity, was also computed. Values of f versus Re_w are plotted in Fig. 27.

There is some scatter in the plots of friction factor, especially for the larger pipe sizes. Discharge remained quite constant during each run and was measured quite accurately. Since diameter was fixed for each pipe size, whether or not it was measured correctly, the probable cause of the scatter was the difficulty in reading the fluctuating manometer tubes. The fluctuations occurred as rather short-term pulses and longer-term surges, neither of which could be damped out completely. The difficulty in reading increased at lower Reynolds numbers because of the smaller head loss.

For the 66 in. pipes, friction factors are essentially constant above a Reynolds number of about 1.5 million. The average f values from Fig. 21 are 0.137 for the annular bolted pipe with 9 in. by 2-1/2 in. corrugations and 0.0617 for the annular riveted pipe with 6 in. by 1 in. corrugations. The corresponding n values are 0.0360 and 0.0242, respectively. Below a Reynolds number of about 1.5 million, the friction factors for the bolted pipe increase with Reynolds number, while for the riveted pipe they decrease.

For the 48 in. annular pipes, friction factor is approximately constant above a Reynolds number of about 2 million. For the helical pipes, the constant regime may extend through all of the data. The average f values from Fig. 22 are 0.0684 for the annular riveted pipe with 6 in. by 1 in. corrugations, 0.0533 for the helical pipe with 2 in. by 1/2 in. corrugations, and 0.0484 for the helical pipe with 2-2/3 in. by 1/2 in. corrugations. The corresponding n values from Fig. 25 are 0.0242, 0.0214, and 0.0204, respectively. For the annular pipe below a Reynolds number of about 2 million, the friction factors appear to be falling with increasing Reynolds number as was the case with the 66 in. annular riveted pipe.

For the 24 in. helical pipe with 2-2/3 by 1/2 in. corrugations, friction factors are constant above a Reynolds number of about 250,000. In this region the average f is about 0.0422 and n about 0.0169. For the 12 in. helical pipe with 2-2/3 by 1/2 in. corrugations, the constant friction factor regime lies above a Reynolds number of about 600,000 with f about 0.0229 and n about 0.0111. In both cases, friction factor decreases as Reynolds number increases.

The friction factor data for all these tests at large Reynolds numbers have been tabulated in Table VIIIa.

IV. DISCUSSION OF FRICTION FACTOR RESULTS

All the present data, as well as the previous data obtained at the St. Anthony Falls Hydraulic Laboratory for helical pipes [1], show a region of more or less constant friction factor at large Reynolds numbers. This is true for both helical and annular corrugated pipe, as can be seen in Figs. 21 through 27 and in Figs. 10 and 11 of the earlier report. The region of constant friction factor can be termed the region of fully rough flow in accordance with the usual practice.

The measured friction factors from the present tests in the fully rough flow regime are summarized in Table VIIIa along with other information. They are plotted in Fig. 28 as $\log f$ versus \log pipe diameter and in Fig. 29 as n versus \log pipe diameter. The points can be identified by the symbols shown in the table. Comparable data from the earlier work at the St. Anthony Falls Hydraulic Laboratory and from the work of others are tabulated in Table VIIIb and are also plotted in Figs. 28 and 29.

Referring first to Figs. 21 through 27, the helical pipe data obtained by others [3,4] are in general agreement with the present data as regards trends of friction factor versus Reynolds number. The annular pipe data obtained by others [6,7], and even those obtained earlier at the St. Anthony Falls Hydraulic Laboratory [5], show some notable differences in trends from those of the present data. For example, all the previous data for annular pipe show a rising friction factor characteristic with increasing Reynolds number at smaller Reynolds numbers, whereas the present data for riveted annular pipe show a falling characteristic (Figs. 21, 22, 24, and 25). Perhaps the opposite trends can be explained by the relative spacing of the corrugations, the present riveted pipe corrugations being 6 by 1 in. whereas all the previous tests on annular pipe were for 2-2/3 by 1/2 in. corrugations as shown in Table VIII. The present bolted pipe results for shorter relative pitch do show a rising friction factor with increasing Reynolds number (Figs. 21 and 24). Another difference occurs for the Webster and Metcalf data [6]. Apparently these data fail to show a region of constant friction factor (fully rough flow) at large Reynolds numbers, but rather seem to peak and fall

back again; this trend is not confirmed with certainty by any other data. One explanation given for the latter phenomenon has been that at higher Reynolds numbers the waviness or corrugation spacing becomes more important than the depth of the corrugations. Nevertheless, on the present riveted annular pipes, pitch over corrugation depth and pitch over pipe diameter are both larger than for the Webster and Metcalf tests, while for the bolted pipe they are both less and the tests show no such peaking. For further analysis, the annular pipe friction factors given in Table VIIIb and plotted in Figs. 28 and 29 have been taken as the peak values at large Reynolds number.

In Fig. 28, all data for riveted pipe with annular corrugations fall approximately on a straight line as is suggested by Neill [7] independently of relative roughness or relative pitch (if the 7 ft diameter pipe data of Webster and Metcalf are not weighted too heavily). The equation for this line can be written

$$f = 0.122 D^{-0.41} \quad (5)$$

where D is the pipe diameter in feet. The line is plotted on the figure. The corresponding equation for n ,

$$n = 0.0257 D^{-0.042} \quad (6)$$

has been plotted in Fig. 29; it is not quite a straight line there because of the semi-logarithmic plotting. It is apparent that for annular riveted pipe, n decreases very slowly with diameter at large Reynolds numbers.

The annular aluminum pipe data fall in nicely with the annular steel pipe data taken by others even though the relative roughness as shown in Table VIII is greater for the aluminum pipe than for the steel pipe at any given diameter. The explanation for this may lie in the greater pitch of the aluminum pipe as just discussed. It is likely that a combination of relative roughness and waviness determines friction factor as a function of diameter for fully rough flow in annular corrugated pipe.

The plotted points for bolted steel and aluminum pipe seem to substantiate this argument. Both plotted points for bolted pipe represent pipes with greater relative roughness and more abrupt waviness than the riveted pipes, and the friction factors are correspondingly larger. The aluminum

bolted pipe has greater relative roughness, but less abrupt waviness than the steel pipe, and this may explain why the two data points fall close to each other. Much more work is necessary to determine the relative contributions of roughness and waviness to friction factors for annular corrugated pipe. (Some of the increase in friction factor for the bolted pipes over that of the riveted pipes is also due to bolt heads in the flow and to the rougher joints associated with field assembly, as shown in Fig. 5. Computations for the bolt head contributions are given by Bossy in Appendix A of Ref. [8].)

For the helical pipe it appears from Figs. 28 and 29 that friction factor increases with diameter for pipe of a given manufacture (i.e., fixed width of sheet from which the pipe is rolled). However, it was observed in an earlier paper by one of the authors [9] that if helical corrugated pipe could be manufactured with helix angle kept constant while the diameter (width of sheet) was increased, the friction factor would actually decrease as diameter increased, much as in the case of annular pipe. To explore this hypothesis further, it was proposed to draw lines parallel to the annular pipe data line in Fig. 28 representing the various helix angles. To this end the f values in Table VIII have been converted to $fD^{0.41}/0.122$ and plotted versus helix angle in Fig. 30. The straight line in Fig. 30 fits most of the data well and tends to substantiate the hypothesis. It has the equation

$$f = 0.945 \times 10^{-8} \frac{\theta^{3.64}}{D^{0.41}} \quad (7)$$

where θ , the helix angle, is in degrees and D , the pipe diameter, is in feet. Straight lines representing this equation have been drawn in Fig. 28 for 60, 70, and 80 degree helix angles. These are of the form

$$f = C D^{-0.41} \quad (8)$$

where C has the values 0.282, 0.491, and 0.805 for 60, 70, and 80 degree helix angles, respectively. Figure 28 now replaces Fig. 1 of Ref. [9].

The corresponding equation for n is

$$n = 7.13 \times 10^{-6} \frac{\theta^{1.82}}{D^{0.042}} \quad (9)$$

and if this is written in the form

$$n = C_1 D^{-0.042} \quad (10)$$

C_1 has the values 0.0122, 0.0160, and 0.0206 for 60, 70, and 80 degree helix angles, respectively. Corresponding lines have been drawn in Fig. 29. Again, the lines are not quite straight because this is a semi-logarithmic plot.

It seems that if helical corrugated pipe of, say, 70 degree helix angle could be fabricated at larger diameters, there would be every reason to expect n values near 0.015 for 3 and 4 ft diameter pipes. A sheet width of about 40 in. would be required for a 3 ft pipe.

In analyzing the effect of helix angle in Fig. 30, no attention has been given to relative roughness or waviness. In fact, inspection of Table VIII shows that relative roughness generally increases with decreasing helix angle and decreasing friction factor, which is the opposite trend from that found in annular pipe. Waviness varies throughout the data. In order to determine whether there is a consistent effect of relative roughness on friction factor for helical pipes, a plot of

$$\frac{f D^{0.41}}{0.945 \theta^{3.64}} \times 10^8$$

versus d/D was made (Fig. 31). This form of plotting removes the influence of helix angle. The plot shows that there may be a trend for increasing friction factor with increasing relative roughness which has previously been masked by the overriding effect of helix angle. Some of the scatter in Fig. 30 may be due to this effect. No trend attributable to waviness could be detected on a similar graph.

The empirical formulas quoted for f and n as functions of θ should not be extended to smaller helix angles. The data point for the 52-1/2 degree helix angle in Fig. 30 already looks suspicious, although its deviation from the empirical correlation line may be due to relative roughness. The problem is that the mechanism by which spiral flow reduces friction is not known, and until it is, the empirical formulas quoted can be used only within the limits in which they appear to fit the data. It was suggested in Ref. [9] that flow

rotation imparted by the spiral corrugations is responsible for friction decrease through reduction in turbulence. Even if this suggestion is valid, it is still necessary to connect the helix angle with the turbulent mixing parameter in the interior of the pipe, and this cannot be done at present.

V. CONCLUSIONS

The experiments described in this report have been conducted using corrugated aluminum pipes flowing full. The measurements were made following an entry region of 20 or more pipe diameters, and although this distance appears to be sufficient, it is not known whether this is a minimum distance for fully developed flow. Measurements were made under laboratory conditions with pipe carefully aligned and joints carefully made so as to avoid introducing additional roughness. The water used in the tests carried a light load of sand, mostly as suspended load, from the Mississippi River. No significant amount of sand was found in the pipes after the flow was shut down; it is not believed that the sand affected the results.

Under these conditions, the following statements can be made regarding friction factors:

1. Aluminum annular riveted pipes with 6 in. by 1 in. corrugations have the same friction factors for fully rough flow as do steel riveted pipes with 2-2/3 by 1/2 in. corrugations. Empirical formulas including both are

$$f = 0.122 D^{-0.41}$$

and

$$n = 0.0257 D^{-0.042}$$

where D is the inside diameter measured in feet. Field assembled and bolted pipes have materially greater friction factors because of both the larger relative depth of corrugations and the presence of bolt heads and rougher joints within the pipes.

2. Helical pipe has lesser friction factors than similar annular pipe of the same diameter; the smaller the helix angle, the less the friction factor. Empirical formulas including both annular and helical pipes of both aluminum and steel are

$$f = 0.945 \times 10^{-8} \frac{\theta^{3.64}}{D^{0.41}}$$

and

$$n = 0.713 \times 10^{-6} \frac{\theta^{1.82}}{D^{0.042}}$$

where θ is the helix angle (measured from the pipe axis) in degrees and D is the inside diameter measured in feet. These formulas are limited to the range of the data available, $52-1/2 \leq \theta \leq 90$. There appears to be little effect of relative roughness on helical pipe friction factors.

3. The thermoplastic sealant provided for the aluminum pipe tests makes a very effective field seal at the pipe joints. However, in the laboratory tests without earth backfill around the pipes, it was found necessary to reinforce the joint seals with corrugated metal bands to prevent the seals from opening due to pressure and vibration. The bands materially increased the rigidity of the pipe line. (Plain metal bands did not protect the seal as well as corrugated bands.) Using corrugated metal bands it was also possible to seal the joints with bands of rubber gasket material placed cold, but several trials were necessary at each joint before a tight seal could be made.
4. The factory-assembled pipes, especially the helical pipes which contained sealant in the spiral joints, were reasonably tight against leakage even without backfill. The field assembled, bolted pipe leaked badly even though sealer strips were used along the bolt rows.
5. In factory assembled pipe, care should be taken to avoid unnecessary joint roughness. Extruding joint sealant from spiral joints on helical pipe, which can introduce roughness, should be avoided.

LIST OF REFERENCES

- [1] Silberman, E. and Dahlin, W. Q., Friction Factors for Helical Corrugated Aluminum Pipe, Project Report No. 112, St. Anthony Falls Hydraulic Laboratory, University of Minnesota, December 1969.
- [2] Silberman, E., The Pitot Cylinder, Circular No. 2, St. Anthony Falls Hydraulic Laboratory, University of Minnesota, October 1947.
- [3] Rice, C. E., Friction Factors for Helical Corrugated Pipe, ARS 41-119, Agricultural Research Service, U.S. Department of Agriculture, February 1966.
- [4] Chamberlain, A. R., Discussion of [6], Journal of the Hydraulics Division, ASCE, Vol. 86, No. HY3, Proc. Paper 2148, March 1960, pp. 67-74.
- [5] Straub, L. G. and Morris, H. M., Hydraulic Tests on Corrugated Metal Culvert Pipes, Technical Paper No. 5-B, St. Anthony Falls Hydraulic Laboratory, University of Minnesota, 1950.
- [6] Webster, M. J. and Metcalf, L. R., "Friction Factors in Corrugated Metal Pipes," Journal of the Hydraulics Division, ASCE, Vol. 85, No. HY9, September 1959, pp. 35-67.
- [7] Neill, C. R., "Hydraulic Roughness of Corrugated Pipes," Journal of the Hydraulics Division, ASCE, Vol. 88, No. HY3, May 1962, pp. 23-44, and Closure of Discussion, Vol. 89, No. HY4, July 1963, pp. 205-208.
- [8] Grace, J. L., Jr., Resistance Coefficients for Structural Plate Corrugated Pipe, Technical Report No. 2-715, U.S. Army Engineer Waterways Experiment Station, February 1966.
- [9] Silberman, E., "Effect of Helix Angle on Flow in Corrugated Pipes," Journal of the Hydraulics Division, ASCE, Vol. 96, No. HY11, November 1970, pp. 2253-2263.

The first part of the document discusses the importance of maintaining accurate records of all transactions and activities. It emphasizes the need for transparency and accountability in financial reporting.

Secondly, it highlights the role of internal controls in preventing fraud and ensuring the integrity of the financial statements. Regular audits and reviews are essential for identifying and addressing any weaknesses in the system.

Furthermore, the document stresses the importance of staying up-to-date with the latest accounting standards and regulations. Continuous professional development is necessary to ensure compliance and accuracy.

In conclusion, the document provides a comprehensive overview of the key principles and practices that govern financial reporting. It serves as a valuable resource for anyone involved in the accounting profession.

The following sections will delve deeper into the specific requirements and procedures for each aspect of financial reporting, providing detailed guidance and examples.

By adhering to these principles and practices, organizations can ensure that their financial statements are reliable and trustworthy, thereby maintaining the confidence of stakeholders and the public.

The document also outlines the consequences of non-compliance with financial reporting standards, including potential legal and financial penalties. It encourages organizations to take a proactive approach to maintaining high standards of financial reporting.

Overall, the document provides a clear and concise framework for financial reporting, ensuring that all relevant parties are aware of their responsibilities and the importance of accurate and transparent financial information.

The document is intended to be a practical guide for accountants and financial managers, providing them with the necessary knowledge and skills to perform their duties effectively and ethically.

It is hoped that this document will be a valuable resource for all those who are committed to the highest standards of financial reporting and transparency.

The document is subject to periodic updates and revisions to reflect changes in accounting standards and regulations. It is recommended that users check for updates regularly to ensure they are using the most current information.

The document is available in both printed and digital formats. It is intended to be a comprehensive and accessible resource for all stakeholders involved in financial reporting.

The document is a key component of the organization's financial reporting framework and is essential for ensuring the accuracy and reliability of financial information.

The document is a valuable tool for promoting transparency and accountability in financial reporting, and for ensuring that all stakeholders have access to accurate and reliable financial information.

T A B L E S
(I thru VIII)

TABLE I. SUMMARY OF FRICTION MEASUREMENTS FOR 66-INCH ANNULAR RIVETED PIPE WITH 6-INCH BY 1-INCH CORRUGATIONS

Average measured diameter = 5.4517 ft

<u>Q</u> cfs	<u>\bar{V}</u> fps	<u>S</u> per cent	<u>Water Temp.</u> Deg. F	<u>v</u> ft ² /sec $\times 10^5$	<u>Re</u> $\times 10^{-6}$	<u>Darcy</u> f	<u>Manning</u> n
302.81*	12.972	2.9537	33.0	1.895	3.7320	0.0616	0.0242
299.81	12.844	2.9537	33.0	1.895	3.6950	0.0628	0.0244
285.84	12.245	2.7152	34.0	1.859	3.5911	0.0635	0.0246
282.78*	12.114	2.4546	33.0	1.895	3.4852	0.0587	0.0236
279.82	11.988	2.5883	33.0	1.895	3.4487	0.0632	0.0245
277.94*	11.907	2.5248	33.0	1.895	3.4255	0.0625	0.0244
253.33	10.853	2.1146	33.0	1.895	3.1222	0.0630	0.0245
253.31*	10.852	1.9032	33.0	1.895	3.1220	0.0567	0.0232
249.92*	10.707	2.0191	33.0	1.895	3.0802	0.0618	0.0242
246.90	10.577	1.9709	33.0	1.895	3.0430	0.0618	0.0242
246.45*	10.558	1.9454	33.0	1.895	3.0374	0.0612	0.0241
246.04*	10.540	2.0115	33.0	1.895	3.0323	0.0635	0.0246
245.84*	10.532	1.7678	33.0	1.895	3.0299	0.0559	0.0231
223.08	9.557	1.5690	34.0	1.859	2.8026	0.0603	0.0239
213.16	9.132	1.4396	34.0	1.859	2.6780	0.0606	0.0240
213.06	9.128	1.3745	33.0	1.895	2.6259	0.0579	0.0235
212.75*	9.114	1.3728	33.0	1.895	2.6221	0.0580	0.0235
211.80	9.074	1.3787	33.0	1.895	2.6104	0.0588	0.0236
201.32	8.625	1.2375	33.0	1.895	2.4812	0.0584	0.0236
179.64	7.696	1.0675	34.0	1.859	2.2569	0.0632	0.0245
165.99	7.111	0.8899	34.0	1.859	2.0854	0.0617	0.0242
154.66	6.626	0.7884	34.0	1.859	1.9430	0.0630	0.0245
138.64	5.939	0.6555	33.0	1.895	1.7087	0.0652	0.0249
124.06	5.315	0.5050	33.0	1.895	1.5290	0.0627	0.0244
109.31	4.683	0.4238	33.0	1.895	1.3472	0.0678	0.0254
93.52	4.006	0.3324	33.0	1.895	1.1526	0.0726	0.0263
77.40	3.316	0.2415	33.0	1.895	0.9539	0.0770	0.0271
58.23	2.495	0.1269	33.0	1.895	0.7177	0.0715	0.0261
39.70	1.701	0.0846	33.0	1.895	0.4893	0.1025	0.0312
22.96	0.984	0.0212	33.0	1.895	0.2830	0.0769	0.0270

*No tailwater

TABLE II. SUMMARY OF FRICTION MEASUREMENTS FOR 66-INCH ANNULAR
BOLTED PIPE WITH 9-INCH BY 2-1/2-INCH CORRUGATIONS

Average measured diameter = 5.38083 ft

<u>Q</u> cfs	<u>\bar{V}</u> fps	<u>S</u> per cent	<u>Water</u> <u>Temp.</u> <u>Deg. F</u>	<u>v</u> <u>ft²/sec</u> <u>$\times 10^5$</u>	<u>Re</u> <u>$\times 10^{-6}$</u>	<u>Darcy</u> <u>f</u>	<u>Manning</u> <u>n</u>
248.64	10.934	4.8451	34.0	1.859	3.1648	0.1403	0.0364
246.09*	10.822	4.5901	34.0	1.859	3.1324	0.1357	0.0358
237.68	10.452	4.3749	34.0	1.859	3.0254	0.1387	0.0362
230.14	10.121	4.0084	34.0	1.859	2.9293	0.1355	0.0358
226.49	9.960	4.0243	34.0	1.859	2.8829	0.1405	0.0365
219.66*	9.660	3.7852	34.0	1.859	2.7960	0.1405	0.0365
216.95*	9.540	3.5860	34.0	1.859	2.7614	0.1364	0.0359
215.99	9.498	3.2114	34.0	1.859	2.7492	0.1232	0.0342
210.31	9.248	3.4027	34.0	1.859	2.6769	0.1377	0.0361
208.49*	9.168	3.4067	34.0	1.859	2.6538	0.1403	0.0364
198.94*	8.748	2.9485	34.0	1.859	2.5323	0.1334	0.0355
187.50	8.245	2.7413	34.0	1.859	2.3866	0.1396	0.0364
180.50*	7.938	2.4624	34.0	1.859	2.2975	0.1353	0.0358
175.79	7.730	2.3349	34.0	1.859	2.2376	0.1353	0.0358
170.58	7.501	2.2154	34.0	1.859	2.1713	0.1363	0.0359
150.96	6.639	1.7332	34.0	1.859	1.9215	0.1362	0.0359
141.91	6.241	1.5436	34.0	1.859	1.8063	0.1372	0.0360
131.88	5.800	1.2846	34.0	1.859	1.6787	0.1322	0.0354
119.61	5.260	1.0543	34.0	1.859	1.5224	0.1319	0.0354
106.72	4.693	0.8296	34.0	1.859	1.3584	0.1304	0.0351
89.84	3.951	0.5778	34.0	1.859	1.1436	0.1282	0.0348
75.18	3.306	0.3985	34.0	1.859	0.9569	0.1262	0.0346
58.55	2.575	0.2207	34.0	1.859	0.7453	0.1153	0.0330
39.72	1.747	0.0797	34.0	1.859	0.5056	0.0904	0.0292
23.27	1.023	0.0281	34.0	1.859	0.2962	0.0930	0.0297

*No tailwater

TABLE III. SUMMARY OF FRICTION MEASUREMENTS FOR 48-INCH ANNULAR RIVETED PIPE WITH 6-INCH BY 1-INCH CORRUGATIONS

Average measured diameter = 3.9683 ft

Q cfs	\bar{V} fps	S per cent	Water Temp. Deg. F	v ft ² /sec $\times 10^5$	Re $\times 10^{-6}$	Darcy f	Manning n
181.73*	14.694	5.6809	56.0	1.289	4.5235	0.0672	0.0240
175.22	14.167	5.2446	58.0	1.253	4.4868	0.0667	0.0239
175.05	14.153	5.3302	58.0	1.253	4.4825	0.0680	0.0241
164.62	13.310	4.7484	58.0	1.253	4.2154	0.0684	0.0242
164.15	13.272	4.6714	58.0	1.253	4.2033	0.0677	0.0241
157.43	12.729	4.3634	59.0	1.235	4.0900	0.0688	0.0243
147.15*	11.898	3.7987	56.0	1.289	3.6628	0.0685	0.0242
147.14*	11.897	3.9958	56.0	1.289	3.6625	0.0721	0.0248
136.28	11.019	3.2426	62.0	1.183	3.6962	0.0682	0.0242
125.62	10.157	2.8148	60.0	1.217	3.3119	0.0697	0.0244
124.70	10.082	2.7122	60.0	1.217	3.2876	0.0681	0.0241
105.49	8.529	1.9422	60.0	1.217	2.7812	0.0682	0.0242
91.37*	7.388	1.4160	56.0	1.289	2.2743	0.0662	0.0238
91.34	7.385	1.4930	60.0	1.217	2.4081	0.0699	0.0245
86.32	6.979	1.2492	64.0	1.151	2.4062	0.0655	0.0237
75.37	6.094	1.0241	59.0	1.235	1.9581	0.0704	0.0246
59.04	4.774	0.6306	59.0	1.235	1.5339	0.0707	0.0246
58.29	4.713	0.6194	63.0	1.167	1.6026	0.0712	0.0247
55.47	4.485	0.5758	64.0	1.151	1.5463	0.0731	0.0250
39.10	3.161	0.3011	56.0	1.289	0.9733	0.0769	0.0257
21.71	1.755	0.0864	56.0	1.289	0.5404	0.0716	0.0248

*No tailwater

TABLE IV. SUMMARY OF FRICTION MEASUREMENTS FOR 48-INCH HELICAL PIPE WITH 2-INCH BY 1/2-INCH CORRUGATIONS

Average measured diameter = 4.0392 ft

<u>Q</u> cfs	<u>\bar{V}</u> fps	<u>S</u> per cent	<u>Water</u> <u>Temp.</u> <u>Deg. F</u>	<u>v</u> <u>ft²/sec</u> <u>$\times 10^5$</u>	<u>Re</u> <u>$\times 10^{-6}$</u>	<u>Darcy</u> <u>f</u>	<u>Manning</u> <u>n</u>
189.74*	14.807	4.3271	54.0	1.328	4.5038	0.0513	0.0210
185.17*	14.451	4.2106	54.0	1.328	4.3953	0.0524	0.0212
179.94	14.043	4.0858	56.0	1.289	4.4004	0.0538	0.0215
178.12*	13.901	4.0025	54.0	1.328	4.2279	0.0538	0.0215
177.01	13.814	3.9027	56.0	1.289	4.3287	0.0532	0.0214
171.23	13.363	3.6947	55.0	1.307	4.1297	0.0538	0.0215
171.01*	13.346	3.5366	54.0	1.328	4.0592	0.0516	0.0211
168.74	13.169	3.6530	56.0	1.289	4.1265	0.0548	0.0217
155.92	12.168	3.1205	56.0	1.289	3.8130	0.0548	0.0217
148.09	11.557	2.8916	54.0	1.328	3.5151	0.0563	0.0220
135.01	10.536	2.4548	54.0	1.328	3.2047	0.0575	0.0222
130.94	10.219	2.0528	54.0	1.328	3.1080	0.0511	0.0210
122.54	9.563	1.8391	54.0	1.328	2.9087	0.0523	0.0212
116.21	9.069	1.7100	56.0	1.289	2.8419	0.0540	0.0216
104.02	8.118	1.3381	56.0	1.289	2.5438	0.0528	0.0213
91.83	7.166	1.0302	56.0	1.289	2.2457	0.0521	0.0212
89.28	6.967	0.9903	56.0	1.289	2.1833	0.0530	0.0214
80.91	6.314	0.8321	56.0	1.289	1.9786	0.0542	0.0216
70.97	5.539	0.5875	56.0	1.289	1.7356	0.0498	0.0207
54.89	4.284	0.3349	57.0	1.271	1.3613	0.0474	0.0202
37.94	2.961	0.1885	56.0	1.289	0.9278	0.0559	0.0219
21.12	1.648	0.0468	55.0	1.307	0.5094	0.0448	0.0196

*No tailwater

TABLE V. SUMMARY OF FRICTION MEASUREMENTS FOR 48-INCH HELICAL PIPE WITH 2-2/3-INCH BY 1/2-INCH CORRUGATIONS

Average measured diameter = 3.9760 ft

<u>Q</u> cfs	<u>\bar{V}</u> fps	<u>S</u> per cent	<u>Water Temp.</u> Deg. F	<u>v</u> ft^2/sec $\times 10^5$	<u>Re</u> $\times 10^{-6}$	<u>Darcy</u> f	<u>Manning</u> n
193.90*	15.617	4.5358	41.0	1.637	3.7931	0.0476	0.0202
189.40*	15.254	4.3027	44.0	1.555	3.9004	0.0473	0.0201
184.89*	14.891	4.1779	44.0	1.555	3.8075	0.0482	0.0203
181.23	14.596	3.9365	42.0	1.610	3.6047	0.0473	0.0201
178.02*	14.338	3.8700	44.0	1.555	3.6661	0.0482	0.0203
174.57*	14.060	3.6952	42.0	1.610	3.4722	0.0478	0.0202
170.88	13.763	3.5953	42.0	1.610	3.3988	0.0486	0.0204
169.24*	13.631	3.5037	44.0	1.555	3.4852	0.0482	0.0203
163.89*	13.200	3.2957	42.0	1.610	3.2598	0.0484	0.0204
158.58	12.772	3.1002	43.0	1.582	3.2100	0.0486	0.0204
149.42	12.034	2.8854	43.0	1.582	3.0246	0.0510	0.0209
148.59*	11.968	2.8296	44.0	1.555	3.0600	0.0506	0.0208
140.66	11.329	2.4161	42.0	1.610	2.7978	0.0482	0.0203
132.60	10.630	2.1389	42.0	1.610	2.6374	0.0480	0.0203
126.77	10.210	2.0282	43.0	1.582	2.5661	0.0498	0.0206
124.34	10.014	1.8850	42.0	1.610	2.4731	0.0481	0.0203
113.73	9.160	1.5563	42.0	1.610	2.2621	0.0475	0.0202
101.52	8.176	1.2983	42.0	1.610	2.0192	0.0497	0.0206
88.68	7.142	0.9695	42.0	1.610	1.7638	0.0486	0.0204
73.39	5.911	0.6774	42.0	1.610	1.4597	0.0496	0.0206
55.20	4.446	0.3970	42.0	1.610	1.0979	0.0514	0.0210
35.46	2.856	0.1540	42.0	1.610	0.7053	0.0483	0.0203
21.60	1.740	0.0600	40.0	1.664	0.4157	0.0507	0.0208

*No tailwater

TABLE VI. SUMMARY OF FRICTION MEASUREMENTS FOR 24-INCH HELICAL PIPE WITH 2-2/3-INCH BY 1/2-INCH CORRUGATIONS

Average measured diameter = 1.9950 ft

<u>Q</u> cfs	<u>\bar{V}</u> fps	<u>S</u> per cent	<u>Water Temp.</u> Deg. F	<u>v</u> ft ² /sec <u>$\times 10^5$</u>	<u>Re</u> <u>$\times 10^{-6}$</u>	<u>Darcy</u> <u>f</u>	<u>Manning</u> <u>n</u>
38.417*	12.290	4.9598	33.0	1.895	1.2938	0.0422	0.0169
37.847	12.108	4.7344	34.0	1.859	1.2993	0.0415	0.0168
36.425*	11.653	4.4422	33.0	1.895	1.2268	0.0420	0.0169
36.068	11.538	4.3837	33.0	1.895	1.2147	0.0423	0.0170
33.661	10.768	3.8576	34.0	1.859	1.1556	0.0427	0.0171
31.311*	10.017	3.2815	33.0	1.895	1.0545	0.0420	0.0169
30.590	9.786	3.0977	34.0	1.859	1.0502	0.0415	0.0168
28.242	9.035	2.6969	34.0	1.859	0.9696	0.0424	0.0170
26.198	8.381	2.1877	33.0	1.895	0.8823	0.0400	0.0165
26.102*	8.350	2.2879	33.0	1.895	0.8791	0.0421	0.0169
24.896	7.964	2.0707	34.0	1.859	0.8547	0.0419	0.0169
21.101	6.750	1.5196	34.0	1.859	0.7244	0.0428	0.0171
19.982*	6.392	1.3443	33.0	1.895	0.6730	0.0422	0.0170
17.558	5.617	1.0236	34.0	1.859	0.6028	0.0416	0.0168
15.304	4.896	0.7932	34.0	1.859	0.5254	0.0425	0.0170
13.688	4.379	0.6397	34.0	1.859	0.4699	0.0428	0.0171
12.226	3.911	0.5010	34.0	1.859	0.4197	0.0420	0.0169
10.594	3.389	0.3707	34.0	1.859	0.3637	0.0414	0.0168
9.168	2.933	0.2856	34.0	1.859	0.3148	0.0426	0.0170
7.606	2.433	0.1970	34.0	1.859	0.2611	0.0427	0.0170
6.348	2.031	0.1252	34.0	1.859	0.2179	0.0390	0.0163
4.820	1.542	0.0836	34.0	1.859	0.1655	0.0451	0.0175
4.546	1.454	0.0836	34.0	1.859	0.1561	0.0507	0.0186
2.649	0.847	0.0274	34.0	1.859	0.0909	0.0491	0.0183

*Downstream valve removed

TABLE VII. SUMMARY OF FRICTION MEASUREMENTS FOR 12-INCH HELICAL PIPE WITH 2-2/3-INCH BY 1/2-INCH CORRUGATIONS

Average measured diameter = 0.9781 ft

Average measured diameter = 0.9781 ft							
Q	\bar{V}	per cent	Water Temp. Deg. F	v	Re	Darcy f	Manning n
cfs	fps	per cent	Temp.	ft/sec	$\times 10^{-6}$	Darcy	Manning
Q	\bar{V}	per cent	Temp.	$\times 10^5$	$\times 10^{-6}$	Darcy	Manning
11.662*	15.521	8.6161	34.0	1.859	0.8166	0.0225	0.0110
11.310	15.052	8.1385	34.0	1.859	0.7920	0.0226	0.0110
11.194	14.898	7.9242	35.0	1.823	0.7992	0.0225	0.0110
10.887	14.439	7.6276	35.0	1.823	0.7774	0.0229	0.0111
10.704	14.246	7.4135	34.0	1.859	0.7495	0.0230	0.0111
10.454*	13.913	6.9357	34.0	1.859	0.7320	0.0226	0.0110
10.449	13.906	6.9851	34.0	1.859	0.7317	0.0227	0.0110
10.113	13.459	6.1449	34.0	1.859	0.7081	0.0214	0.0107
9.226	12.279	5.4202	34.0	1.859	0.6460	0.0226	0.0110
9.193*	12.235	5.4860	34.0	1.859	0.6437	0.0231	0.0111
8.754	11.651	4.9754	34.0	1.859	0.6130	0.0231	0.0111
7.930	11.554	4.1021	35.0	1.823	0.5662	0.0232	0.0112
7.716	10.269	3.9209	35.0	1.823	0.5510	0.0234	0.0112
7.246*	9.644	3.4513	34.0	1.859	0.5074	0.0234	0.0112
6.856	9.125	3.1054	34.0	1.859	0.4801	0.0235	0.0112
6.566	8.739	2.7677	35.0	1.823	0.4689	0.0228	0.0111
5.396	7.181	1.9226	35.0	1.823	0.3853	0.0235	0.0112
4.937*	6.571	1.6507	34.0	1.859	0.3457	0.0241	0.0114
3.801	5.059	0.9786	35.0	1.823	0.2714	0.0241	0.0114
3.128	4.163	0.6836	35.0	1.823	0.2234	0.0248	0.0115
2.606	3.468	0.4909	35.0	1.823	0.1861	0.0257	0.0117
2.100	2.795	0.3296	36.0	1.791	0.1526	0.0265	0.0119
1.784	2.374	0.2194	35.0	1.823	0.1274	0.0245	0.0115
1.680	2.236	0.2072	36.0	1.791	0.1211	0.0261	0.0118
1.452	1.932	0.1645	36.0	1.791	0.1055	0.0277	0.0122
1.254	1.669	0.1071	35.0	1.823	0.0895	0.0243	0.0114
1.193	1.588	0.1020	36.0	1.791	0.0867	0.0255	0.0117
0.966	1.286	0.0656	35.0	1.823	0.0690	0.0250	0.0116
0.948	1.262	0.0656	36.0	1.791	0.0689	0.0260	0.0118
0.660	0.878	0.0329	35.0	1.823	0.0471	0.0269	0.0120
0.626	0.833	0.0371	36.0	1.791	0.0455	0.0336	0.0134
*Downstream valve removed			36.0	1.791	0.0455	0.0336	0.0134

*Downstream valve removed

TABLE VII. [Continued] SUMMARY OF FRICTION MEASUREMENTS FOR 12-INCH
HELICAL PIPE WITH 2-2/3-INCH BY 1/2-INCH CORRUGATIONS

Average measured diameter = 0.9781 ft

<u>Q</u> cfs	<u>\bar{V}</u> fps	<u>S</u> per cent	<u>Water</u> <u>Temp.</u> <u>Deg. F</u>	<u>v</u> <u>ft²/sec</u> <u>x 10⁵</u>	<u>Re</u> <u>x 10⁻⁶</u>	<u>Darcy</u> <u>f</u>	<u>Manning</u> <u>n</u>
11.718*	15.595	8.9620	53.0	1.348	1.1316	0.0232	0.0112
11.422*	15.201	8.4678	53.0	1.348	1.1030	0.0231	0.0111
11.166*	14.861	8.0724	53.0	1.348	1.0783	0.0230	0.0111
10.512*	13.990	7.2817	53.0	1.348	1.0151	0.0234	0.0112
9.982*	13.285	6.4909	53.0	1.348	0.9639	0.0232	0.0111

*Downstream valve removed

TABLE VIII. FRICTION FACTORS AT HIGH REYNOLDS NUMBERS AND OTHER DATA

Ref.	PIPE DATA							FRICTION FACTORS				
	Dia. D ft	Corrugation p x d In.	Helix Angle θ Deg	p/d	d/D	Nom. sheet width in.	Material	Graph symbol	f	n	$\frac{fD^{0.41}}{0.122}$	$\frac{fD^{0.41}}{0.945 \theta^{3.64}} \times 10^8$
<u>a. Present Tests</u>												
0.978	$2\frac{2}{3} \times 0.496$	$52\frac{1}{2}$	5.37	0.0424	24	Aluminum	⊠	0.023	0.0111	0.1885	1.340	
1.995	$2\frac{2}{3} \times 0.519$	$72\frac{1}{4}$	5.15	0.0216	24	"	⊠	0.042	0.0169	0.457	1.022	
3.976	$2\frac{2}{3} \times 0.517$	81	5.15	0.0108	24	"	⊠	0.048	0.0204	0.694	1.023	
4.039	2 x 0.490	$82\frac{1}{2}$	4.08	0.0101	20	"	⊙	0.053	0.0214	0.770	1.060	
3.97	6 x 0.941	90	6.36	0.0198	--	"	⊕	0.068	0.0242	0.981	--	
5.45	6 x 0.958	90	6.26	0.0146	--	"	⊕	0.062	0.0242	1.018	--	
5.38	9 x 2.484	90	3.62	0.040	--	" *	⊕	0.137	0.0360	--	--	
<u>b. Previous Tests</u>												
[1]	0.993	2 x 0.460	$59\frac{1}{2}$	4.35	0.0386	20	Aluminum	⊙	0.0272	0.0122	0.223	1.009
[1]	1.508	2 x 0.44	70	4.55	0.0243	20	"	⊙	0.036	0.015	0.350	0.876
[1]	1.998	2 x 0.449	75	4.45	0.0187	20	"	⊙	0.041	0.0167	0.446	0.884

[3]	0.677	$1\frac{1}{2}$ x 0.24	62*	6.25	0.0295	12	Steel	⊙	0.036	0.0130	0.252	0.973
[3]	1.00	2 x 0.43	66*	4.65	0.0358	16	"	⊙	0.043	0.0152	0.352	1.090
[4]	1.01	2 x 0.44*	66*	4.55	0.0363	16	"	⊙	0.040	0.0146	0.328	1.015
[4]	1.01	$2\frac{2}{3}$ x 0.5*	90	5.33	0.0412	--	"	⊙	0.120	0.0254	0.985	--
[5]	1.51	$2\frac{2}{3}$ x 0.5*	90	5.33	0.0276	--	"	△	0.101 [#]	0.0250	0.980	--
[5]	2.03	$2\frac{2}{3}$ x 0.5*	90	5.33	0.0205	--	"	△	0.092 [#]	0.0250	1.006	--
[5]	3.00	$2\frac{2}{3}$ x 0.5*	90	5.33	0.0139	--	"	△	0.078 [#]	0.0246	1.002	--
[6]	2.996	$2\frac{2}{3}$ x 0.5*	90	5.33	0.0139	--	"	▽	0.077 [#]	0.0243	0.990	--
[6]	4.95	$2\frac{2}{3}$ x 0.5*	90	5.33	0.0084	--	"	▽	0.0638 [#]	0.0242	1.007	--
[6]	7.05	$2\frac{2}{3}$ x 0.5*	90	5.33	0.0059	--	"	▽	0.0538 [#]	0.0235	0.984	--
[7]	1.25*	$2\frac{2}{3}$ x 0.5*	90	5.33	0.0333	--	"	⊙	0.114	0.0257	1.022	--
[7]	4.925*	6 x 2*	90	3.00	0.0338	--	" *	⊙	0.134 [#]	0.0350	--	--

- [1] Silberman and Dahlin, Friction Factors for Helical Corrugated Aluminum Pipe, P.R. 112, SAFHL, 1969.
 [3] Rice, Friction Factors for Helical Corrugated Pipe, ARS 41-119, ARS, USDA, 1966.
 [4] Chamberlain, disc. of [6], Jr. Hydr. Div., ASCE, Vol. 86, No. HY3, March 1960, pp. 67-74.
 [5] Straub and Morris, Hydraulic Tests on Corrugated Metal Culvert Pipes, T.P. 5-B, SAFHL, 1950.
 [6] Webster and Metcalf, "Friction Factors in Corrugated Metal Pipes," Jr. Hydr. Div., ASCE, Sept. 1959, pp. 35-67.
 [7] Neill, "Hydraulic Roughness of Corrugated Pipes," Jr. Hydr. Div. ASCE, May 1962, pp. 23-44, and disc. closure July 1963, pp. 205-208.

*Nominal, not known whether measurement was made. Otherwise, measured.

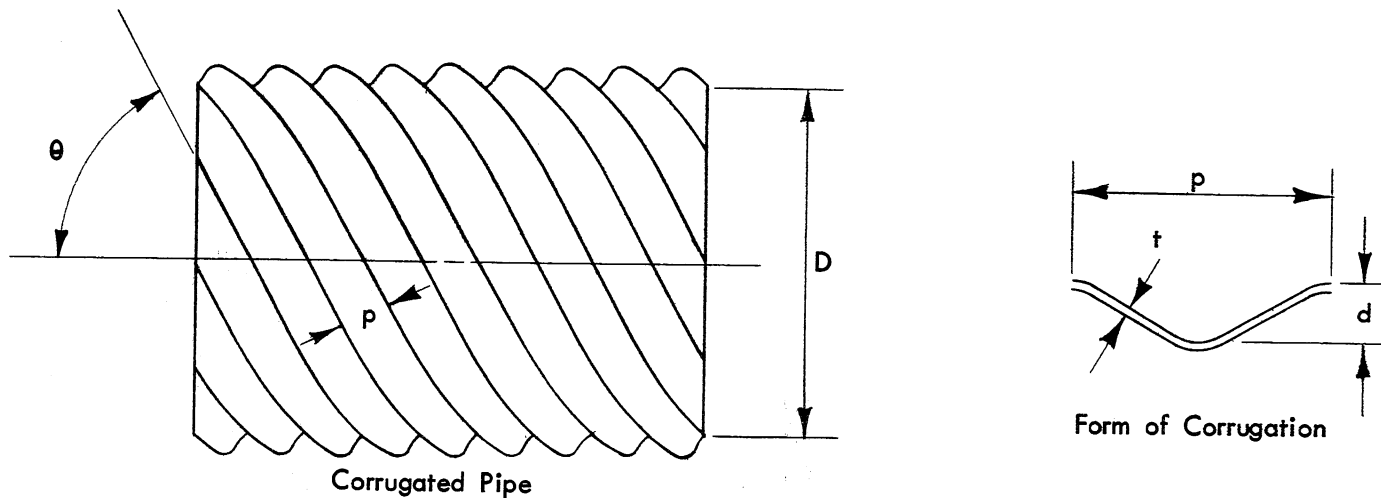
#Maximum value (at high Reynolds number).

*Bolted joints. All other annular pipe riveted. Helical pipe has crimped seams.



I L L U S T R A T I O N S

(Figs. 1 thru 31)



From Factory Specifications

Measured

Type	Nominal	Helix Angle	p - in.	t - in.	d - in.	Average	Standard	Helix Angle	d - in.
	Pipe Dia.								
*Annular Riveted	66	90	6	0.105	1	65.42	0.719	90	0.958
*Annular Bolted	66	90	9	0.100	2-1/2	64.57	0.492	90	2.484
*Annular Riveted	48	90	6	0.075	1	47.62	0.332	90	0.941
*Helical	48	82° - 28'	2	0.105	1/2	48.47	0.204	82.5	0.490
#Helical	48	80° - 58'	2-2/3	0.105	1/2	47.71	0.218	81.0	0.517
#Helical	24	71° - 58'	2-2/3	0.105	1/2	23.94	0.099	72.2	0.519
#Helical	12	50° - 51'	2-2/3	0.060	1/2	11.737	0.030	52.5	0.496

*Supplied by Kaiser Aluminum & Chemical Sales, Inc.

#Supplied by Reynolds Metals Co.

Fig. 1 - Pipe Details

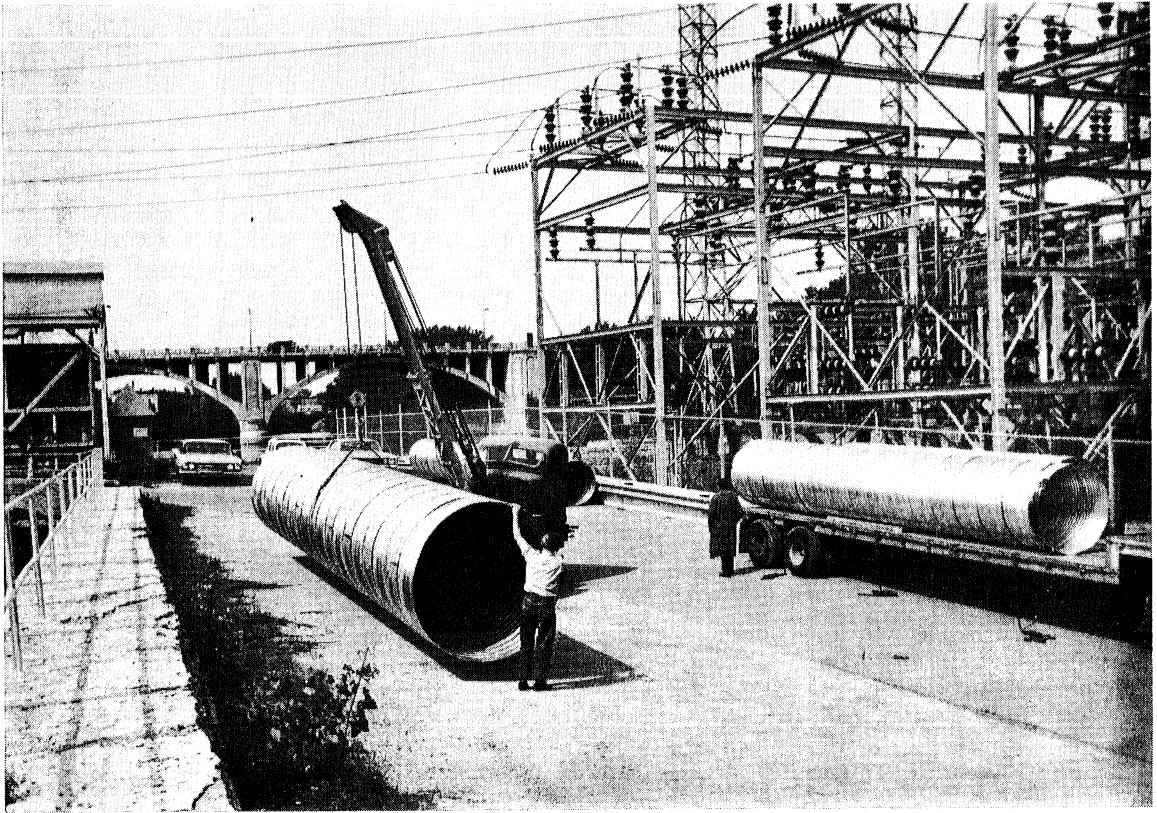


Fig. 2 - Unloading the 48 in. Pipe

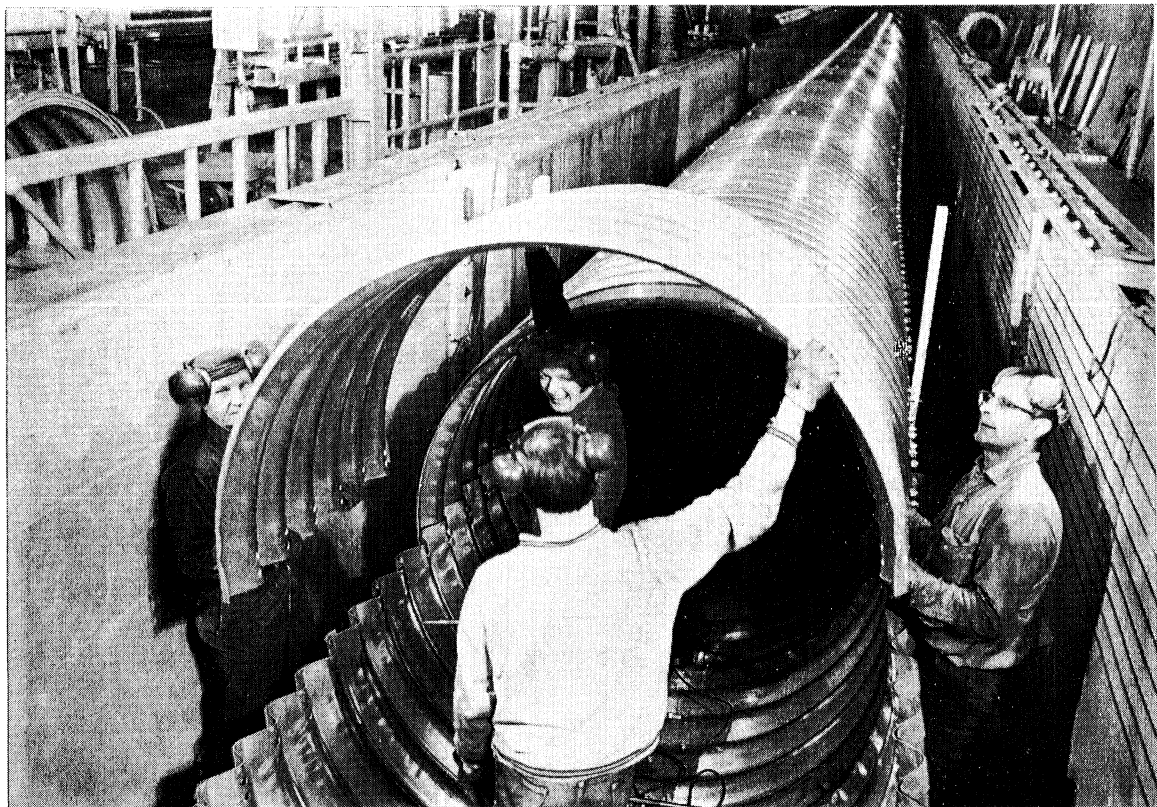


Fig. 3 - Assembly of the 66 in. Bolted Pipe

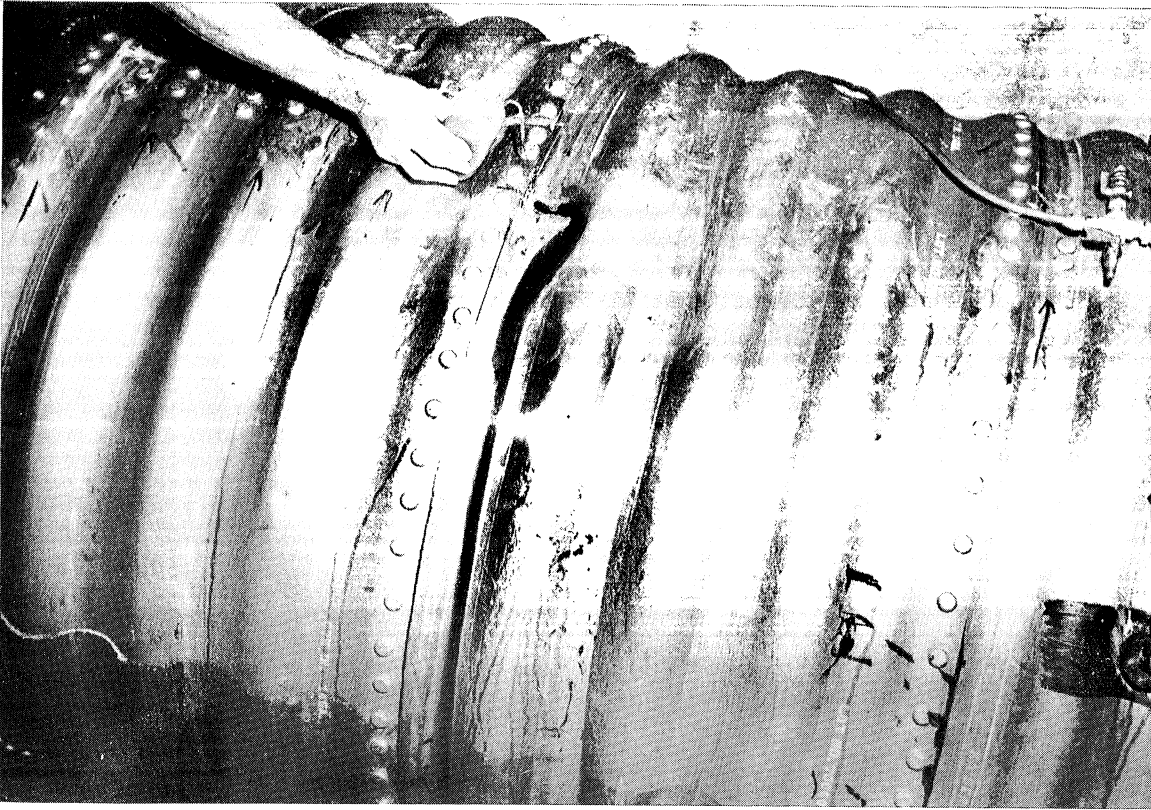


Fig. 4 - A Typical Leak in a Riveted Joint of the 48 in. Annular Pipe (Dye colors the leaking water)

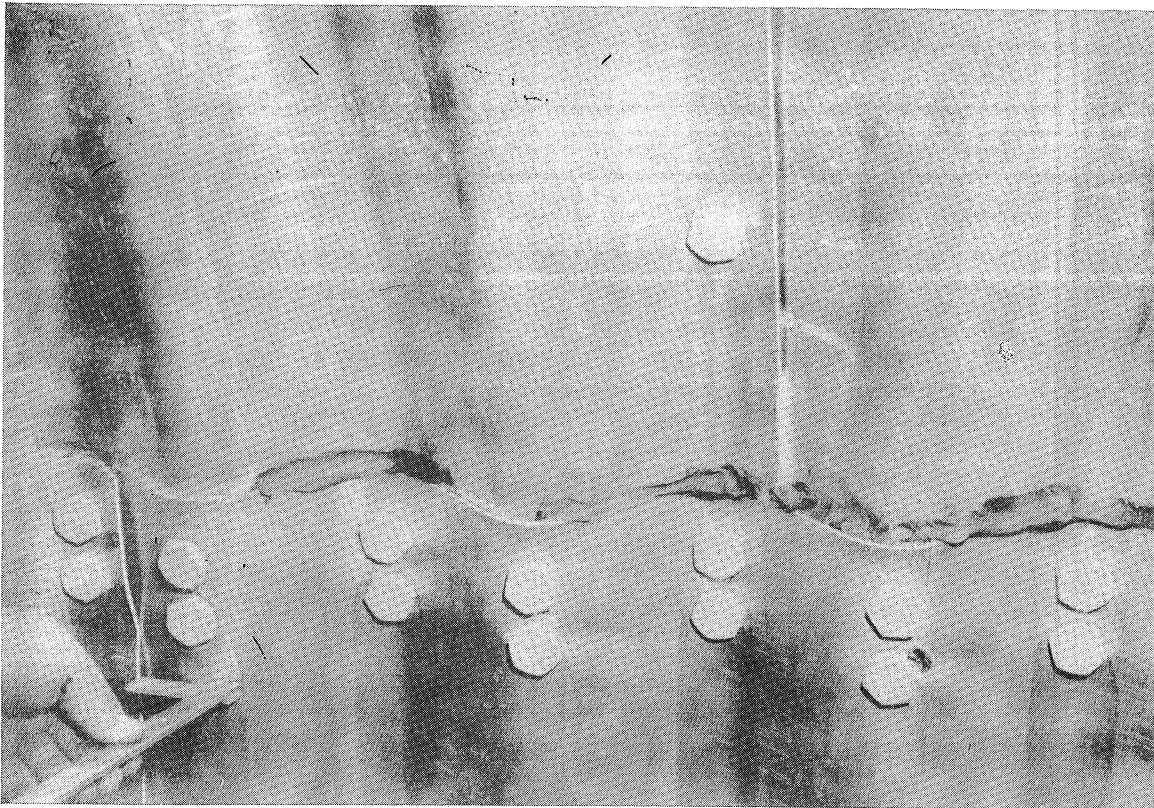
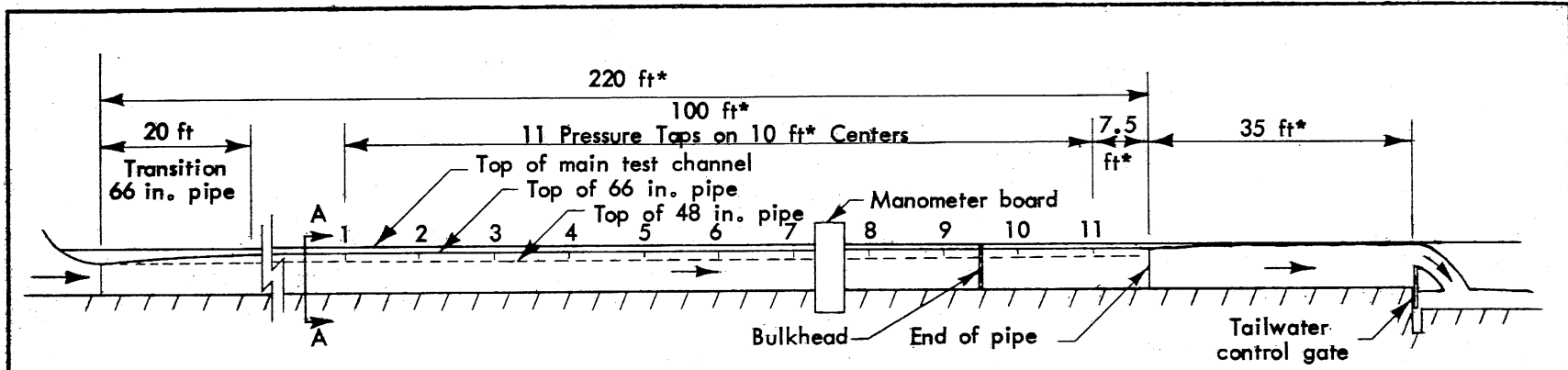


Fig. 5 - Joint Detail inside the 66 in. Bolted Pipe



Test pipe on main channel floor with 0.133 per cent slope
 *Dimensions vary slightly for different pipes

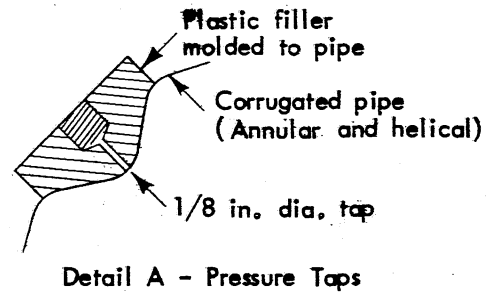
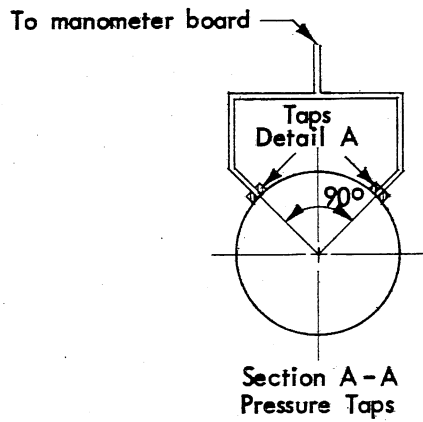


Fig. 6 - Test Arrangement in Main Test Channel for 48 in. and 66 in. Pipe

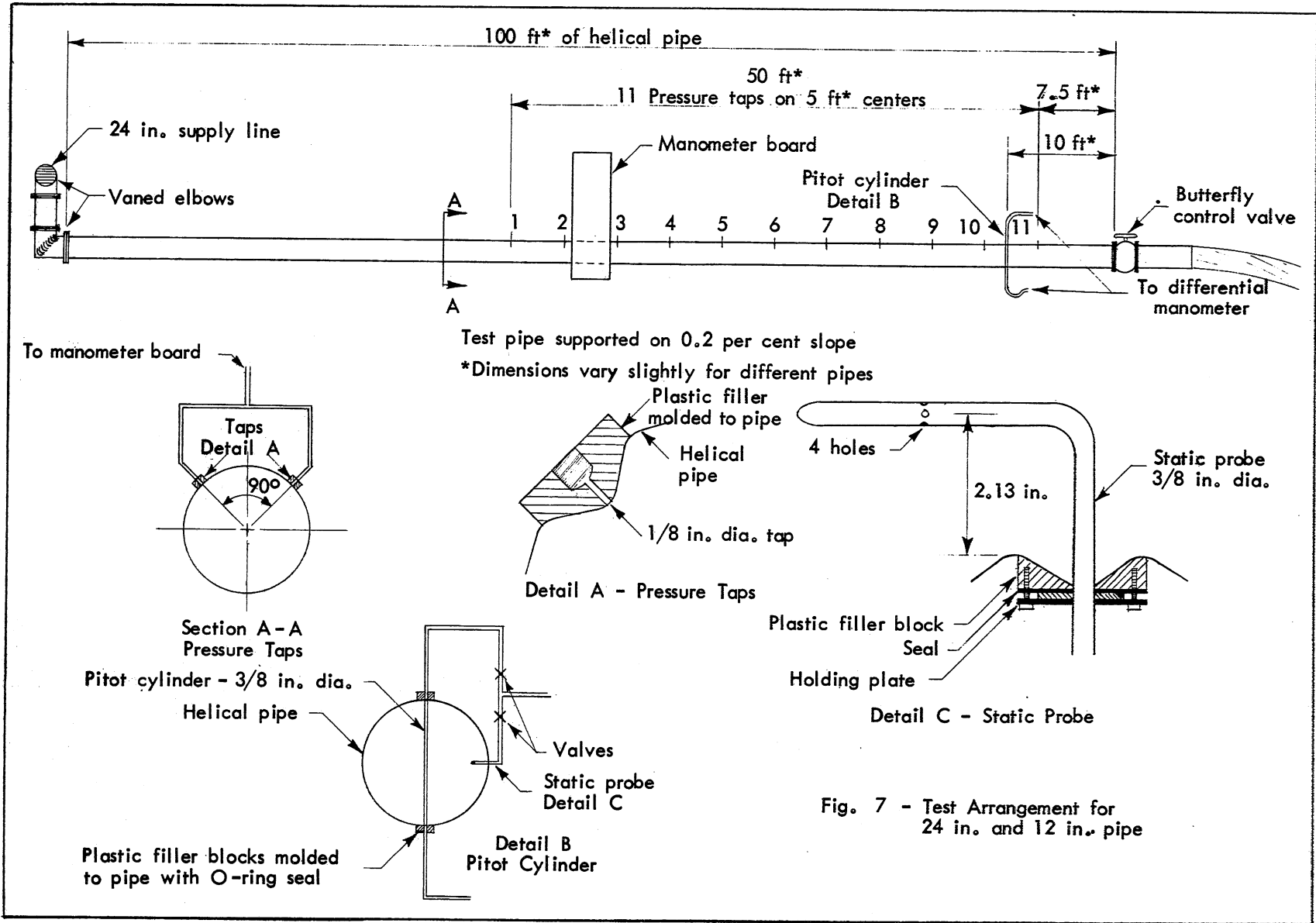


Fig. 7 - Test Arrangement for 24 in. and 12 in. pipe

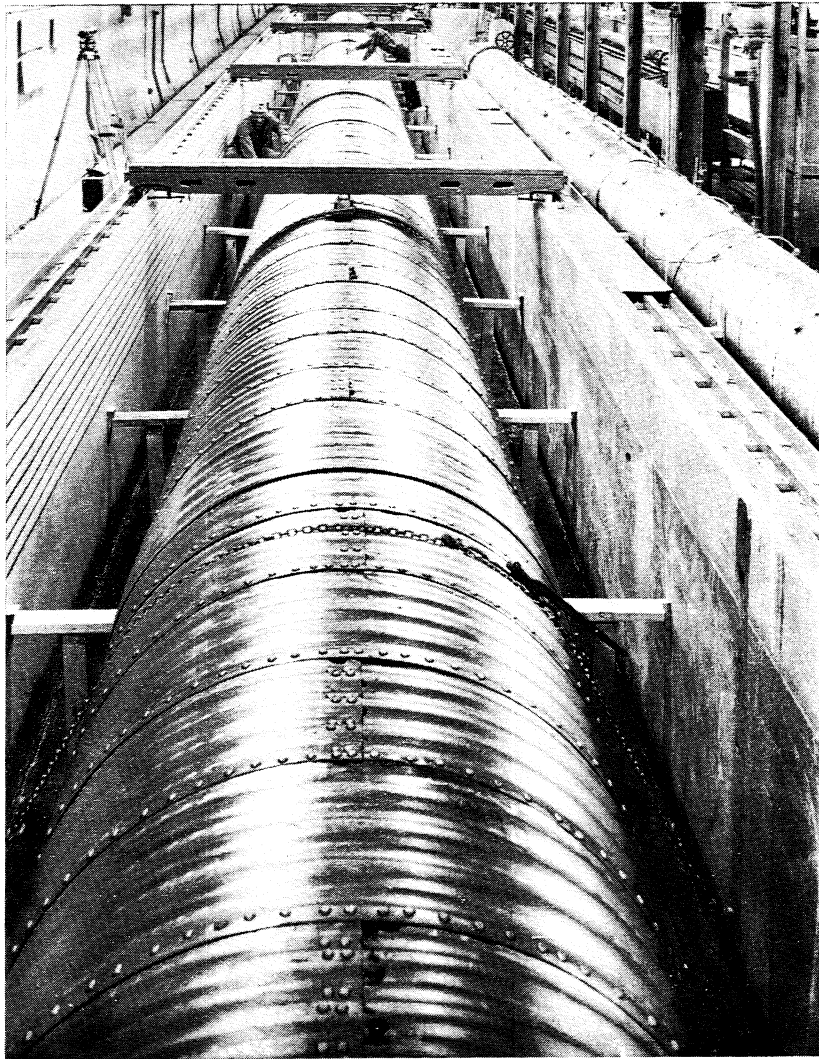


Fig. 8 - The 66 in. Annular Riveted Pipe
Installed in the Main Channel with
24 in. Helical Pipe along the Side

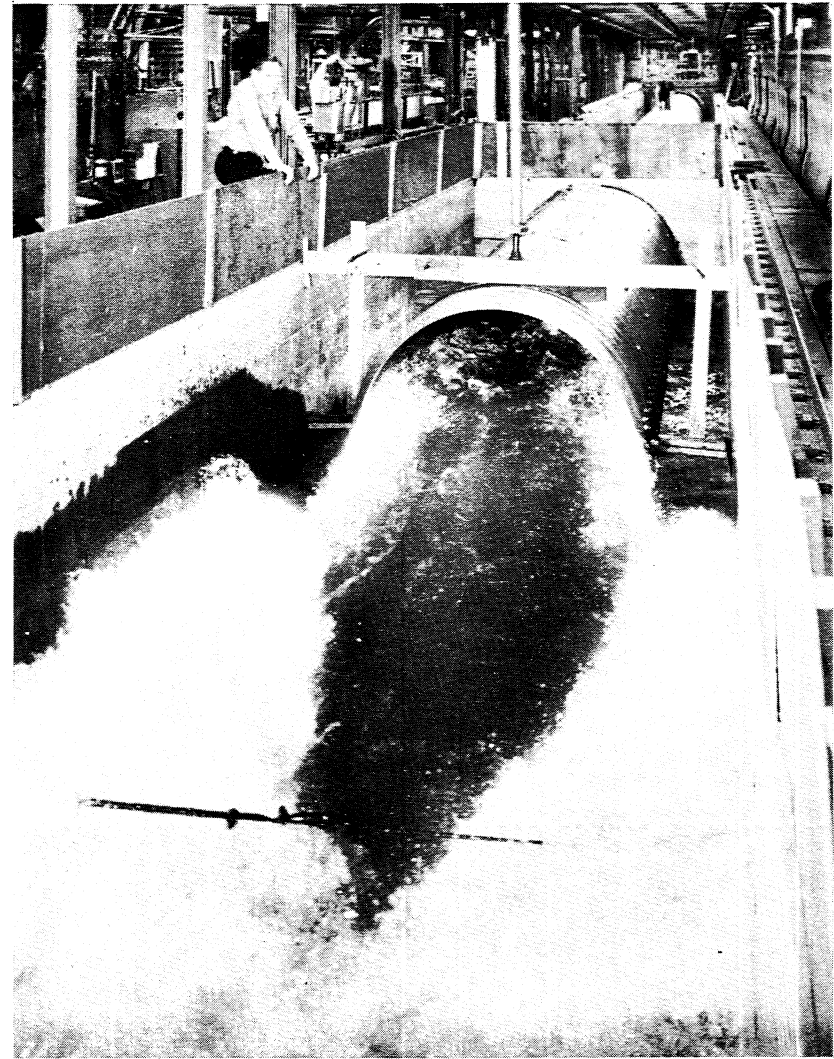


Fig. 9 - Flow at the Exit of the 66 in.
Bolted Pipe (240 cfs)

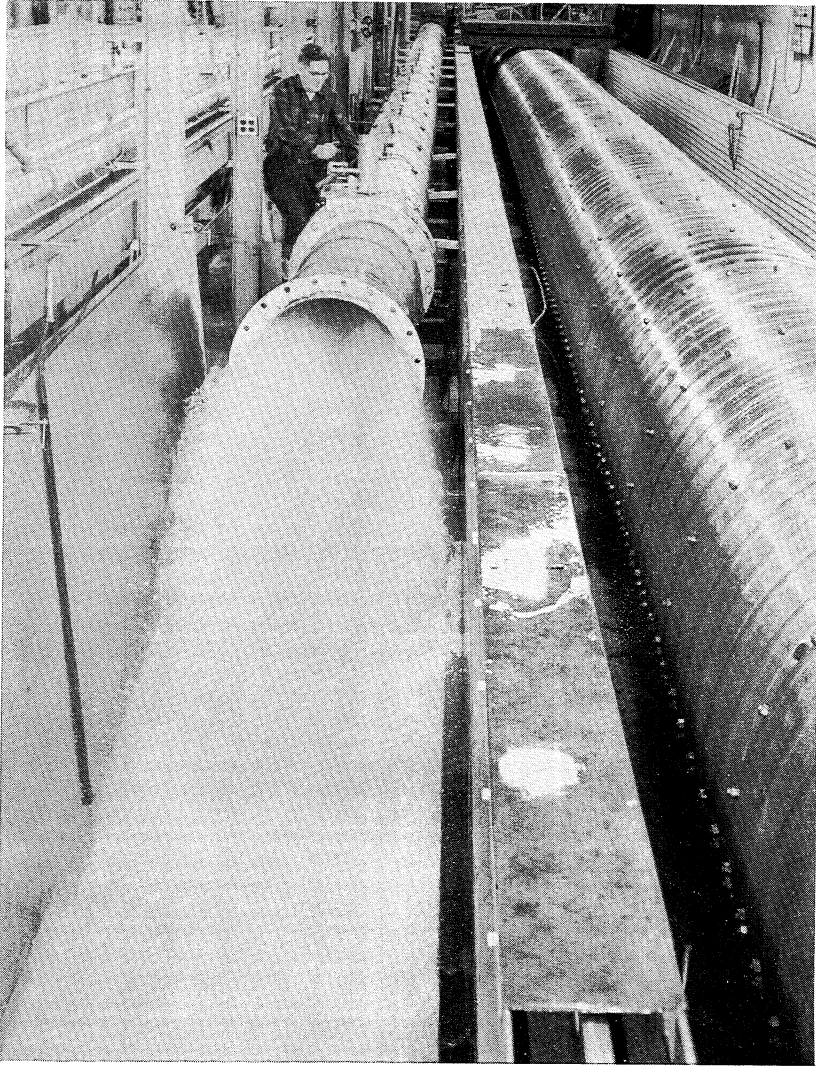


Fig. 10 - Flow at the Exit of the 24 in. Helical Pipe (38 cfs); 66 in. Bolted Pipe Installed in Main Channel along Side

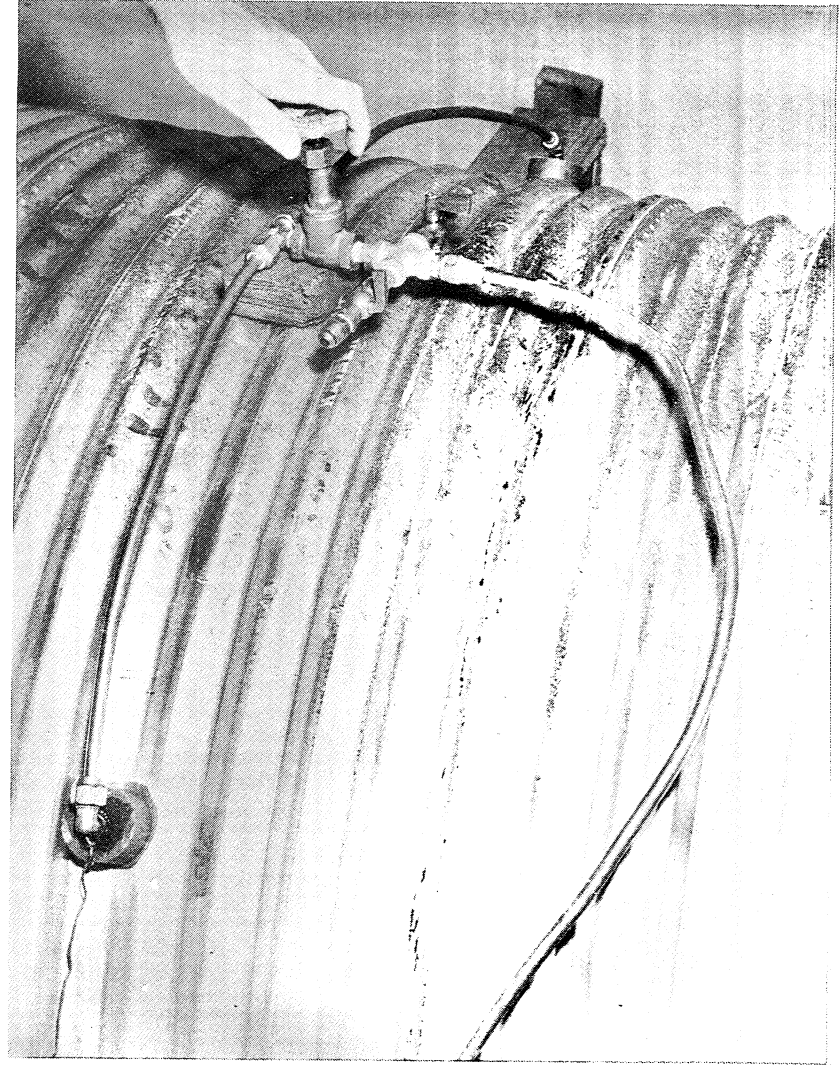


Fig. 11 - Piezometer Tap Arrangement (48 in. Helical Pipe)

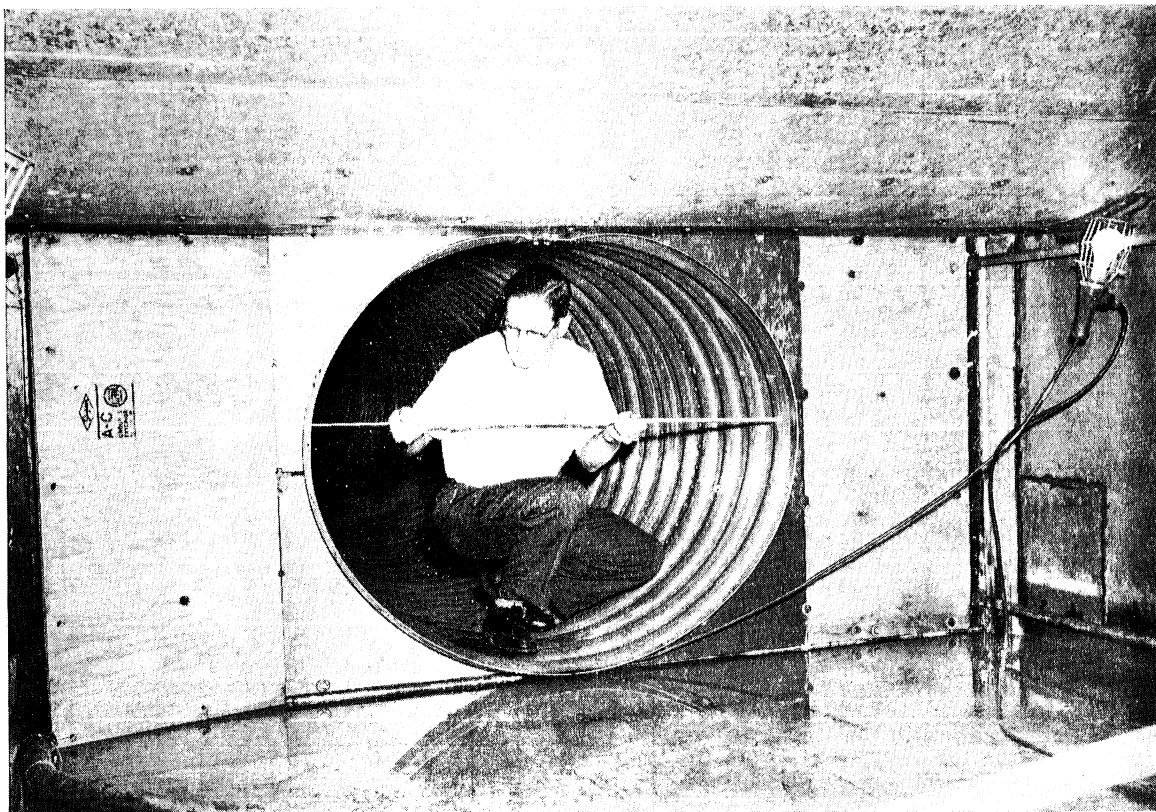


Fig. 12 - The Inlet for the 48 in. Pipes

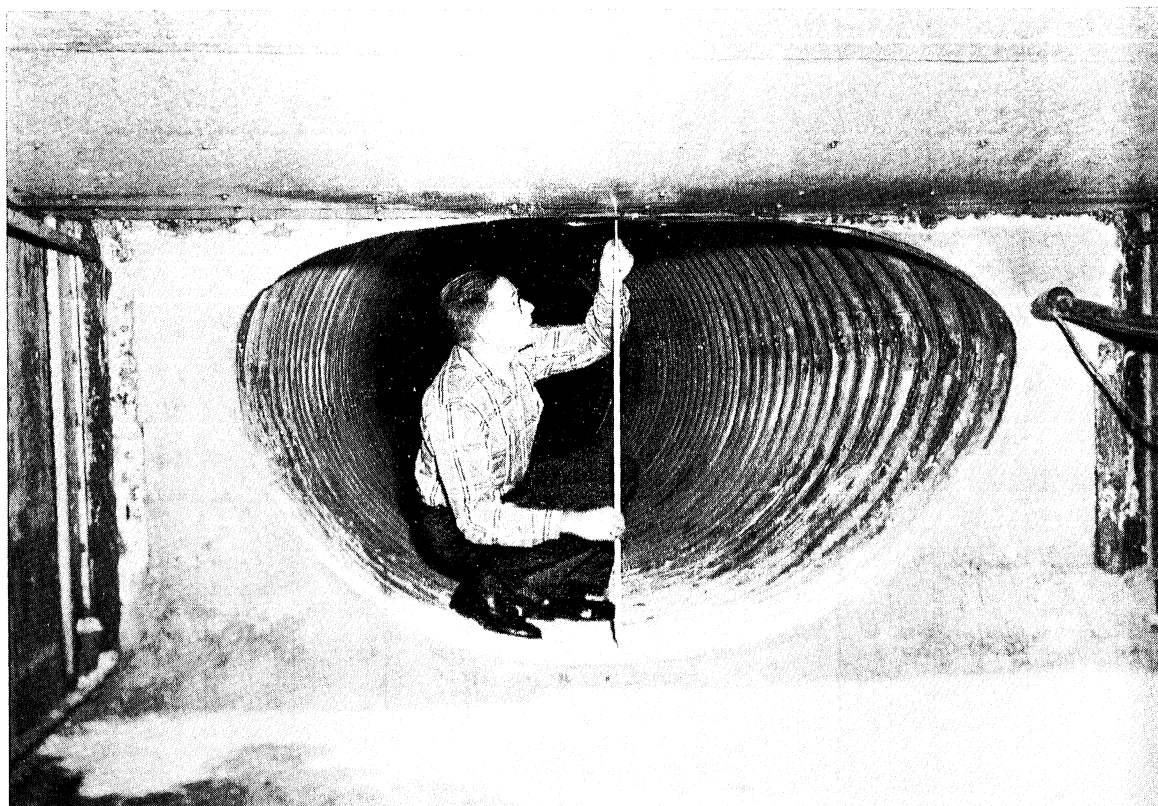
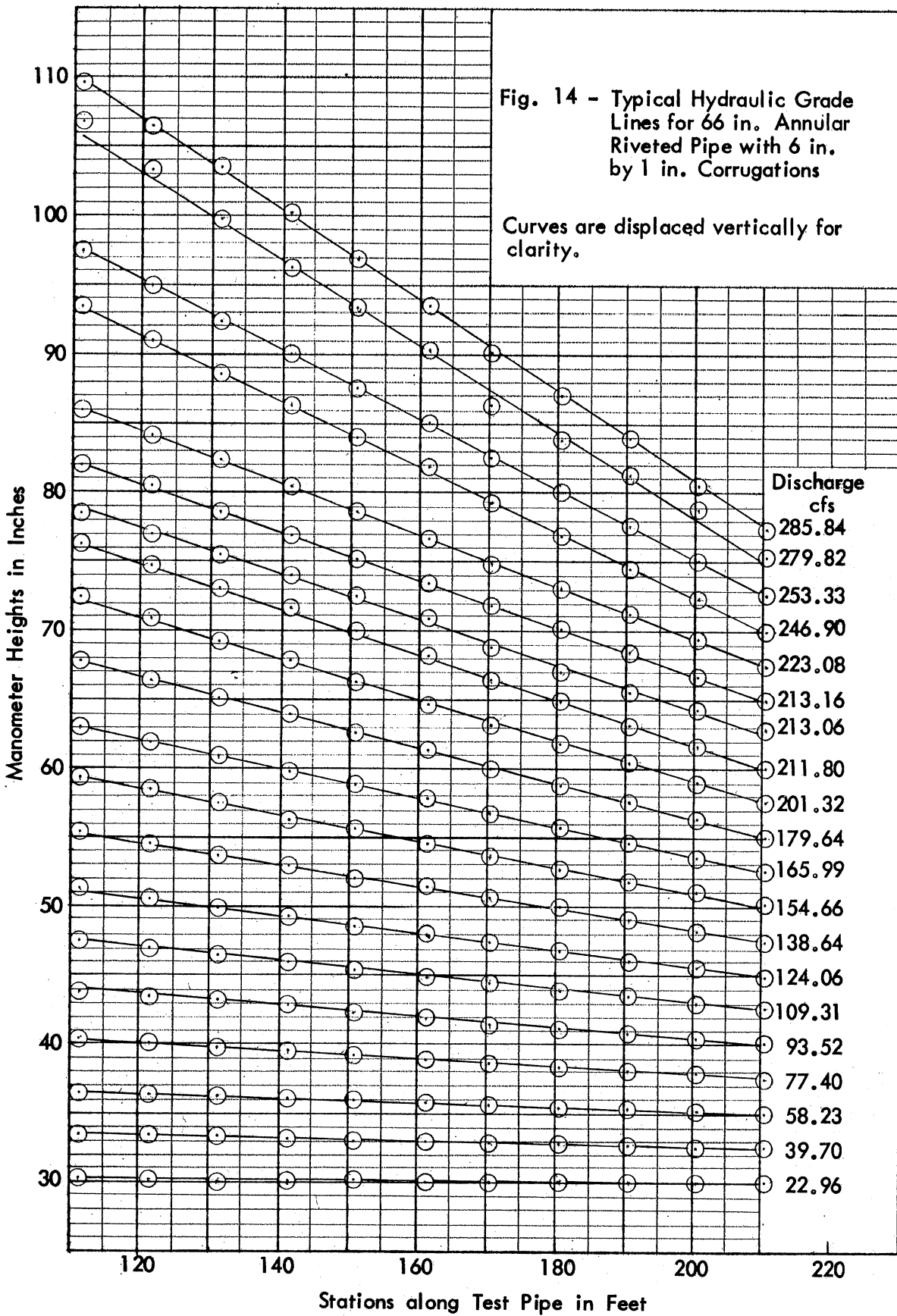
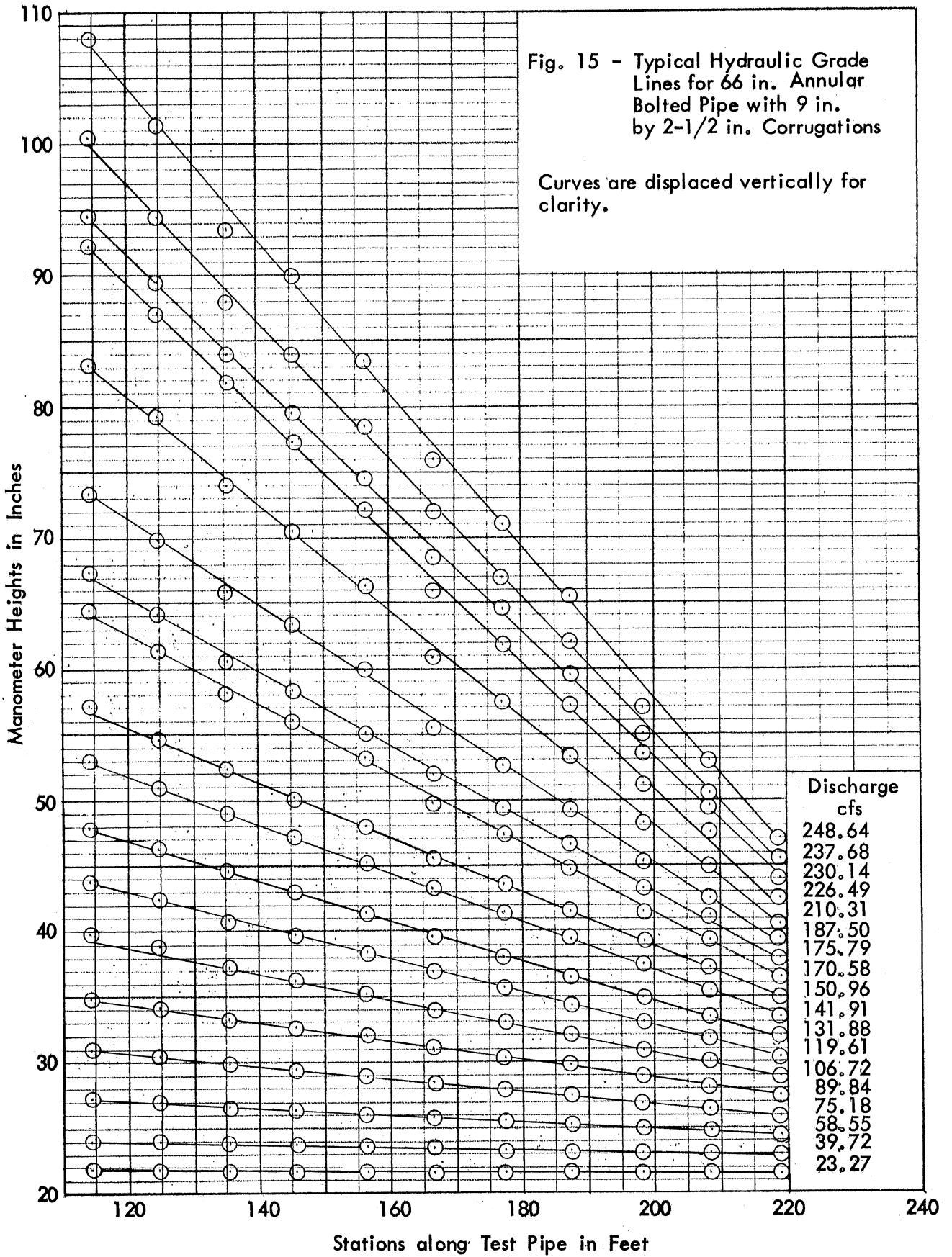
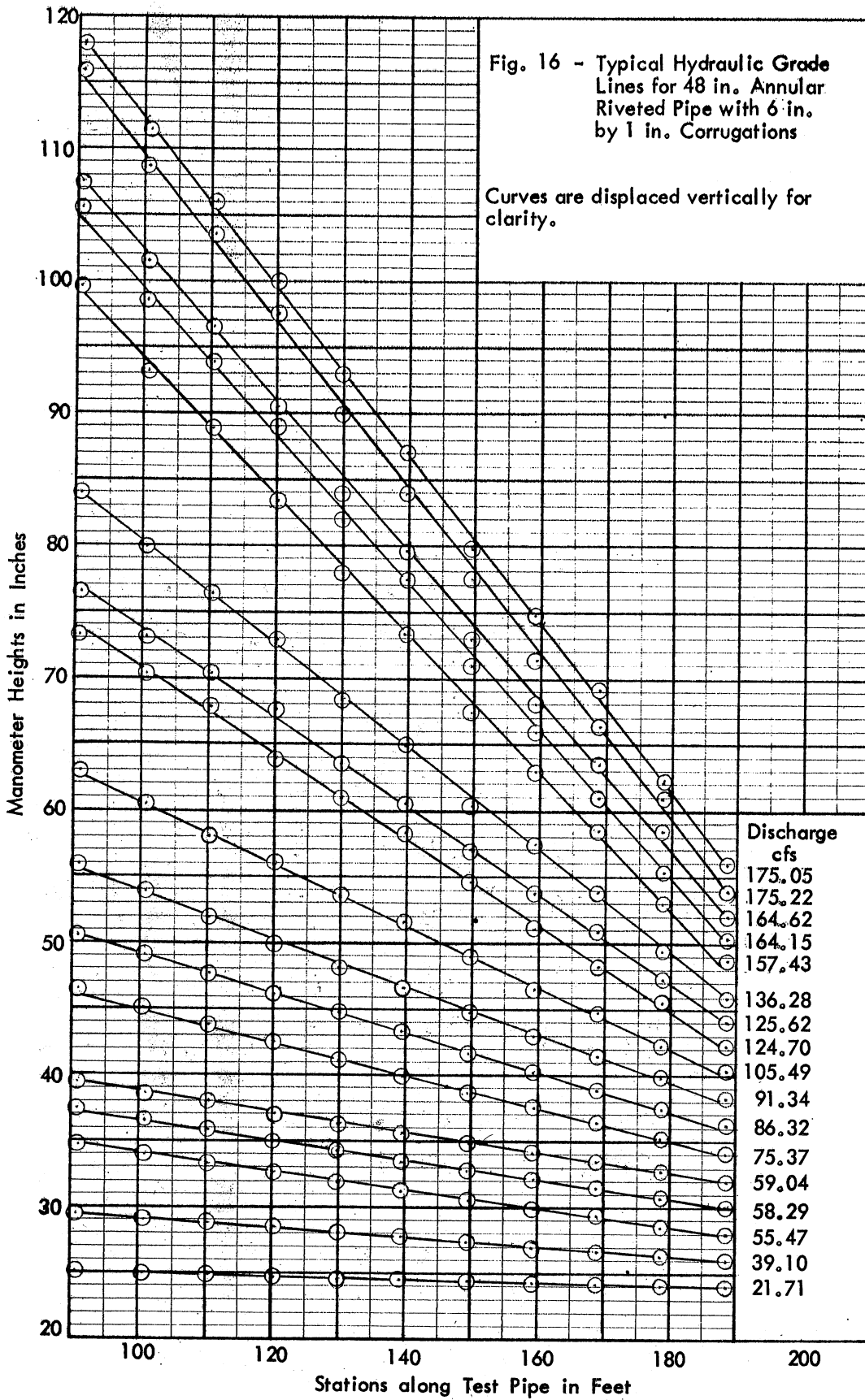
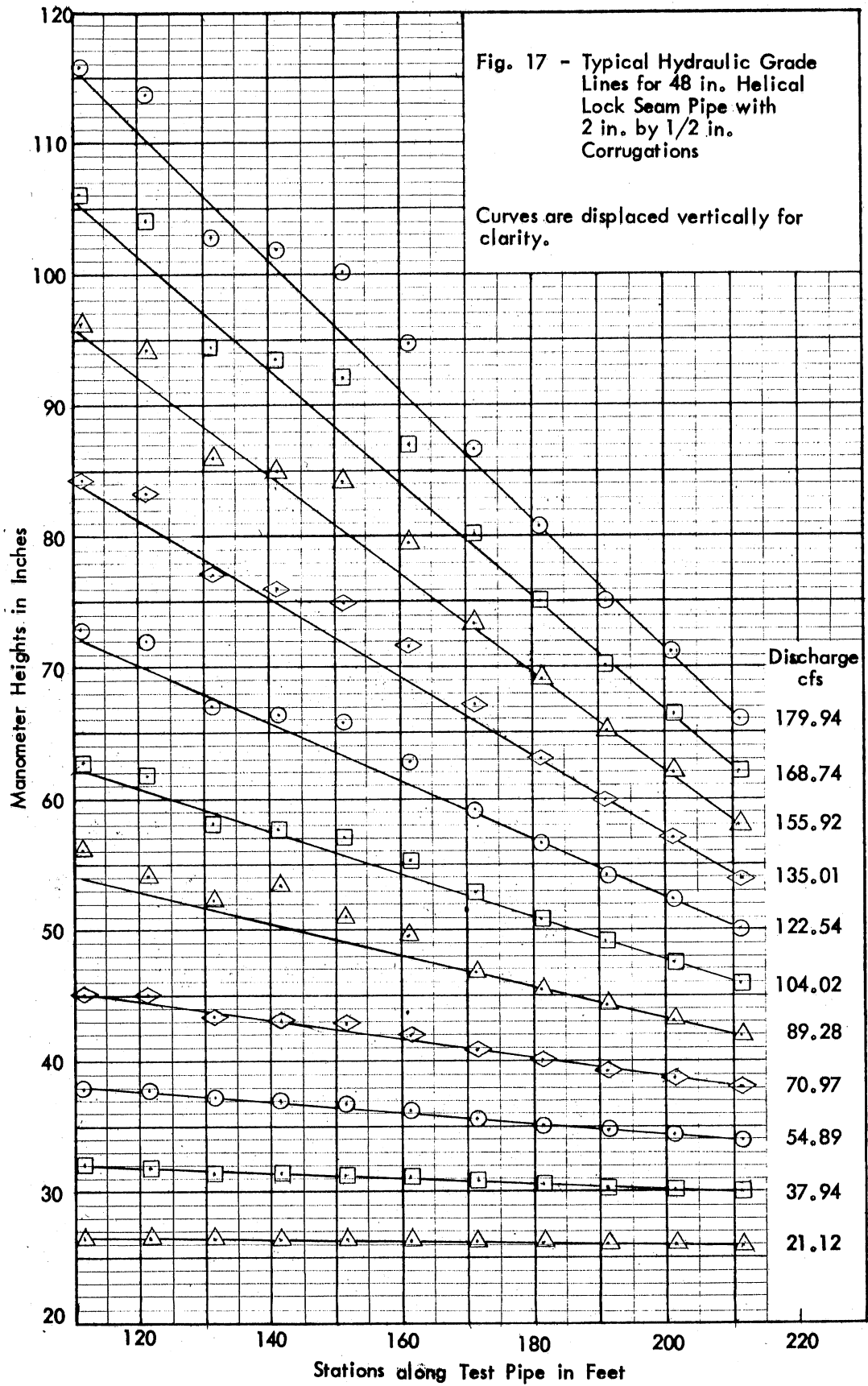


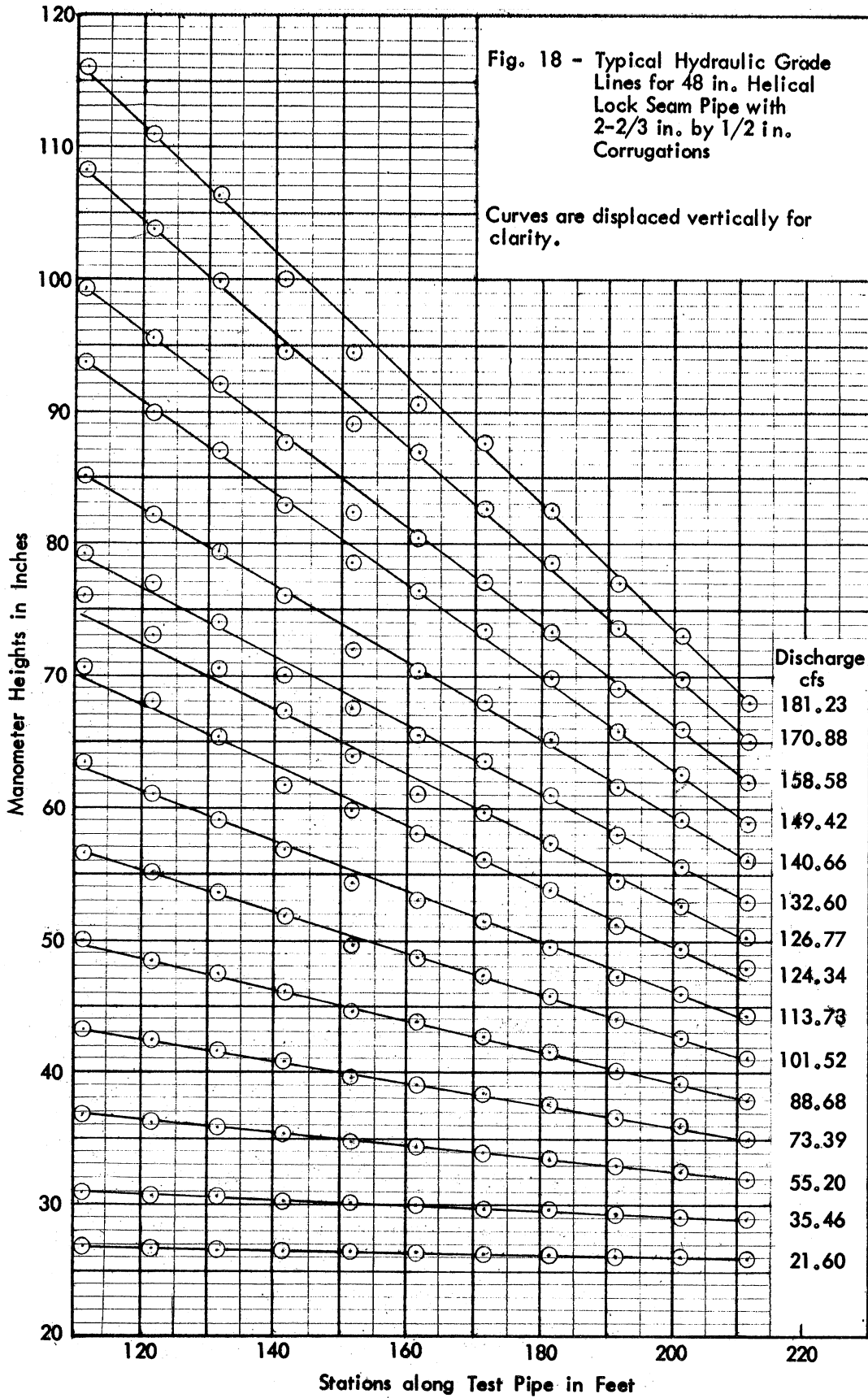
Fig. 13 - The Inlet for the 66 in. Pipes

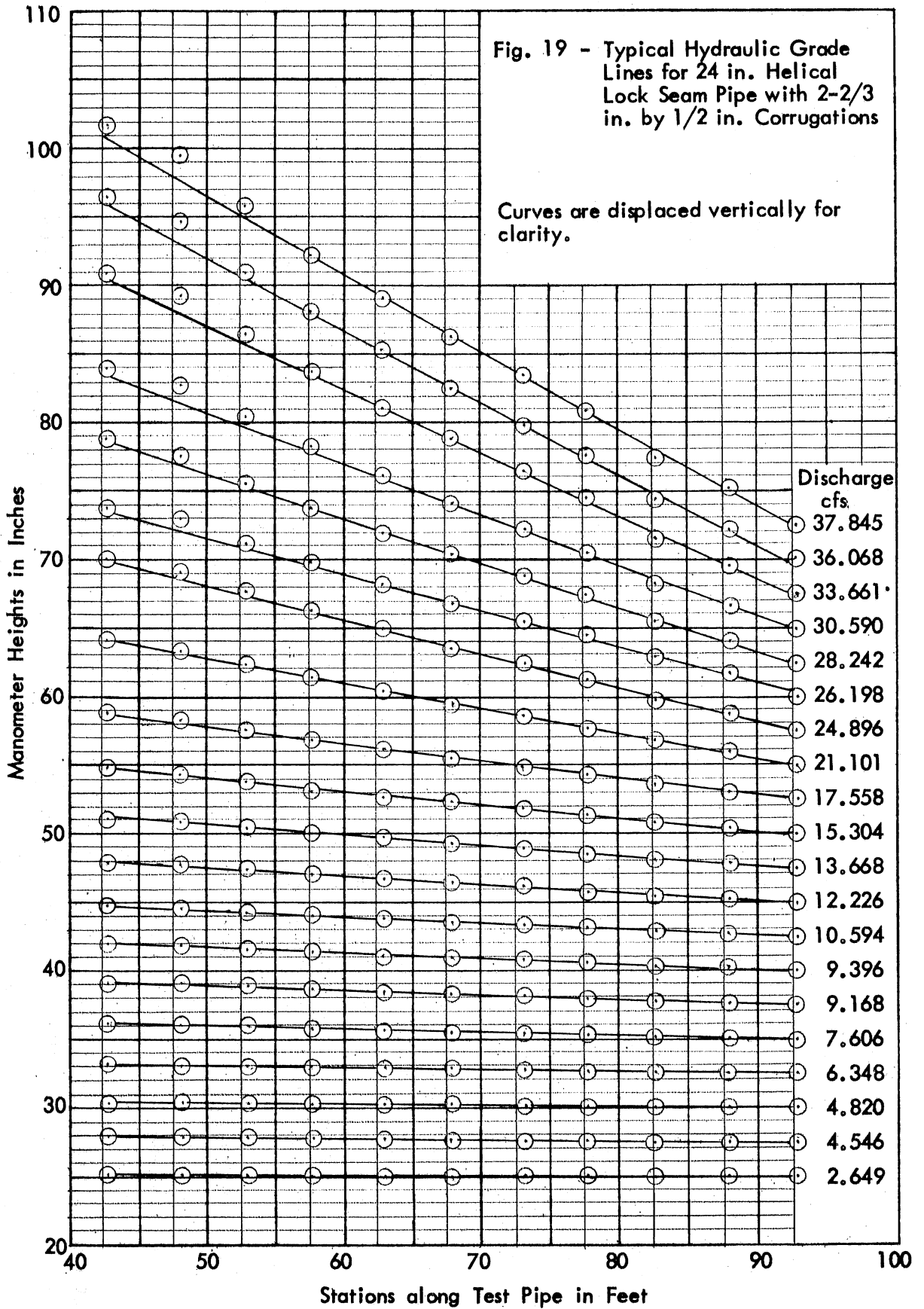


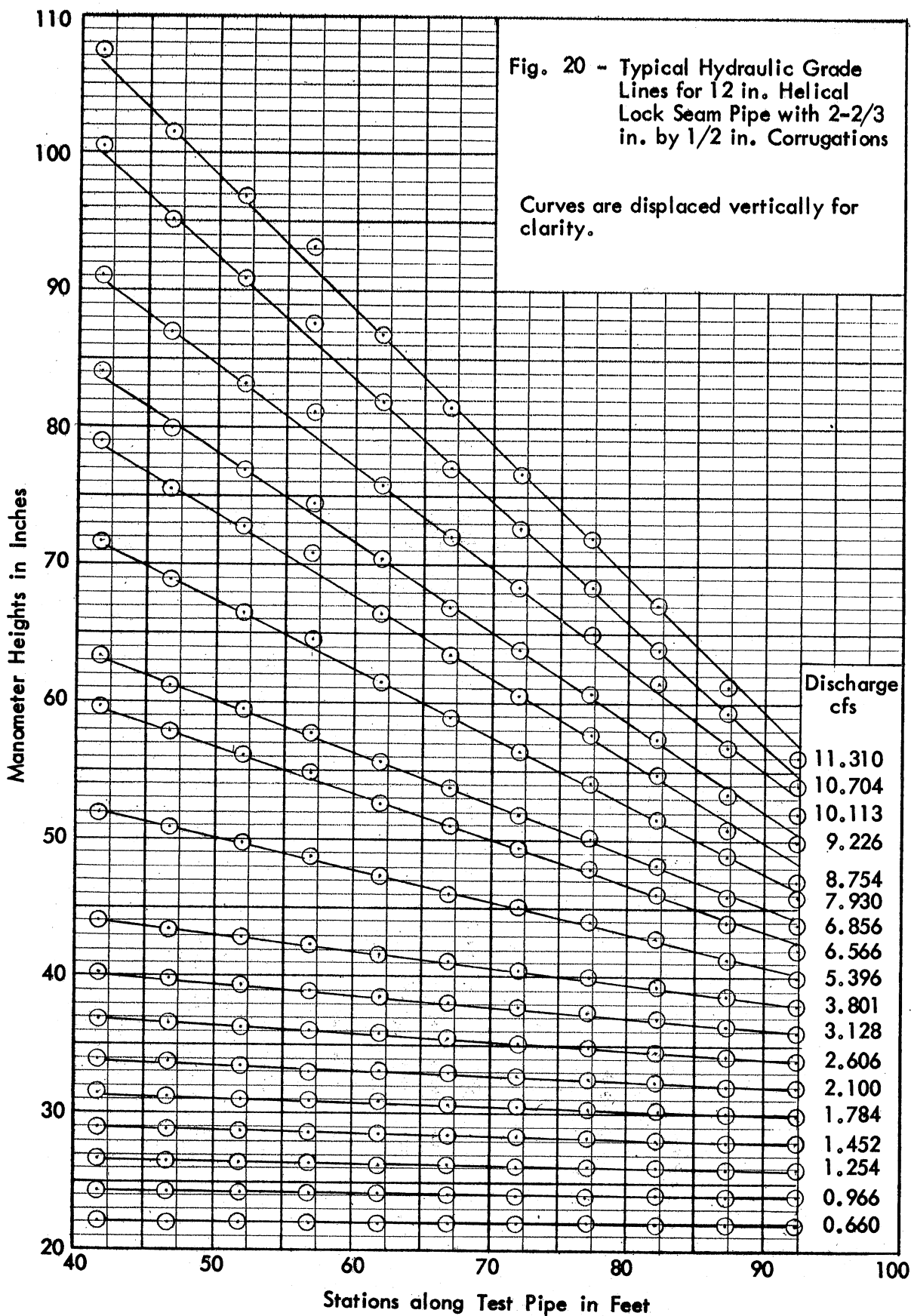












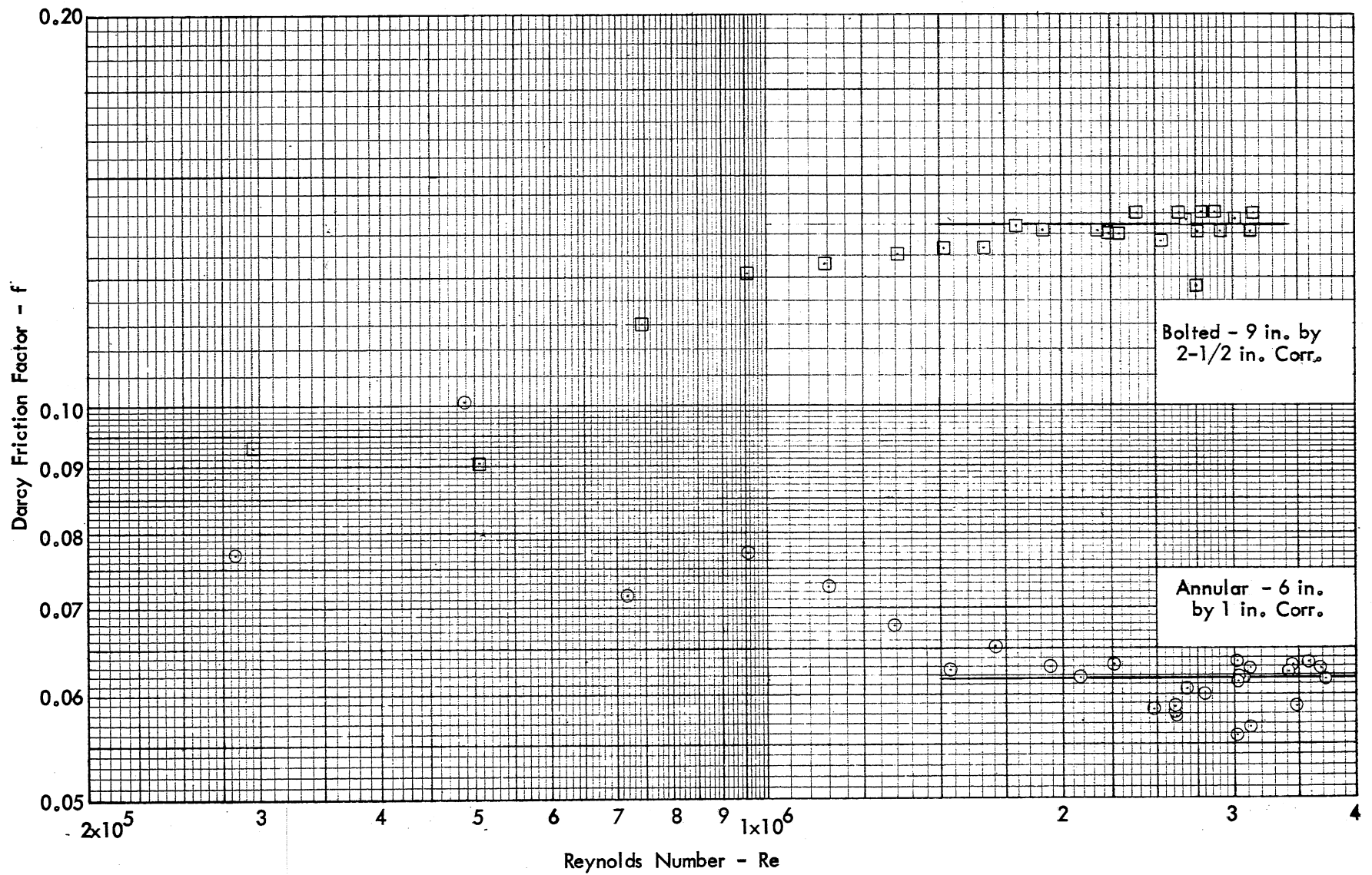


Fig. 21 - Variation of Darcy Friction Factor f with Reynolds Number - 66 Inch Corrugated Pipe

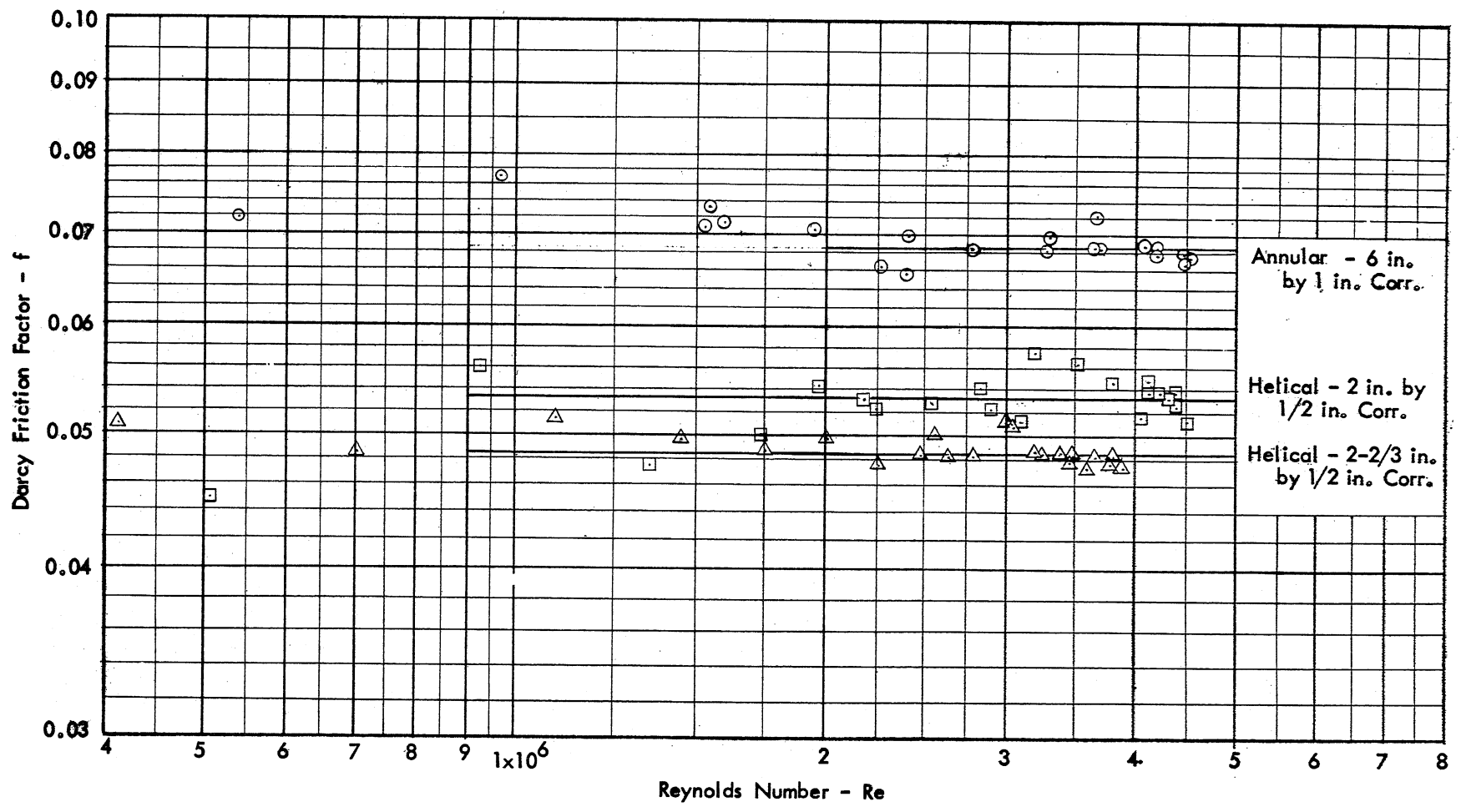


Fig. 22 - Variation of Darcy Friction Factor f with Reynolds Number - 48 Inch Corrugated Pipe

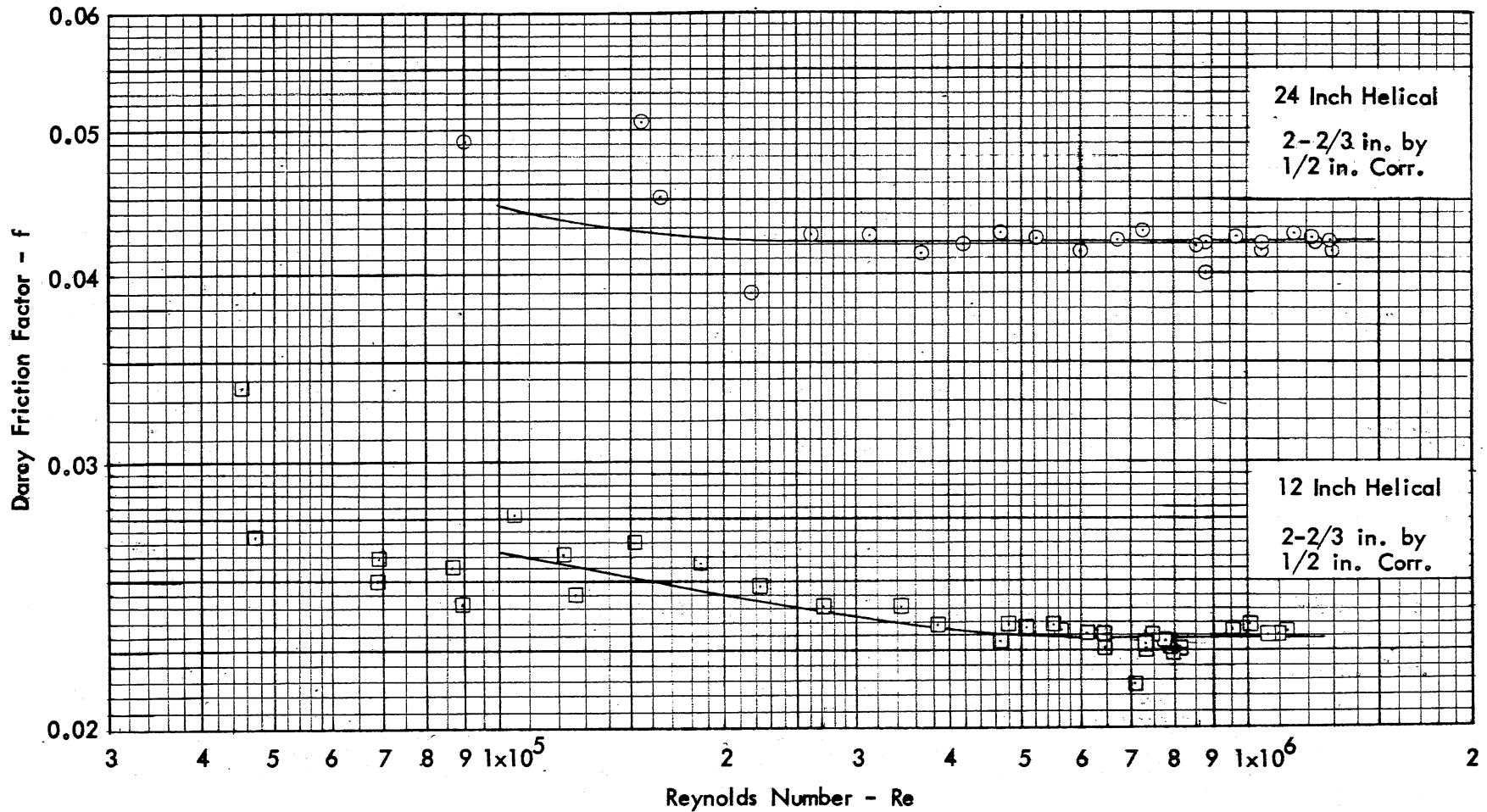


Fig. 23 - Variation of Darcy Friction Factor f with Reynolds Number - 12 Inch and 24 Inch Corrugated Pipe

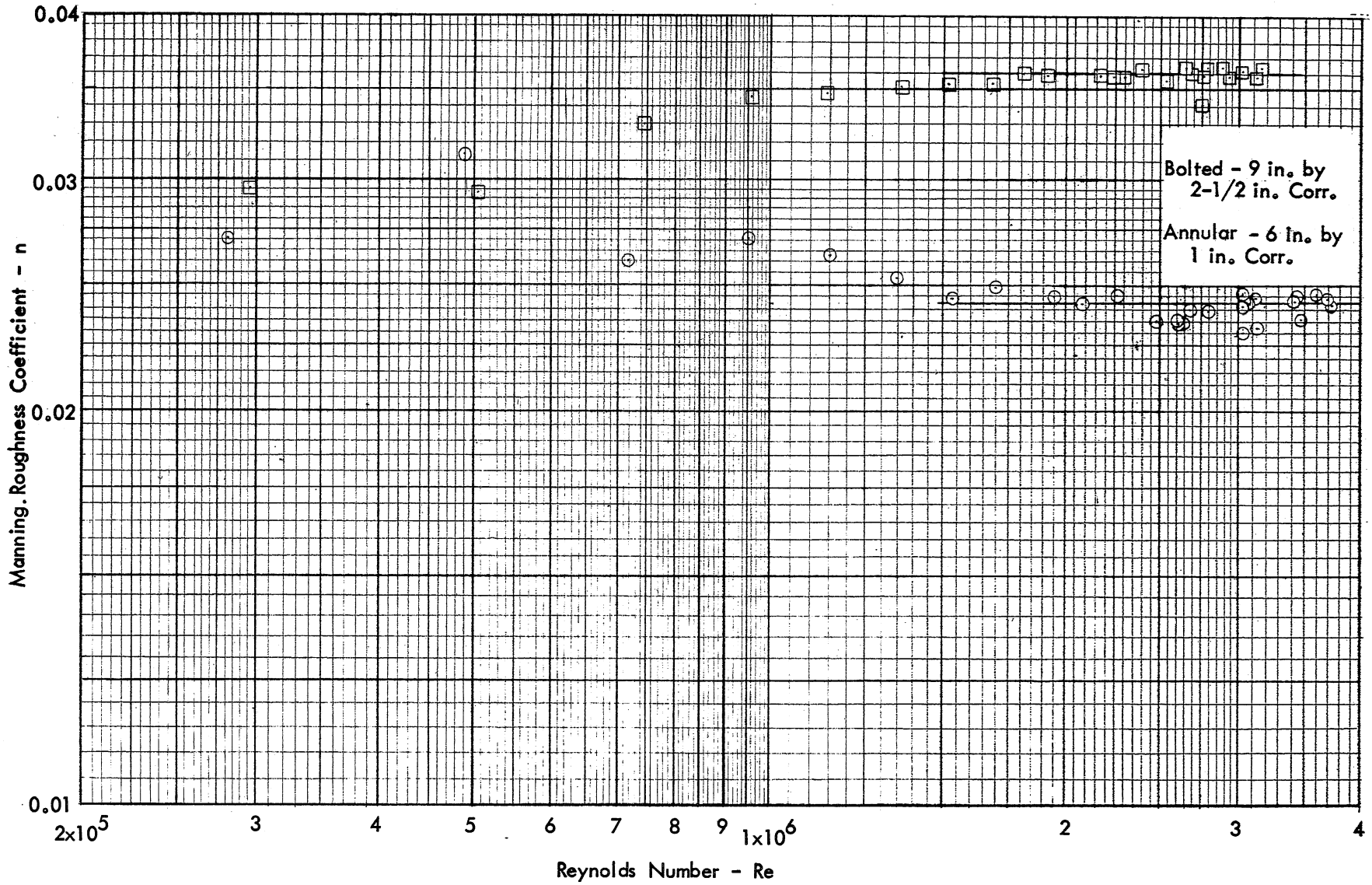


Fig. 24 - Variation of Manning n with Reynolds Number - 66 Inch Corrugated Pipe

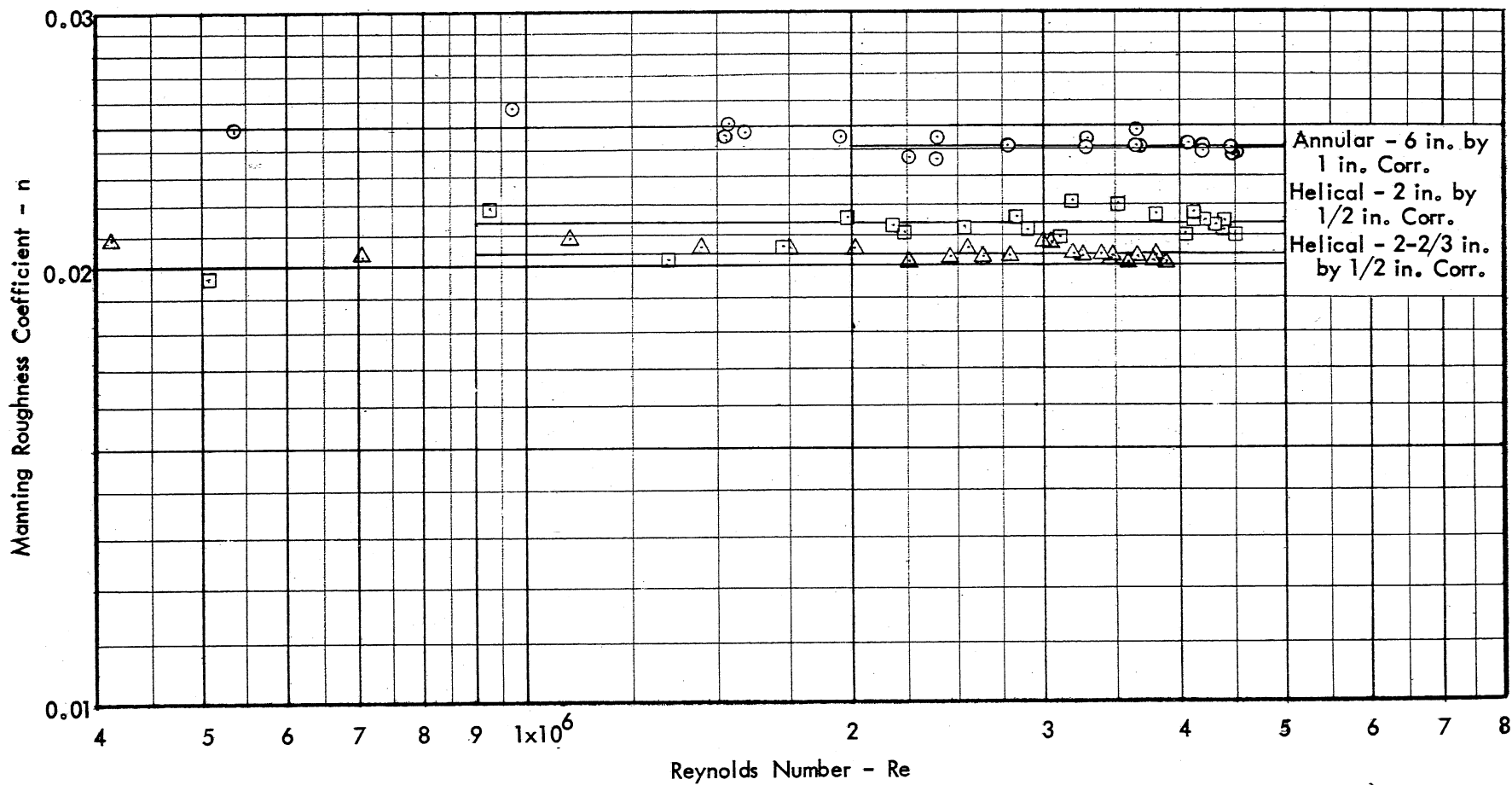


Fig. 25 - Variation of Manning n with Reynolds Number - 48 Inch Corrugated Pipe

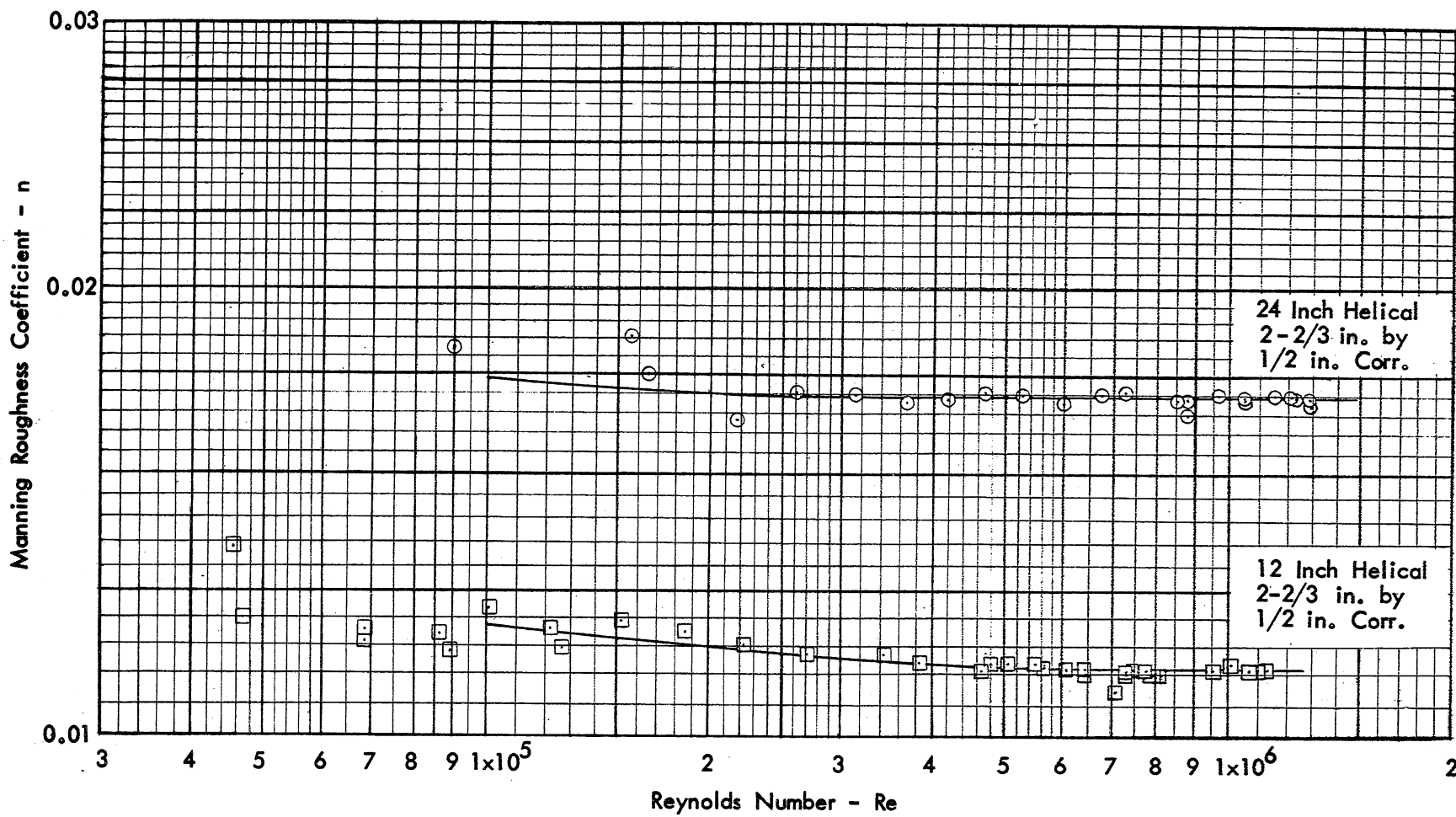


Fig. 26 - Variation of Manning n with Reynolds Number - 12 Inch and 24 Inch Corrugated Pipe

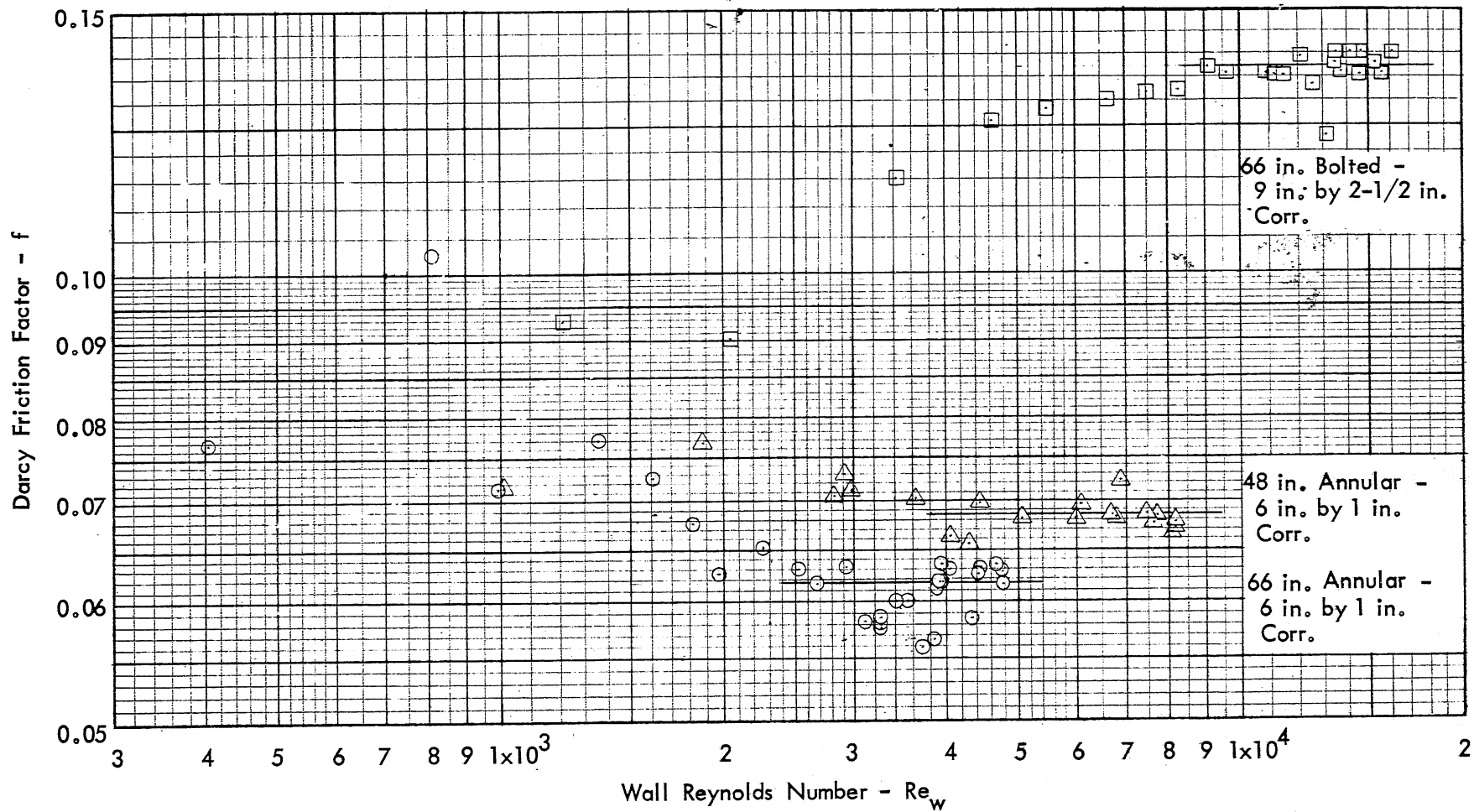


Fig. 27 - Variation of Darcy Friction Factor f with Wall Reynolds Number - Annular Corrugated Pipe

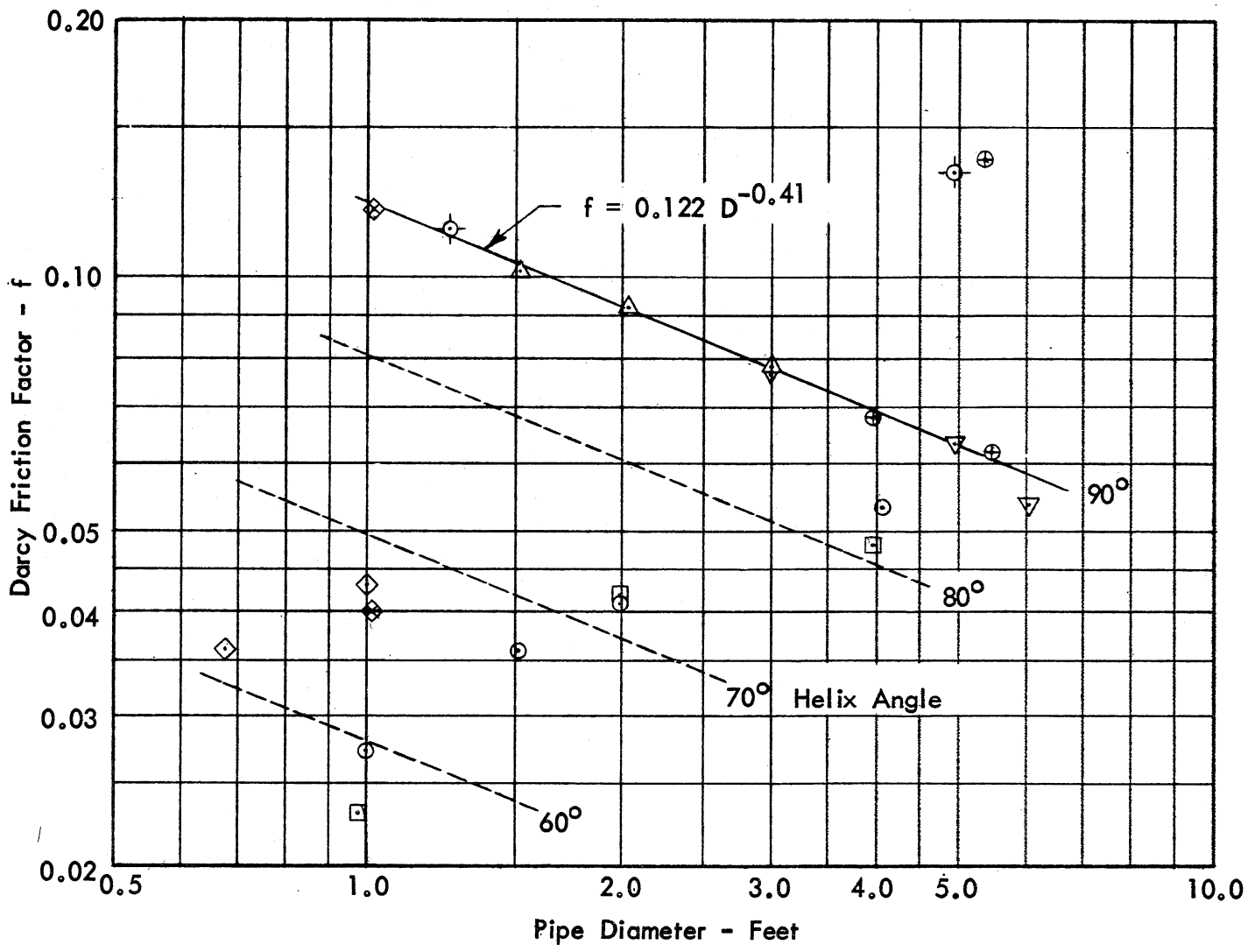


Fig. 28 - Darcy Friction Factor f as a Function of Pipe Diameter at High Reynolds Numbers

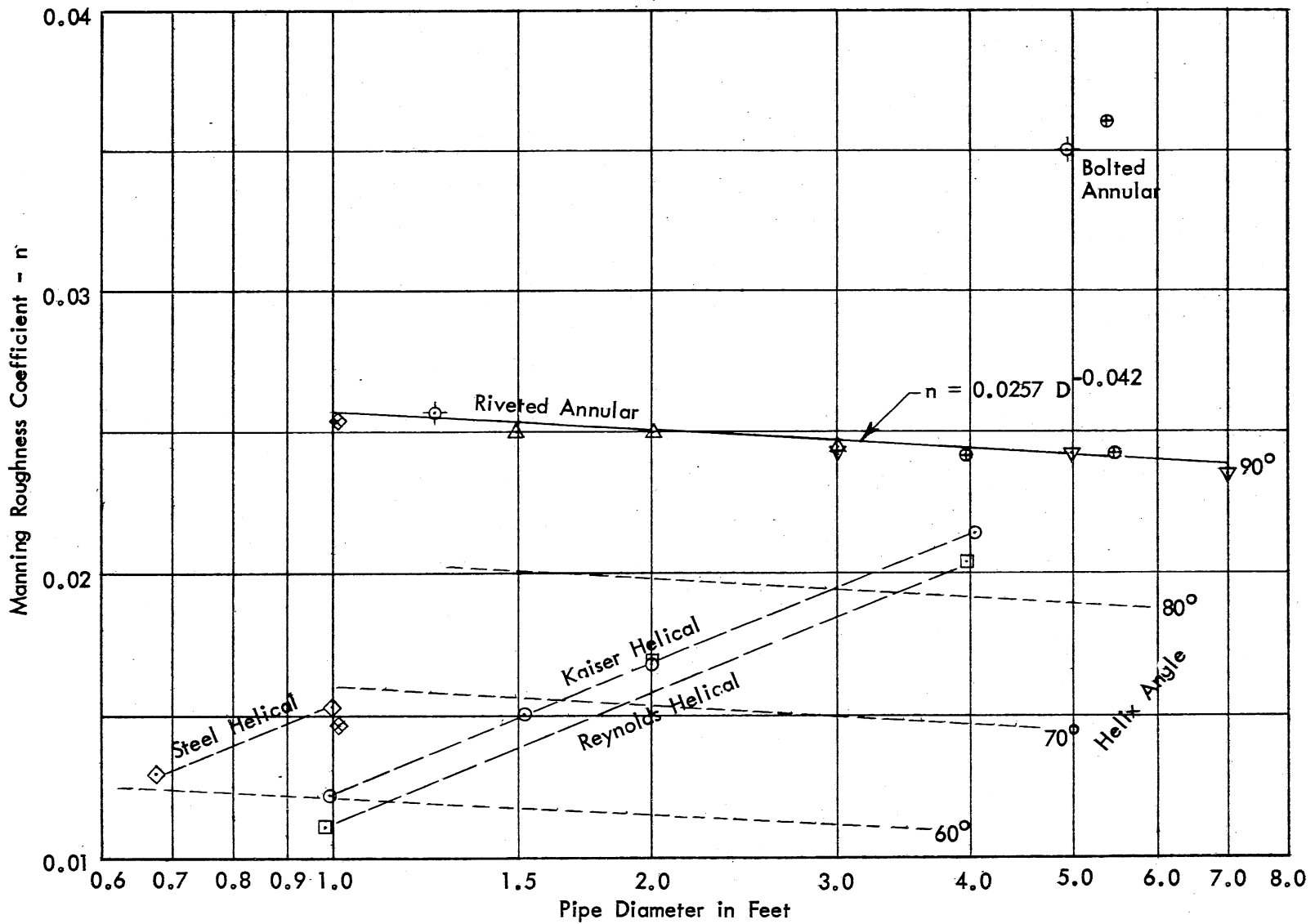


Fig. 29 - Manning Roughness Coefficient n as a Function of Pipe Diameter at High Reynolds Numbers

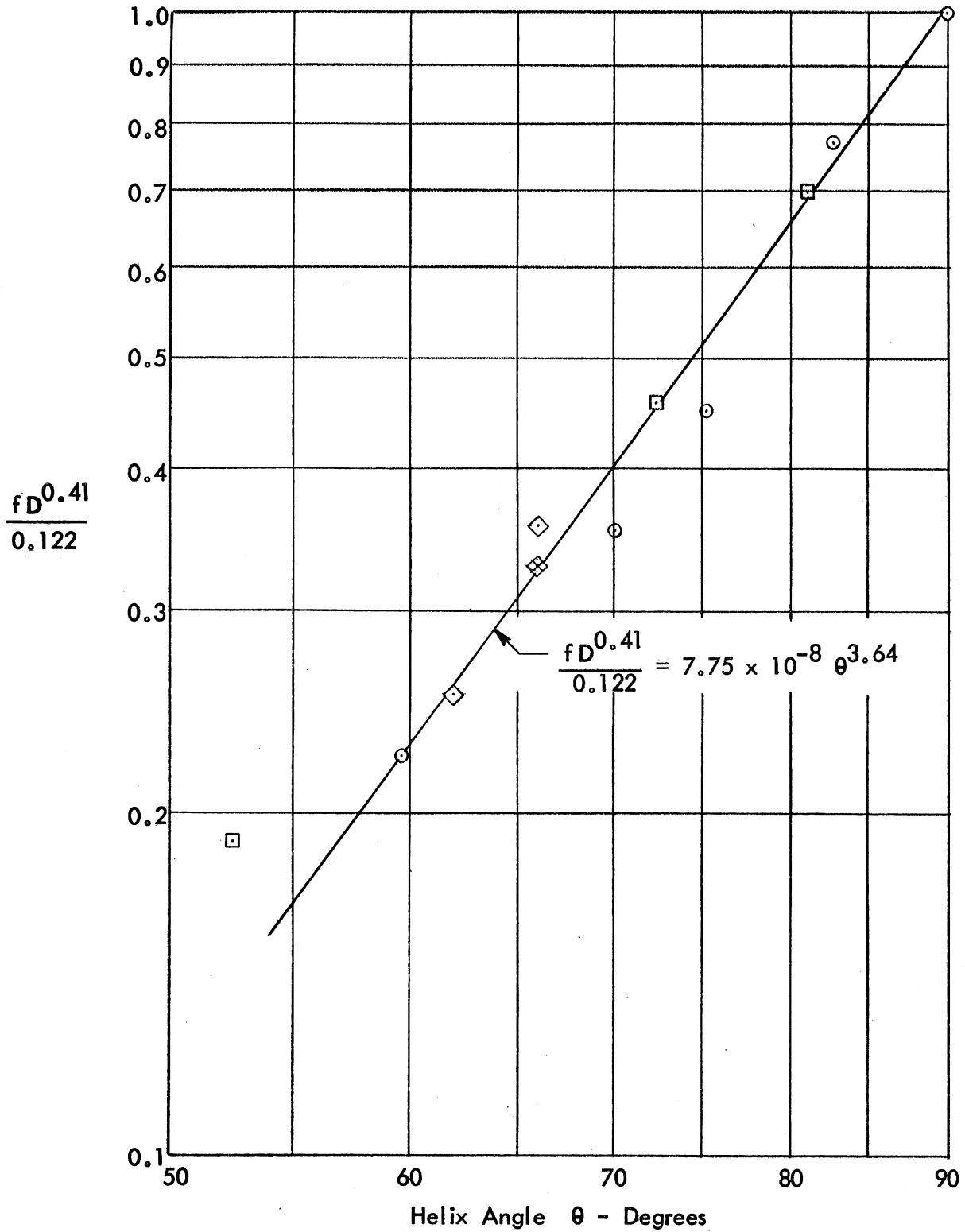


Fig. 30 - Friction Factor as a Function of Helix Angle at High Reynolds Numbers

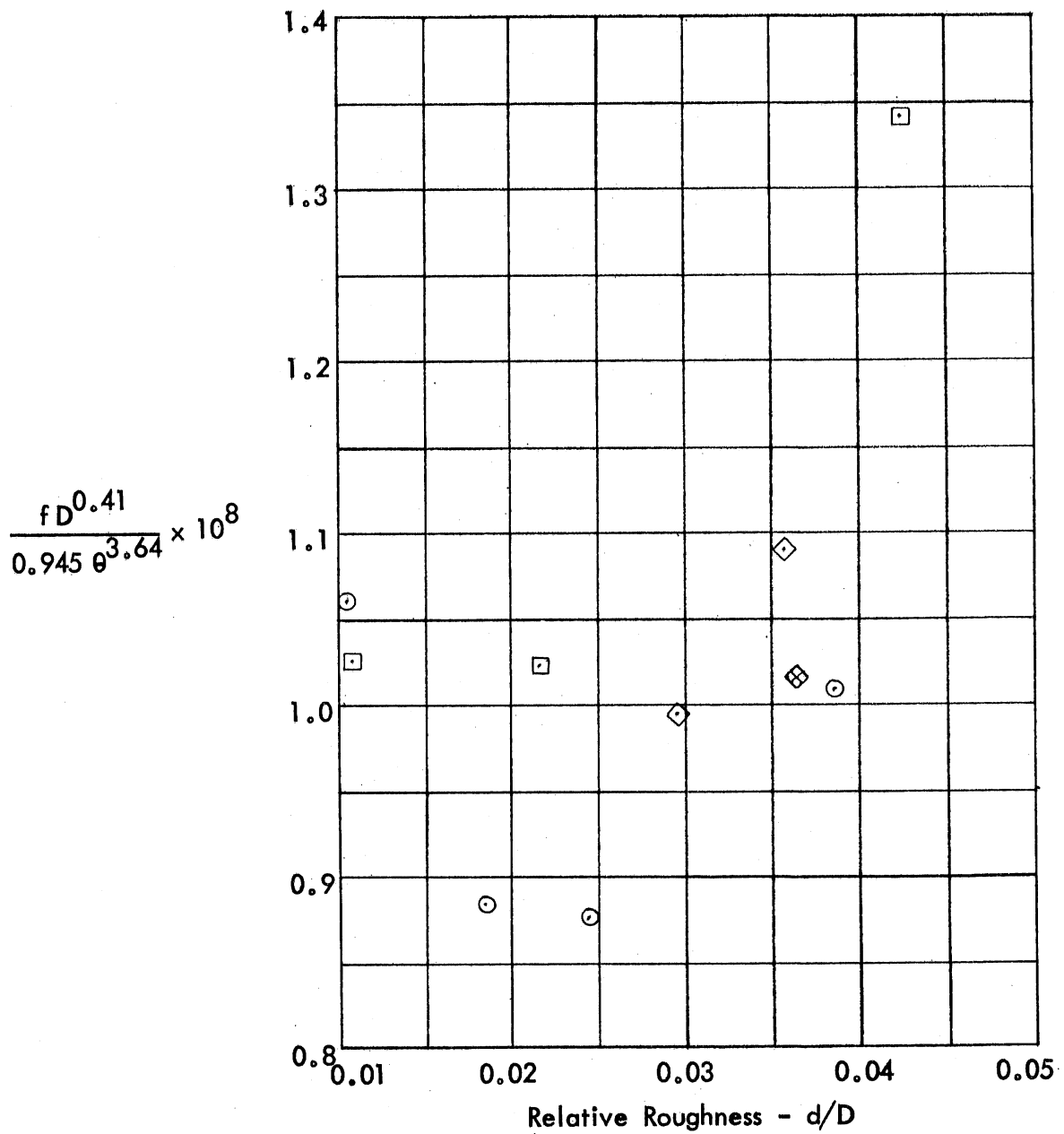


Fig. 31 - Friction Factor as a Function of Relative Roughness for Helical Pipes at High Reynolds Numbers

Appendix A

POSITION OF HYDRAULIC GRADE LINE AT THE PIPE OUTLET



Appendix A

POSITION OF HYDRAULIC GRADE LINE AT THE PIPE OUTLET

Following the test runs in the main channel on the larger pipes with raised tailwater and on the smaller pipes with the downstream valve in place, test runs were made with the tailwater control gate down in the main channel and the downstream valve removed from the smaller pipes. In this manner the maximum discharge was obtained, along with several lower flows, by controlling the inflow at the upstream end. The procedure described earlier was used to measure the discharge, hydraulic grade lines, and water temperature. Typical hydraulic grade lines for the seven pipes tested are shown in Figs. A-1 through A-7 in actual relationship to the test pipe.

The friction factors computed from these data are consistent with the results found with raised tailwater or with the valve in place and are included in Tables I through VII as well as in the graphs of Figs. 21 through 27.

Also computed from these data were the values of y/D and $Q/D^{5/2}$, where y is the vertical distance between the pipe invert and the hydraulic grade line at the end of the pipe. These values are presented in Table A-1 and are plotted in Fig. A-8 along with the results presented in the authors' earlier study [1]. In Fig. A-8, the line drawn through the data points represents the results reported in the earlier study. The plots of data points for all pipes appear reasonable with the noticeable exception of the 12 in. helical pipe with 2-2/3 in. by 1/2 in. corrugations. The point with values of 0.735 for y/D and 5.22 for $Q/D^{5/2}$ plots near the curve drawn through the earlier data, but then with increasing values of $Q/D^{5/2}$, y/D changes from a decreasing to an increasing characteristic. A second series of tests was run to verify this at a later date, and similar results were obtained. Without further detailed study it is difficult to explain this phenomenon, although it might be attributable to the stronger rotations associated with the helix angle, which is 52-1/2 degrees for the 12 in. pipe tested currently and 59-1/2 degrees for the 12 in. pipe tested earlier.

TABLE A-1. POSITION OF HYDRAULIC GRADE LINE AT THE PIPE OUTLET

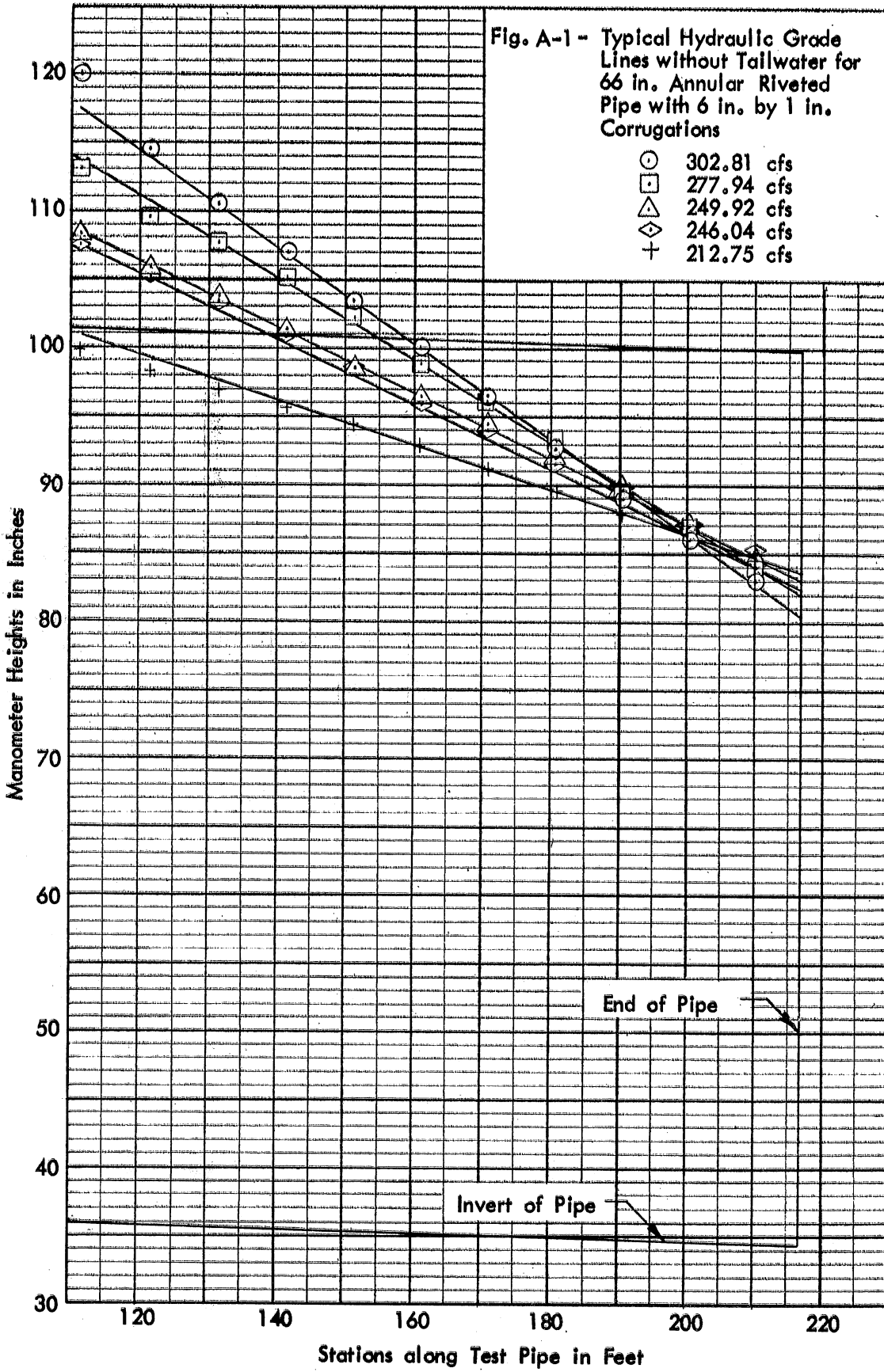
<u>Q</u>	<u>D</u>	<u>y</u>	<u>y/D</u>	<u>Q/D^{5/2}</u>
<u>cfs</u>	<u>ft</u>	<u>ft</u>		<u>ft^{1/2}/sec</u>
66 in. Annular Riveted Pipe with 6 in. by 1 in. Corrugations				
302.81	5.4517	3.820	0.701	4.36
282.78	5.4517	3.970	0.728	4.07
277.94	5.4517	3.967	0.728	4.00
253.31	5.4517	4.134	0.758	3.65
249.92	5.4517	4.058	0.744	3.60
246.45	5.4517	4.102	0.753	3.55
246.04	5.4517	3.985	0.731	3.55
245.84	5.4517	4.080	0.748	3.54
212.75	5.4517	4.103	0.753	3.07
66 in. Annular Bolted Pipe with 9 in. by 2-1/2 in. Corrugations				
246.09	5.3808	3.910	0.727	3.66
219.66	5.3808	3.852	0.716	3.27
216.95	5.3808	3.948	0.734	3.23
208.49	5.3808	3.858	0.717	3.10
198.94	5.3808	3.939	0.732	2.96
180.50	5.3808	3.806	0.707	2.69
48 in. Annular Riveted Pipe with 6 in. by 1 in. Corrugations				
181.73	3.9683	1.419	0.358	5.79
147.15	3.9683	2.519	0.635	4.69
147.14	3.9683	2.531	0.638	4.69
91.37	3.9683	3.040	0.766	2.91
48 in. Helical Lock Seam Pipe with 2 in. by 1/2 in. Corrugations				
189.74	4.0392	2.583	0.640	5.79
185.17	4.0392	2.684	0.664	5.65
178.12	4.0392	2.716	0.672	5.43
171.01	4.0392	2.875	0.712	5.21
48 in. Helical Lock Seam Pipe with 2-2/3 in. by 1/2 in. Corrugations				
193.90	3.9760	2.013	0.506	6.15
189.40	3.9760	2.097	0.528	6.01
184.89	3.9760	2.115	0.532	5.87
178.02	3.9760	2.305	0.580	5.65
174.57	3.9760	2.518	0.633	5.54
169.24	3.9760	2.607	0.656	5.37
163.89	3.9760	2.673	0.672	5.20

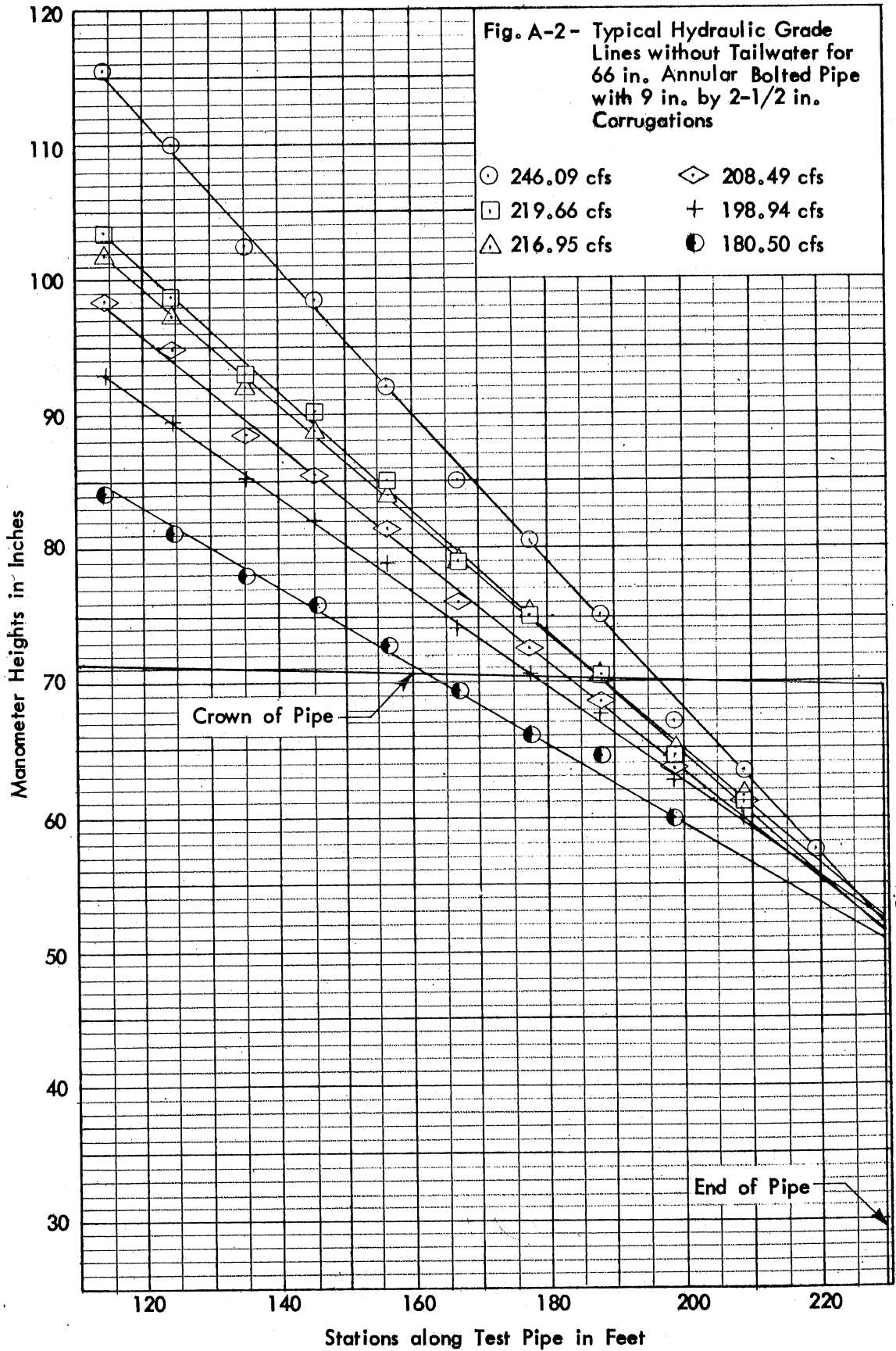
TABLE A-1. [Continued]

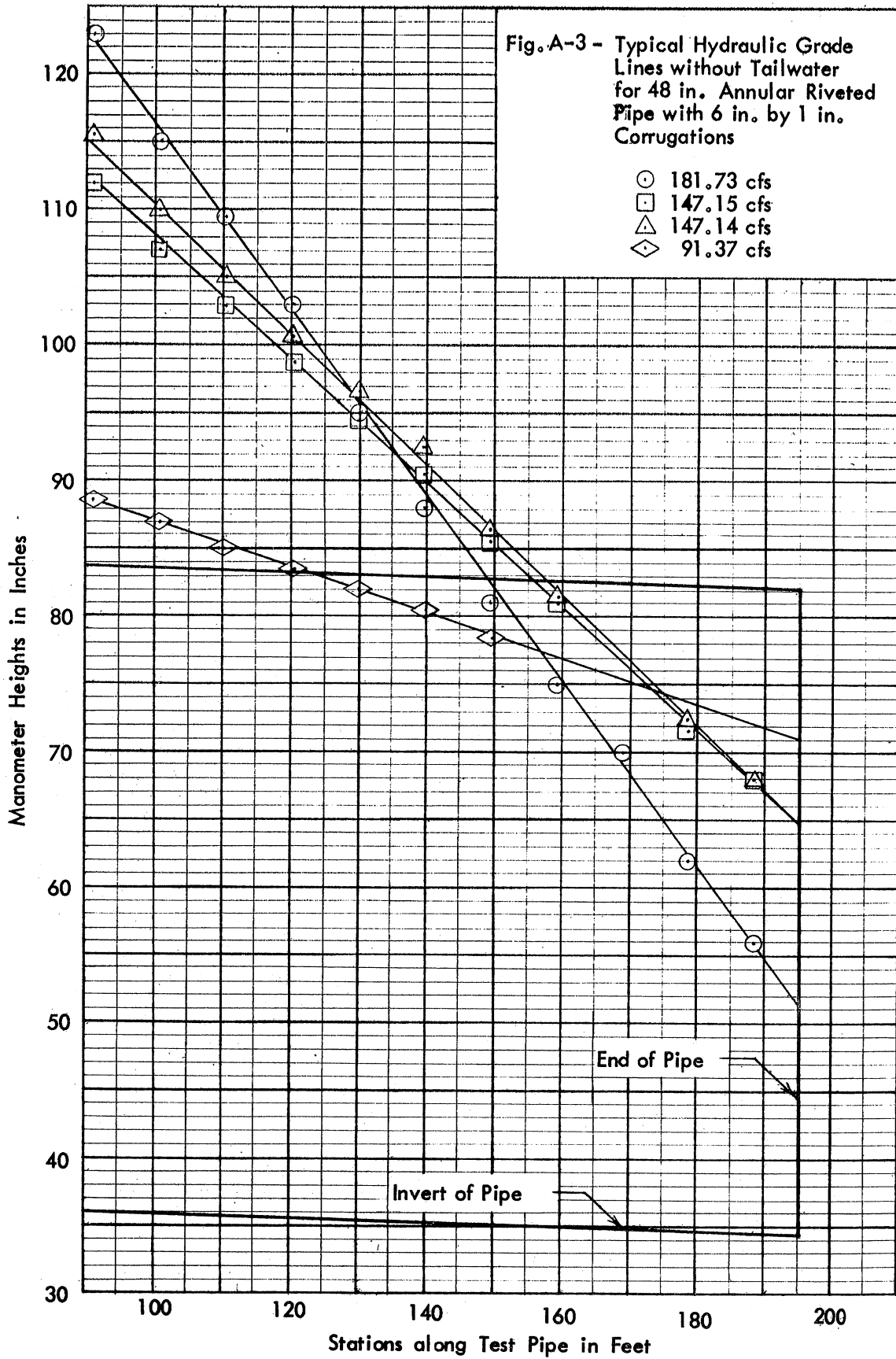
<u>Q</u>	<u>D</u>	<u>y</u>	<u>y/D</u>	<u>Q/D^{5/2}</u>
<u>cfs</u>	<u>ft</u>	<u>ft</u>		<u>ft^{1/2}/sec</u>
24 in. Helical Lock Seam Pipe with 2-2/3 in. by 1/2 in. Corrugations				
38.417	1.9950	0.904	0.453	6.83
36.425	1.9950	0.993	0.498	6.48
31.311	1.9950	1.288	0.646	5.57
26.102	1.9950	1.505	0.754	4.64
19.982	1.9950	1.718	0.861	3.55
12 in. Helical Lock Seam Pipe with 2-2/3 in. by 1/2 in. Corrugations				
11.662	0.9781	0.843	0.862	12.33
10.454	0.9781	0.785	0.803	11.05
9.193	0.9781	0.685	0.700	9.72
7.246	0.9781	0.645	0.660	7.66
4.937	0.9781	0.719	0.735	5.22

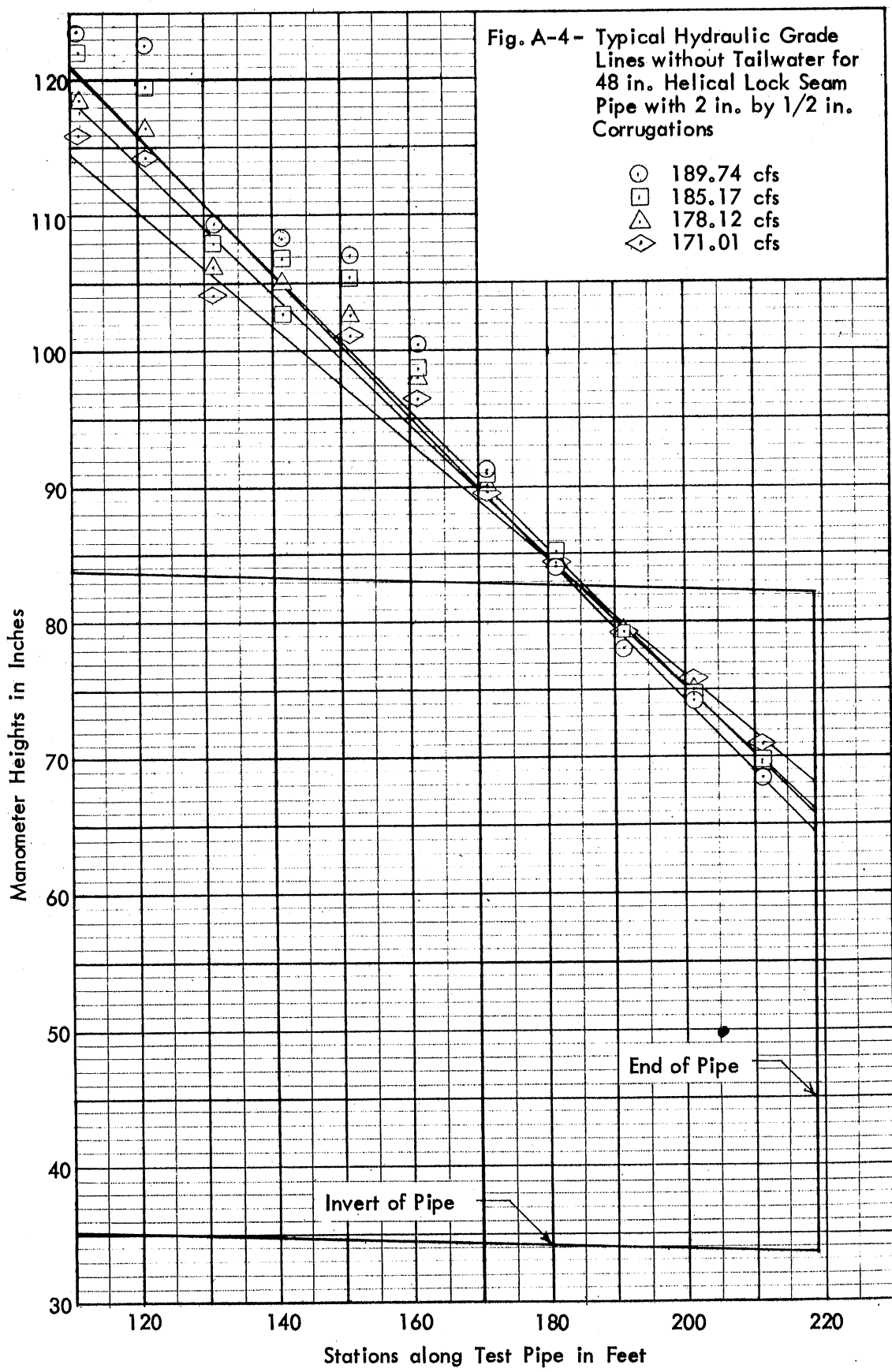
I L L U S T R A T I O N S -- Appendix A

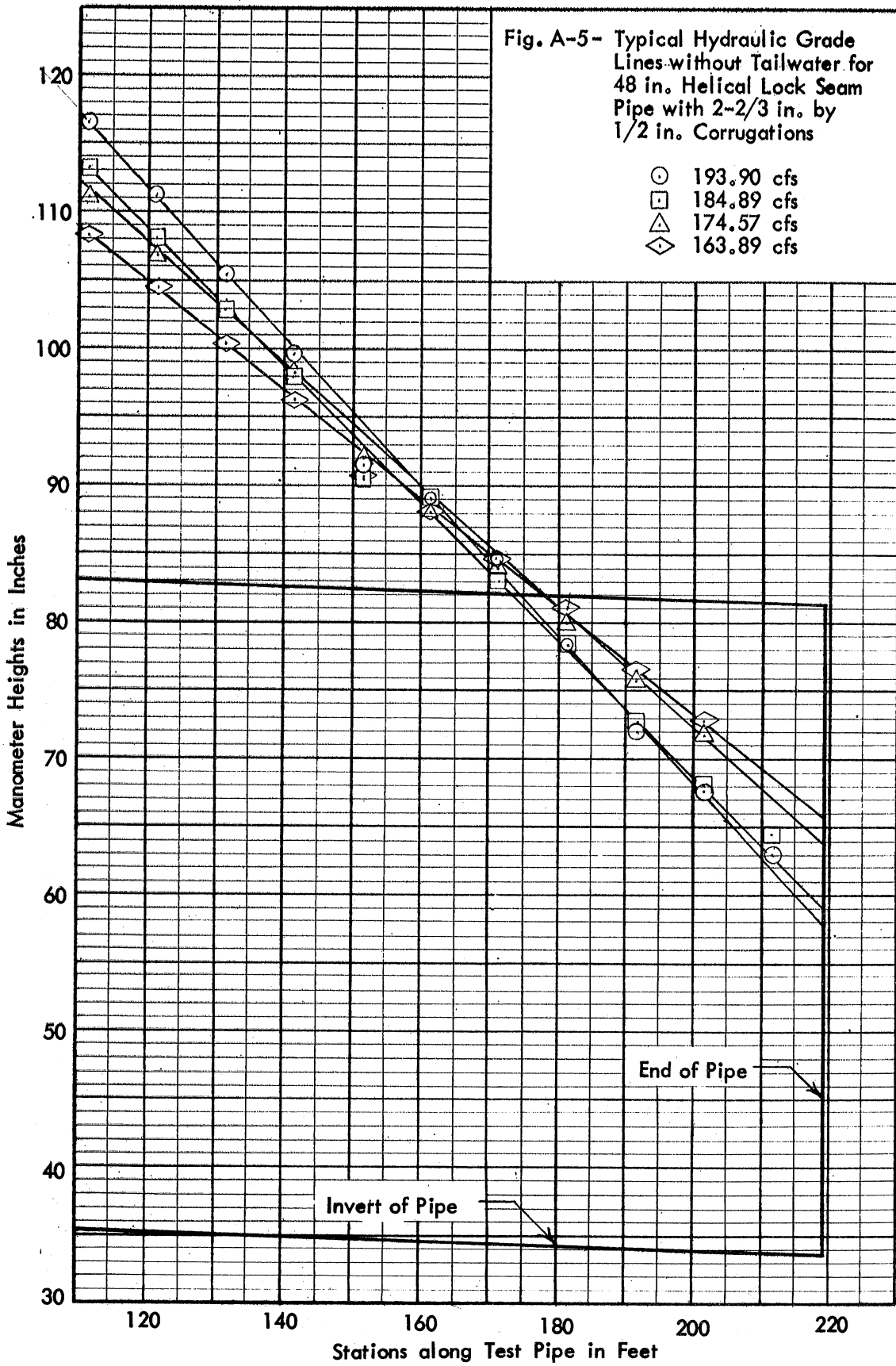
(Figs. A-1 thru A-8)

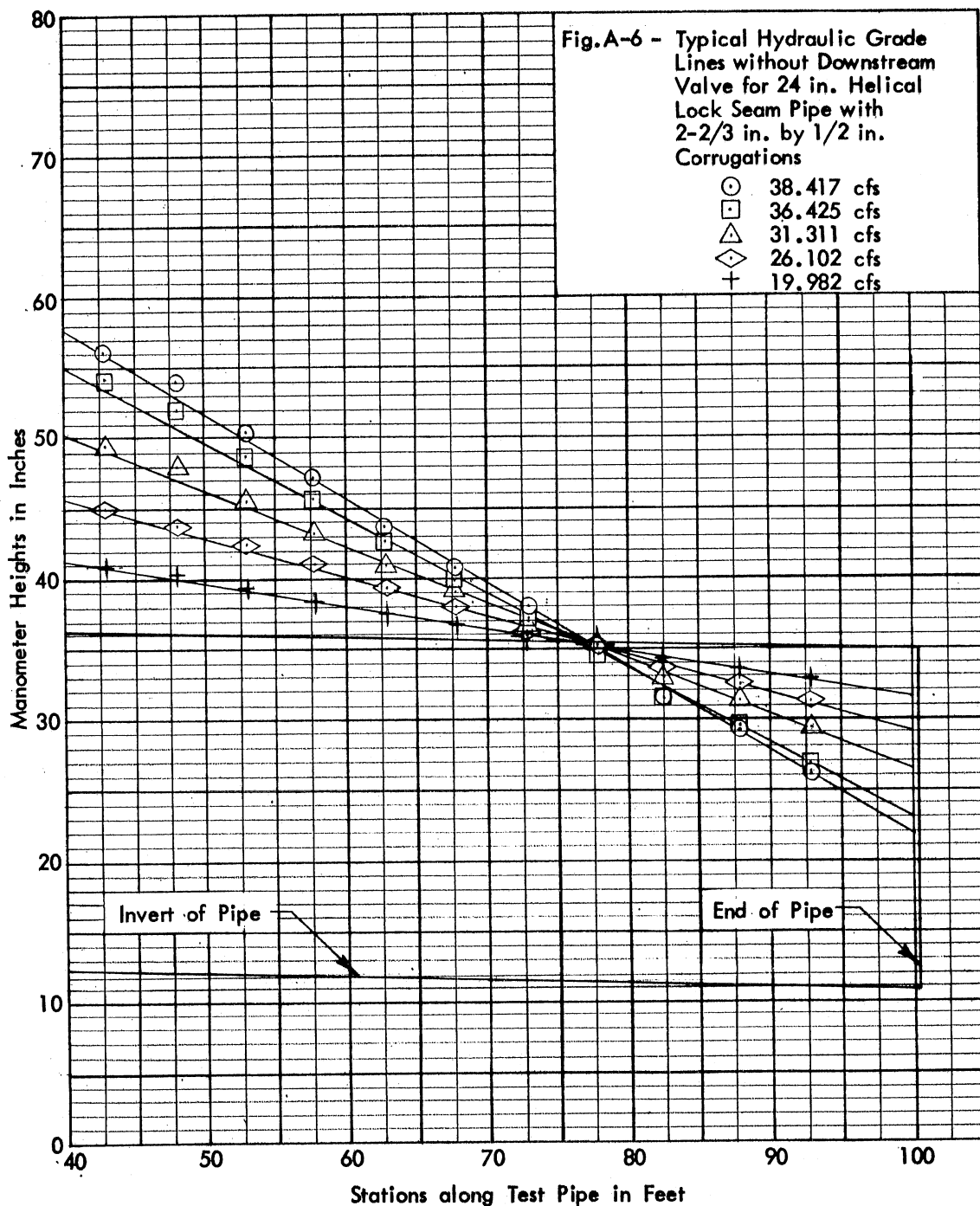


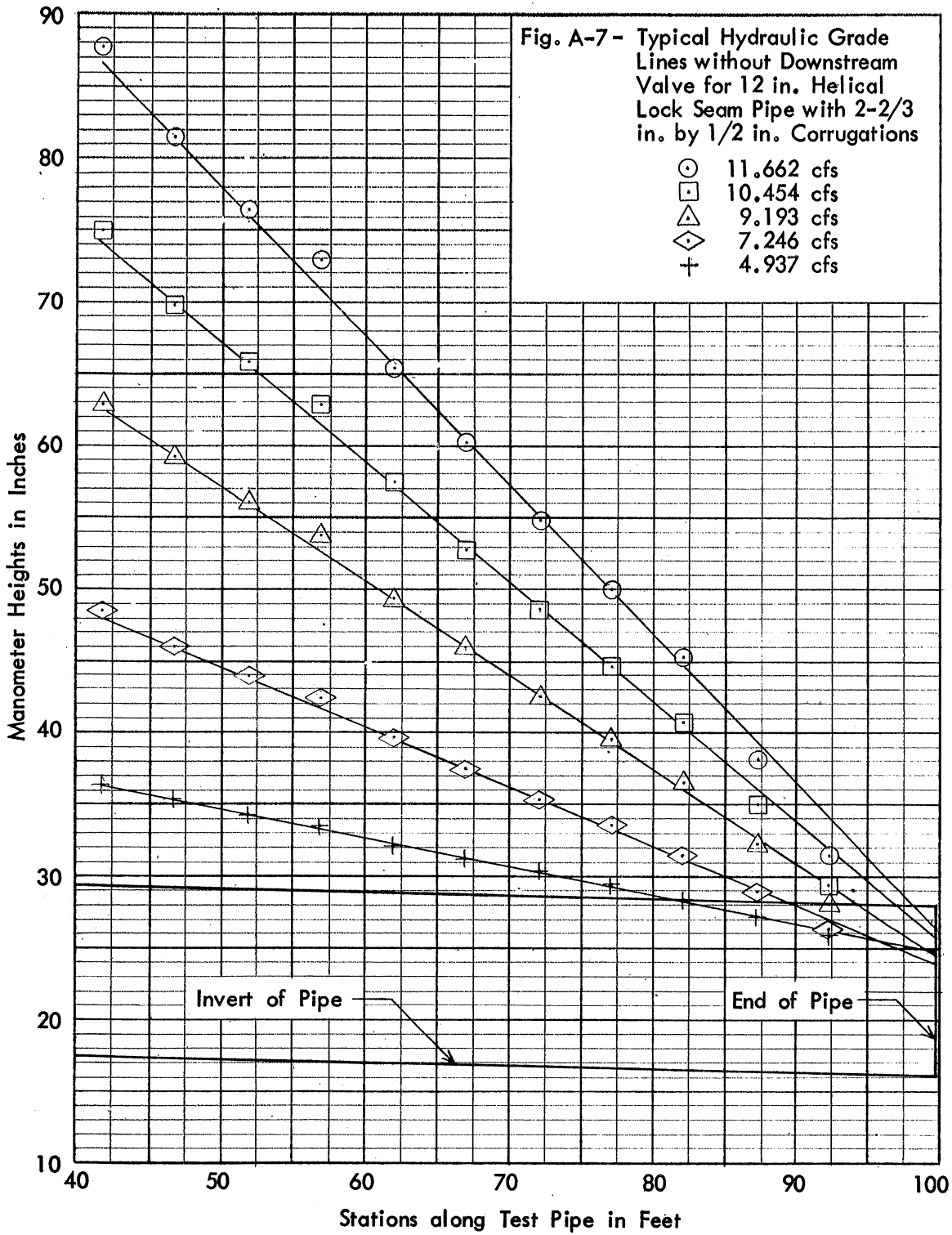


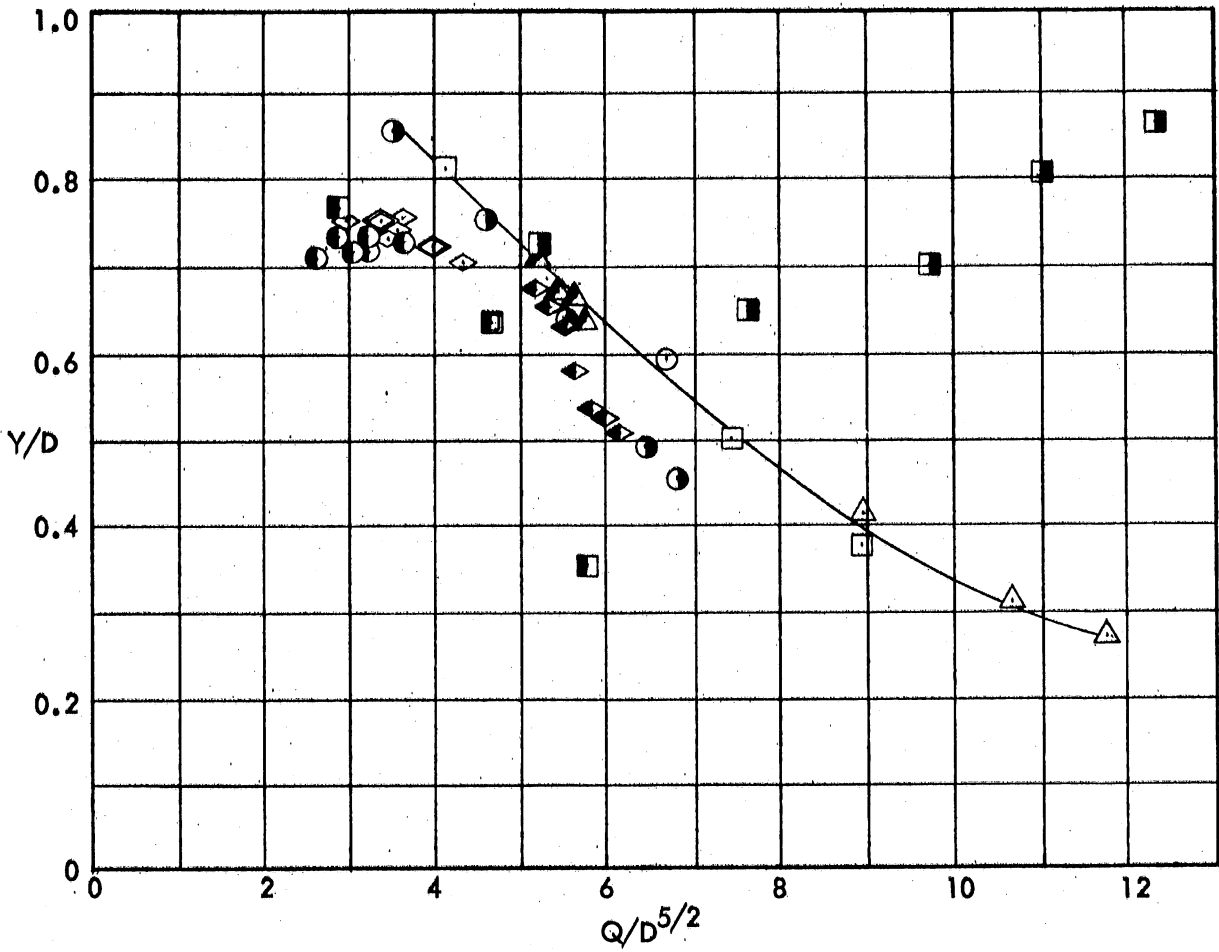












Type of Pipe	Pipe Dia. in.	Corrugations in.	
○	Helical	24	2 x 1/2
□	Helical	18	2 x 1/2
△	Helical	12	2 x 1/2
◇	Annular Riveted	66	6 x 1
●	Annular Bolted	66	9 x 2-1/2
■	Annular Riveted	48	6 x 1
▲	Helical	48	2 x 1/2
◀	Helical	48	2-2/3 x 1/2
⊙	Helical	24	2-2/3 x 1/2
◼	Helical	12	2-2/3 x 1/2

} 1969 Study

} This Work

These tests were made with no tailwater.

Fig. A-8- Position of Hydraulic Grade Line at the Pipe Outlet

Appendix B
VELOCITY PROFILES

Appendix B
VELOCITY PROFILES

Velocity profiles were obtained along the vertical diameter at 10 ft from the end for the 24 in. and 12 in. pipes. The velocity direction and magnitude were measured with a 3/8 in. diameter pitot cylinder [2] used in conjunction with a static tube. The location of these measurements was shown in Fig. 7. As the flow is not parallel to the pipe axis, the static probe had to be directed into the flow. To accomplish this, the direction of flow was determined first with the pitot cylinder at a distance of 2.13 in. from the top and bottom of the pipe, this being the distance the static tube protruded into the pipe. The direction of the static tube was set to the average of these two directions. The tube reading served as a reference against which to measure total heads with the pitot cylinder. Traverses of the static tube from the 2.13 in. position toward the wall with the pitot cylinder held at a fixed position as reference showed that there was practically no static pressure variation over this distance.

Velocity profiles were obtained for the following runs:

RUNS FOR WHICH VELOCITY PROFILES WERE OBTAINED

Pipe size in.	Q Meas. cfs	D ft	\bar{v} fps	$v \times 10^5$ ft ² /sec	Re $\times 10^{-6}$	f (Fig. 23)	Q Integrated cfs
24	26.198	1.9950	8.380	1.895	0.8822	0.0422	26.10
12	8.258	0.9781	10.990	1.859	0.5782	0.0229	8.35
12	8.148	0.9781	10.844	1.859	0.5705	0.0229	8.20

Tables B-1, B-2, and B-3 contain the basic measured data along with some computations based thereon. Figures B-1 and B-2 show the velocity magnitude plotted along the vertical diameter for the two pipes. Velocity readings above +11.90 inches in the 24 in. pipe (Fig. B-1) and above +5.85 inches in the 12 in. pipe (Fig. B-2) were measured within the corrugation at the top of the pipe.

Figure B-3 shows the velocity magnitude and direction in the top halves of the pipes. The center flow was axial for the 12 in. pipe and 2 degrees from axial in the 24 in. pipe, the latter direction being used as the

reference or zero angle. Figure B-3 shows that close to the wall the flow approaches the helical direction and that in the corrugation it is essentially in the helical direction. The photographs in Fig. B-4 show the flow directions at the outlet for the two 48 in. pipes, one annular and the other helical. The spiral nature of the flow along the wall of a helical pipe is clearly shown by a comparison of the two photos.

The velocity profiles have been plotted in the form of the velocity defect law in Fig. B-5 and in law-of-the-wall form in Fig. B-6. For comparison, similar plots from the earlier work [1] have also been placed on these graphs. The results are quite comparable, although the new data indicate, from Fig. B-5, that the reduction in turbulence may not be quite so great for the new pipes as it was in the earlier tests. The reason for the slight difference is not readily apparent.

The law-of-the-wall plot in Fig. B-6 shows that the roughness of the 24 in. helical pipe in the present tests should be somewhat less than in the previous tests. This was not borne out by the friction factor measurements displayed in Figs. 28 and 29. Figure B-6 also seems to indicate that the present 12 in. pipe has about the same roughness as the previous 12 in. pipe of larger helix angle. Again, the friction factor measurements displayed in Figs. 28 and 29 show a different result, the smaller helix angle pipe showing a lesser friction factor. The discrepancies are not large, and certainly the direct measurements of friction factor should be given precedence.

TABLE B-1. VELOCITY PROFILE DATA FOR 24 IN. PIPE - 2-2/3 in. by 1/2 in. Corrugations

$$\bar{V} = 8.38 \text{ fps}, V_* = 0.61 \text{ fps}, \nu = 1.90 \times 10^{-5} \text{ ft}^2/\text{sec}$$

Dis- tance from pipe C L, in.	Dis- tance from outer wall y, ft	yV_*/ν $\times 10^{-4}$	y/R	TOP OF PIPE					BOTTOM OF PIPE				
				V fps	α , Deg.	U = V cos α fps	U/V*	$\frac{U_{\max} - U}{V_*}$	V fps	α , Deg.	U = V cos α fps	U/V*	$\frac{U_{\max} - U}{V_*}$
0.00	1.035	3.320	1.000	11.84	0.0	11.84	19.40	0.00	11.84	0.0	11.84	19.40	0.00
2.00	0.868	2.785	0.840	11.51	2.0	11.50	18.85	0.56	11.48	2.0	11.47	18.80	0.77
4.00	0.702	2.555	0.676	10.88	2.0	10.87	17.80	1.59	10.82	4.0	10.80	17.70	1.71
6.00	0.535	1.720	0.516	9.89	4.0	9.87	16.20	3.24	9.76	4.5	9.73	15.90	3.46
7.00	0.452	1.453	0.436	9.38	6.0	9.31	15.30	4.15	9.35	6.5	9.26	15.20	4.24
8.00	0.368	1.180	0.356	8.75	9.0	8.65	14.20	5.23	8.86	10.0	8.71	14.30	5.14
8.50	0.327	1.050	0.315	8.60	10.0	8.45	13.85	5.56	8.64	10.0	8.50	13.90	5.49
9.00	0.285	0.915	0.275	8.22	12.0	8.04	13.20	6.24	8.14	12.5	7.94	13.00	6.40
9.50	0.243	0.780	0.235	8.02	12.0	7.85	12.90	6.55	7.86	16.0	7.55	12.40	7.04
9.76	0.222	0.712	0.214	7.78	14.5	7.51	12.30	7.10	7.78	17.0	7.53	12.30	7.07
10.00	0.202	0.649	0.195	7.56	16.0	7.26	11.90	7.51	7.48	18.0	7.10	11.65	7.77
10.25	0.181	0.580	0.175	7.39	19.5	6.96	11.40	8.00	7.39	21.0	6.90	11.30	8.10
10.50	0.160	0.514	0.155	7.31	22.0	6.77	11.10	8.33	7.27	21.0	6.79	11.10	8.29
10.75	0.139	0.445	0.134	7.17	25.0	6.50	10.65	8.75	7.13	24.0	6.50	10.65	8.75
11.00	0.117	0.376	0.114	7.03	29.0	6.15	10.10	9.33	6.95	27.5	6.16	10.10	9.32
11.25	0.0975	0.313	0.094	6.85	31.0	5.86	9.60	9.81	6.71	29.0	5.86	9.60	9.81
11.50	0.077	0.247	0.074	6.51	34.5	5.36	8.80	10.62	6.51	30.0	5.64	9.25	10.13
11.60	0.068	0.218	0.066						6.42	32.0	5.45	8.94	10.48
11.70	0.060	0.193	0.058						6.31	33.0	5.30	8.70	10.72
11.75	0.056	0.180	0.054	6.16	40.0	4.71	7.71	11.70					
11.80	0.052	0.167	0.050						5.88		5.19	8.50	10.90
12.00	0.035	0.112	0.034	5.61	52.0	3.46	5.66	13.72					
12.10	0.027	0.086	0.026	5.44	57.0	2.96	4.85	14.56					
12.20	0.018	0.058	0.018	5.44	65.5	2.25	3.69	15.70					
12.30	0.010	0.032	0.010	5.38	68.0	2.01	3.30	16.11					

TABLE B-2. VELOCITY PROFILE DATA FOR 12 IN. PIPE - RUN 1 - 2-2/3 in. by 1/2 in. Corrugations

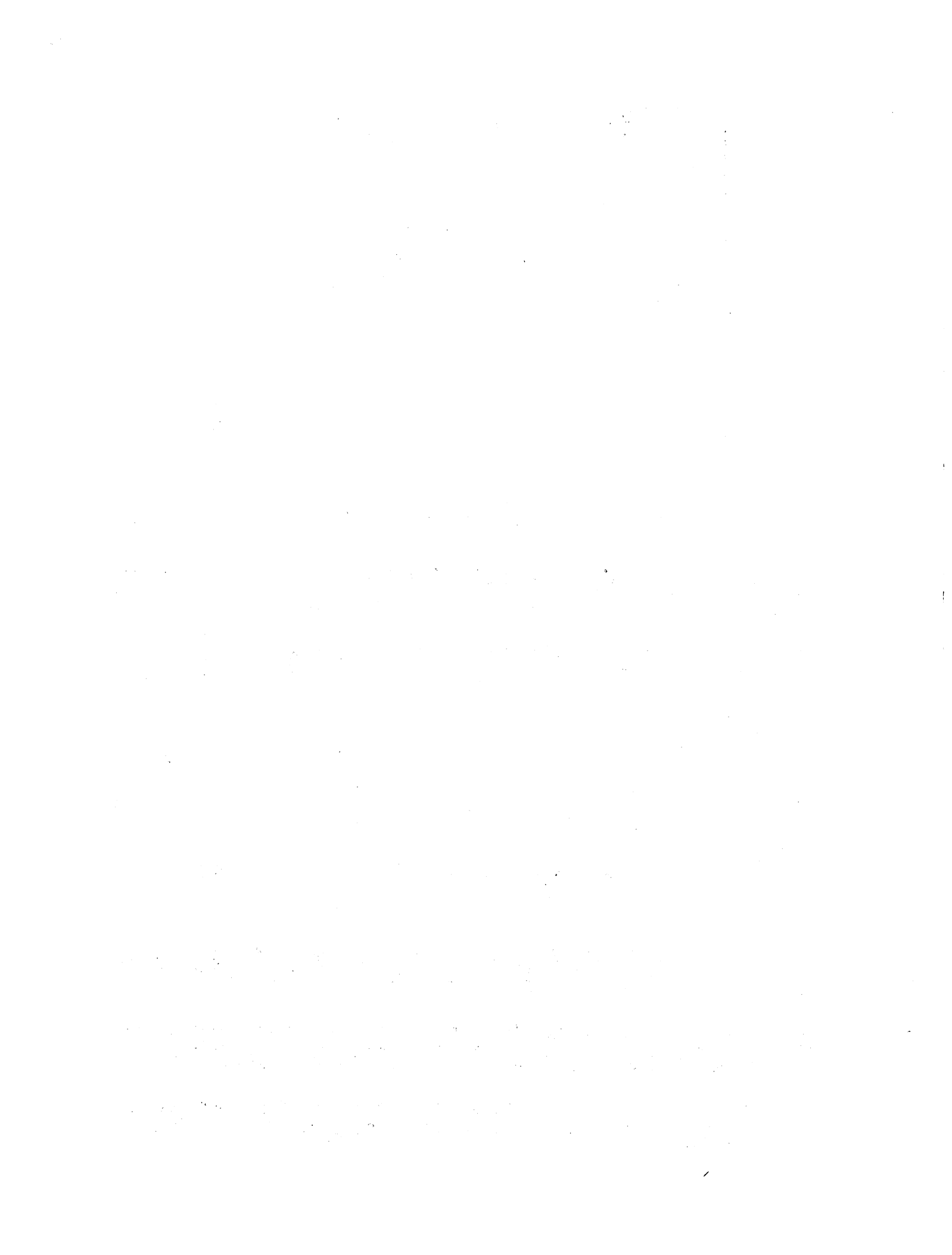
$\bar{V} = 10.990 \text{ fps}, V_* = 0.590 \text{ fps}, \nu = 1.859 \times 10^{-5} \text{ ft}^2/\text{sec}$

Dis- tance from pipe C L, in.	Dis- tance from outer wall y, ft	yV_*/ν $\times 10^{-4}$	y/R	TOP OF PIPE					BOTTOM OF PIPE				
				V fps	$\alpha,$ Deg.	U = V cos α fps	U/V _*	$\frac{U_{\text{max}} - U}{V_*}$	V fps	$\alpha,$ Deg.	U = V cos α fps	U/V _*	$\frac{U_{\text{max}} - U}{V_*}$
0.00	0.528	1.667	1.000	14.123	0.0	14.120	24.00	0.00	14.123	0.0	14.120	24.00	0.00
0.50	0.487	1.533	0.921	14.123	-1.0	14.120	24.00	0.00	14.147	1.0	14.150	24.00	0.00
1.00	0.445	1.402	0.842	14.003	-1.0	14.000	23.75	0.20	14.003	1.5	14.000	23.75	0.20
1.50	0.403	1.270	0.764	13.706	0.0	13.710	23.25	0.70	13.730	4.0	13.700	23.20	0.71
2.00	0.362	1.140	0.684	13.345	0.5	13.345	22.60	1.31	13.417	4.0	13.385	22.70	1.25
2.50	0.320	1.010	0.605	12.960	1.0	12.960	22.00	1.96	13.008	4.5	12.970	22.00	2.12
3.00	0.278	0.879	0.527	12.447	1.5	12.440	21.10	2.84	12.551	4.5	12.510	21.20	2.73
3.50	0.237	0.747	0.449	11.974	4.5	11.940	20.25	3.70	12.166	9.0	12.020	20.40	3.56
3.65	0.224	0.708	0.425	11.870	5.0	11.825	20.05	3.89	11.894	8.5	11.760	19.90	4.00
3.75	0.216	0.681	0.409	11.701	6.5	11.630	19.70	4.22	11.870	9.5	11.710	19.85	4.09
4.00	0.195	0.615	0.370	11.485	8.0	11.370	19.30	4.66	11.597	11.0	11.400	19.30	4.61
4.25	0.174	0.550	0.330	11.316	11.5	11.190	18.95	4.96	11.428	13.0	11.130	18.90	5.07
4.50	0.153	0.484	0.290	10.939	15.0	10.565	17.90	6.03	11.172	15.5	10.770	18.25	5.69
4.75	0.1325	0.419	0.251	10.819	19.0	10.230	17.40	6.60	10.963	18.5	10.430	17.70	6.25
5.00	0.112	0.352	0.222	10.667	22.0	9.890	16.75	7.16	10.763	20.0	10.110	17.15	6.80
5.25	0.091	0.287	0.172	10.458	24.5	9.520	16.15	7.80	10.514	22.0	9.750	16.50	7.41
5.50	0.070	0.221	0.133	10.298	28.0	9.090	15.40	8.52	10.209	24.0	9.320	15.80	8.14
5.60	0.062	0.194	0.117						10.081	26.5	9.020	15.30	8.65
5.70	0.053	0.168	0.101						9.921	27.0	8.840	15.00	8.95
5.75	0.049	0.155	0.093	9.985	31.5	8.510	14.40	9.52					
5.80	0.045	0.142	0.085						9.688	23.0	8.820	14.95	8.99
5.85	0.041	0.129	0.077	9.592	33.5	7.840	13.30	10.63					
5.95	0.0325	0.1025	0.062	9.351	40.0	6.880	11.65	12.27					
6.05	0.024	0.0763	0.046	9.319	44.5	6.650	11.30	12.66					
6.15	0.016	0.050	0.030	9.215	48.0	6.160	10.45	13.50					
6.25	0.0075	0.0236	0.014	9.215	48.0	6.160	10.45	13.50					

TABLE B-3. VELOCITY PROFILE DATA FOR 12 IN. PIPE - RUN 2 - 2-2/3 in. by 1/2 in. Corrugations

$$\bar{V} = 10.844 \text{ fps}, V_* = 0.584 \text{ fps}, v = 1.859 \times 10^{-5} \text{ ft}^2/\text{sec}$$

Dis- tance from pipe CL, in.	Dis- tance from outer wall y, ft	yV_*/v $\times 10^{-4}$	y/R	TOP OF PIPE					BOTTOM OF PIPE				
				V fps	$\alpha,$ Deg.	U = V cos α fps	U/V*	$\frac{U_{\max} - U}{V_*}$	V fps	$\alpha,$ Deg.	U = V cos α fps	U/V*	$\frac{U_{\max} - U}{V_*}$
0.00	0.528	1.655	1.000	13.891	0.0	13.891	23.80	0.00	13.891	0.0	13.891	23.80	0.00
0.50	0.487	1.530	0.921	13.843	0.5	13.843	23.80	0.08	13.778	-1.0	13.775	23.60	0.20
1.00	0.445	1.400	0.842	13.730	1.5	13.726	23.55	0.28	13.634	0.5	13.634	22.40	0.44
1.50	0.403	1.265	0.764	13.538	1.5	13.534	23.25	0.61	13.442	0.5	13.442	23.10	0.77
2.00	0.362	1.135	0.684	13.249	3.0	13.230	22.70	1.13	13.105	0.5	13.105	22.50	1.35
2.50	0.320	1.003	0.605	12.880	3.0	12.862	22.05	1.72	12.728	1.0	12.725	21.85	2.00
3.00	0.278	.873	0.527	12.375	5.0	12.328	21.20	2.68	12.319	3.5	12.296	21.10	2.74
3.50	0.237	.745	0.449	11.870	7.5	11.768	20.20	3.64	11.789	7.5	11.688	20.00	3.78
3.64	0.225	.706	0.426	11.733	7.0	11.645	20.00	3.85					
3.65	0.224	.704	0.425						11.597	7.5	11.497	19.70	4.10
3.75	0.216	.679	0.409	11.677	7.5	11.577	19.80	3.96	11.509	8.0	11.397	19.60	4.28
4.00	0.195	.611	0.370	11.396	8.0	11.285	19.30	4.65	11.396	8.5	11.271	19.30	4.50
4.25	0.174	.546	0.330	11.140	13.0	10.855	18.60	5.20	11.172	10.0	11.002	18.90	4.95
4.50	0.153	.480	0.290	10.963	15.5	10.564	18.10	5.70	10.875	11.5	10.656	18.30	5.54
4.75	0.1325	.416	0.251	10.699	17.5	10.204	17.50	6.31	10.643	15.5	10.256	17.60	6.23
5.00	0.112	.352	0.222	10.546	20.5	9.878	16.90	6.85	10.490	18.5	9.948	17.05	6.76
5.25	0.091	.286	0.172	10.330	24.0	9.436	16.15	7.81	10.242	20.5	9.594	16.45	7.35
5.50	0.070	.220	0.133	10.113	28.5	8.887	15.20	8.57	10.017	22.0	9.288	15.90	7.90
5.60	0.062	.195	0.117						9.857	24.0	9.004	15.40	8.36
5.70	0.053	.166	0.101						9.760	24.0	8.916	15.30	8.54
5.75	0.049	.154	0.093	9.688	32.5	8.171	14.00	9.80					
5.80	0.045	.141	0.085						9.520	23.5	8.731	14.95	8.85
5.85	0.041	.129	0.077	9.456	35.0	7.746	13.30	10.50					
5.95	0.0325	.102	0.062	9.183	40.0	7.034	12.05	11.75					
6.05	0.024	.075	0.046	9.039	42.5	6.664	11.40	12.37					
6.15	0.016	.0502	0.030	9.039	42.5	6.664	11.40	12.37					
6.25	0.0075	.0235	0.014	8.998	47.5	6.079	10.40	13.40					



I L L U S T R A T I O N S -- Appendix B

(Figs. B-1 thru B-6)

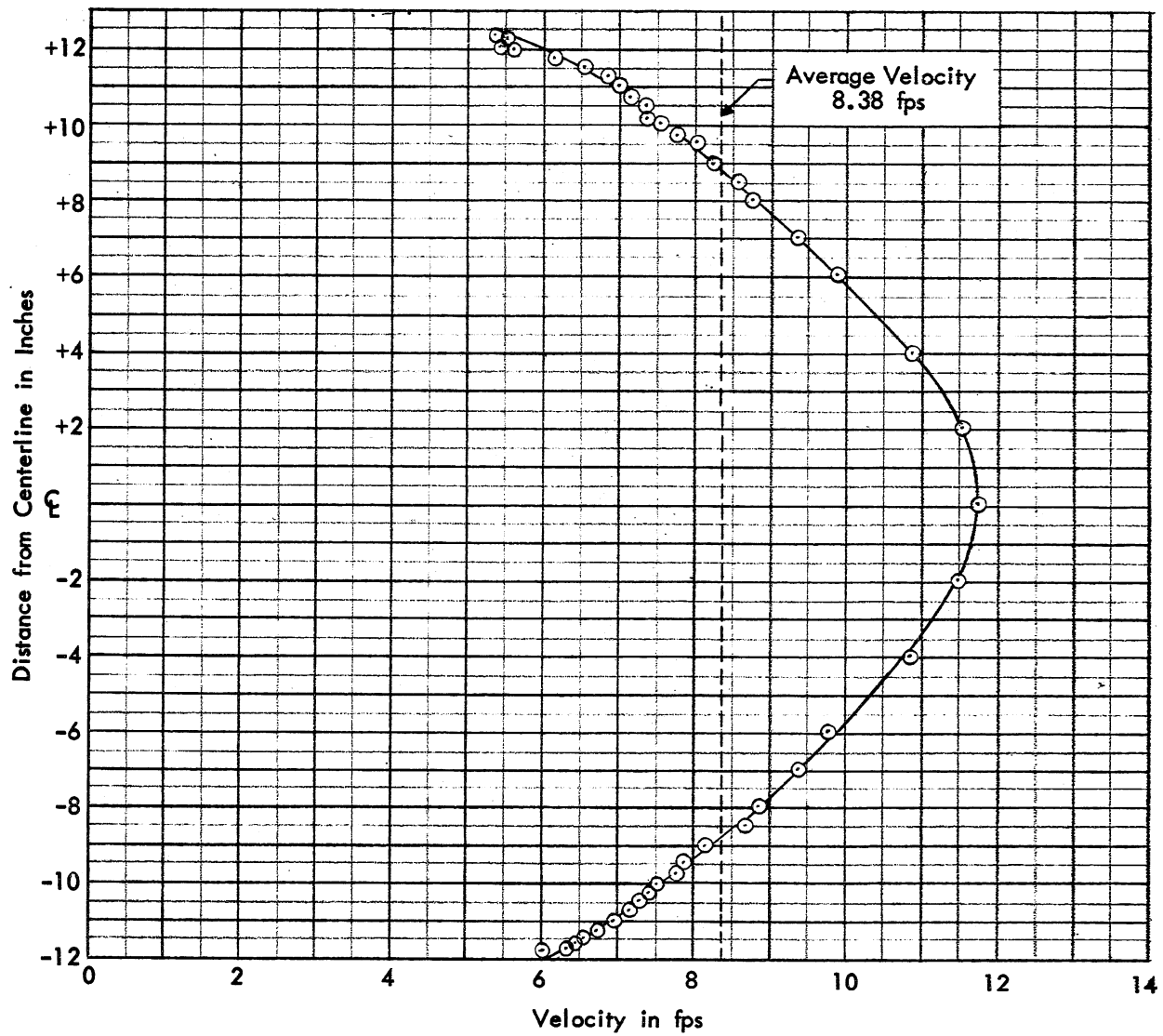


Fig. B-1 - Velocity Distribution in 24 In. Helical Lock Seam Pipe with 2-2/3 in. by 1/2 in. Corrugations

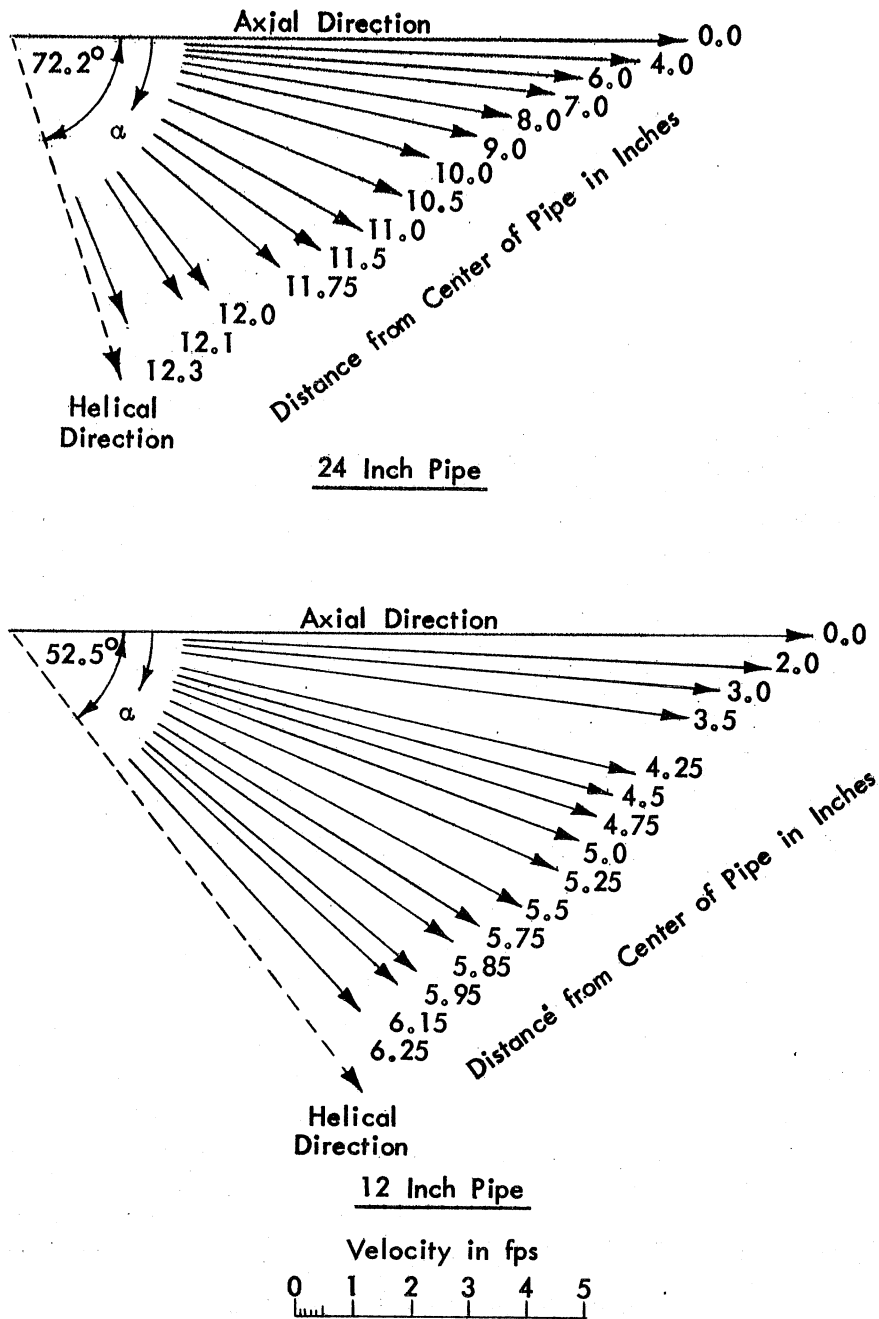
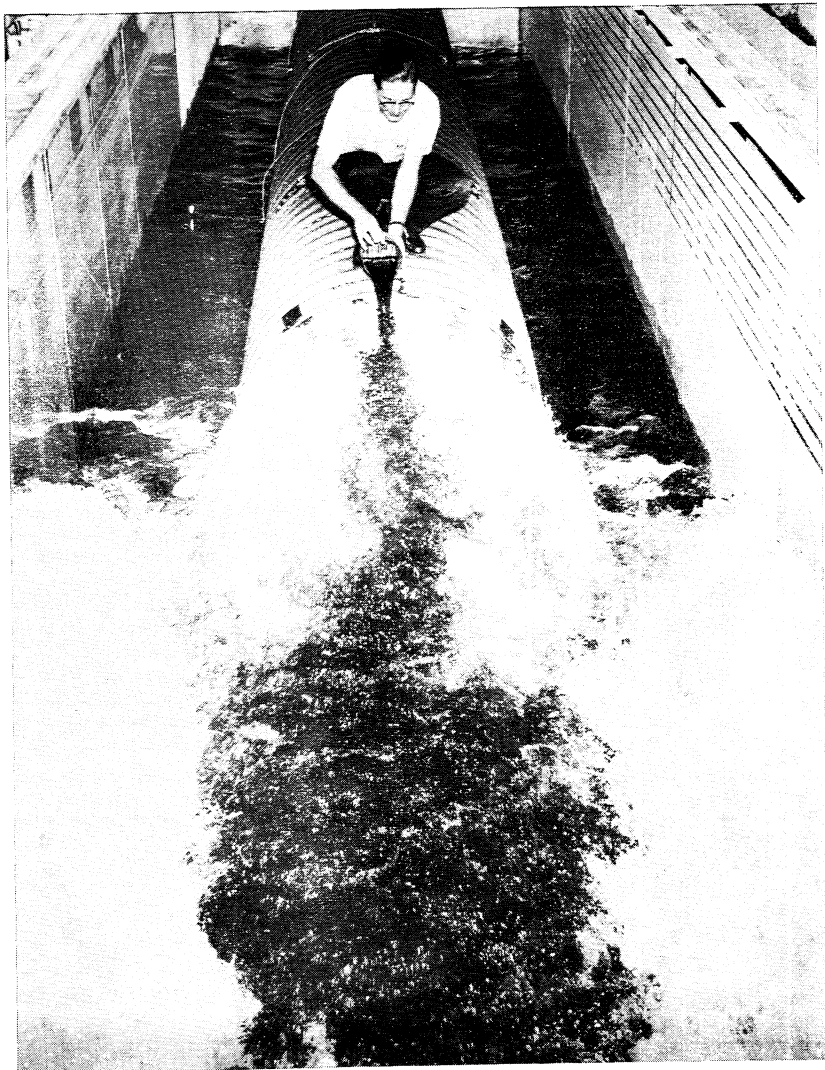
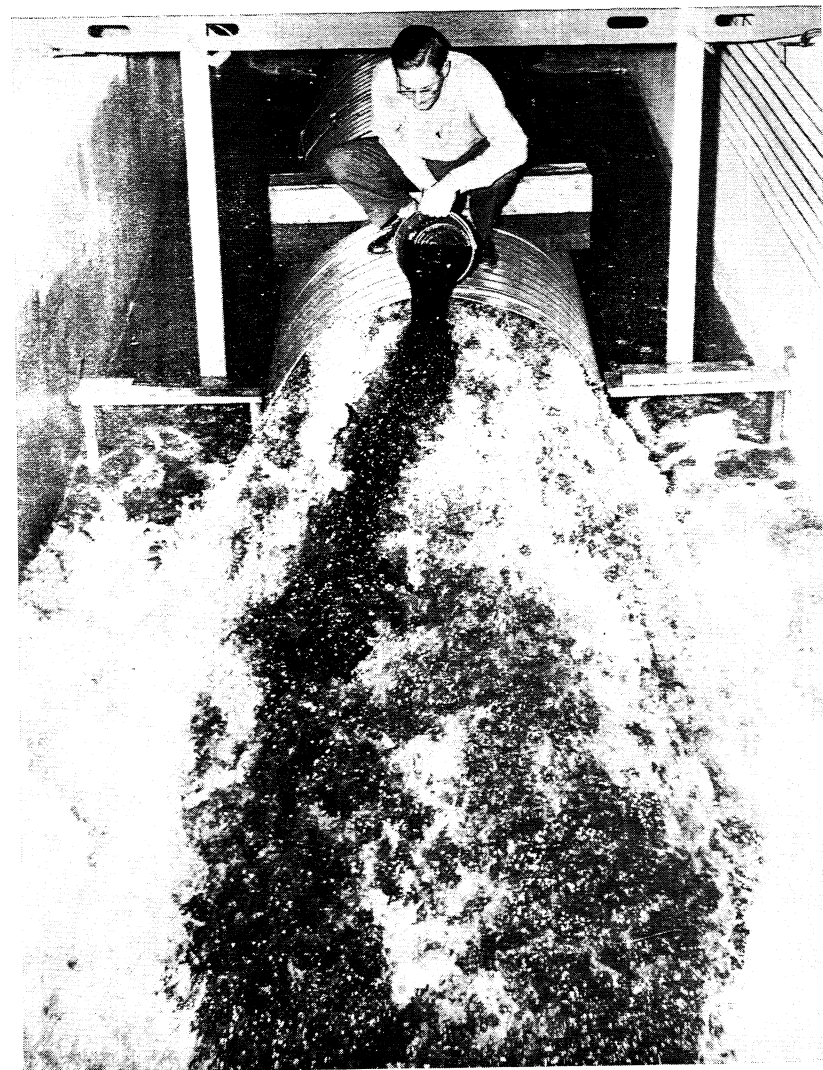


Fig. B-3 - Velocity Vectors, Top Halves of Pipes for 24 in. and 12 in. Helical Lock Seam Pipe with 2-2/3 in. by 1/2 in. Corrugations



a. Annular Pipe, 6 in. by 1 in. Corrugations



b. Helical Pipe, 2-2/3 in. by 1/2 in. Corrugations

Fig. B-4 - Flow Direction at 48 in. Pipe Outlets

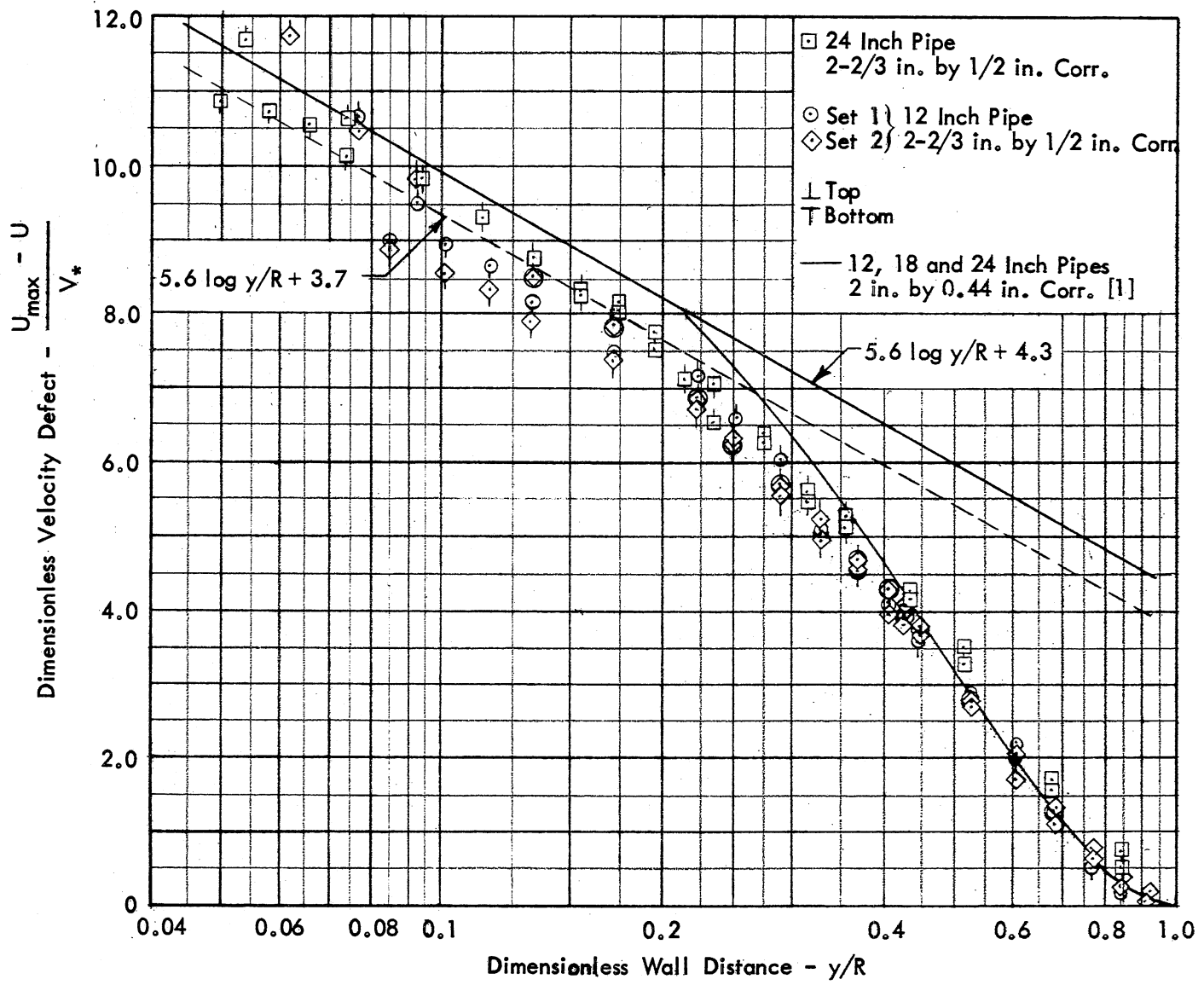


Fig. B-5 - Velocity Profiles in Defect-Law Form

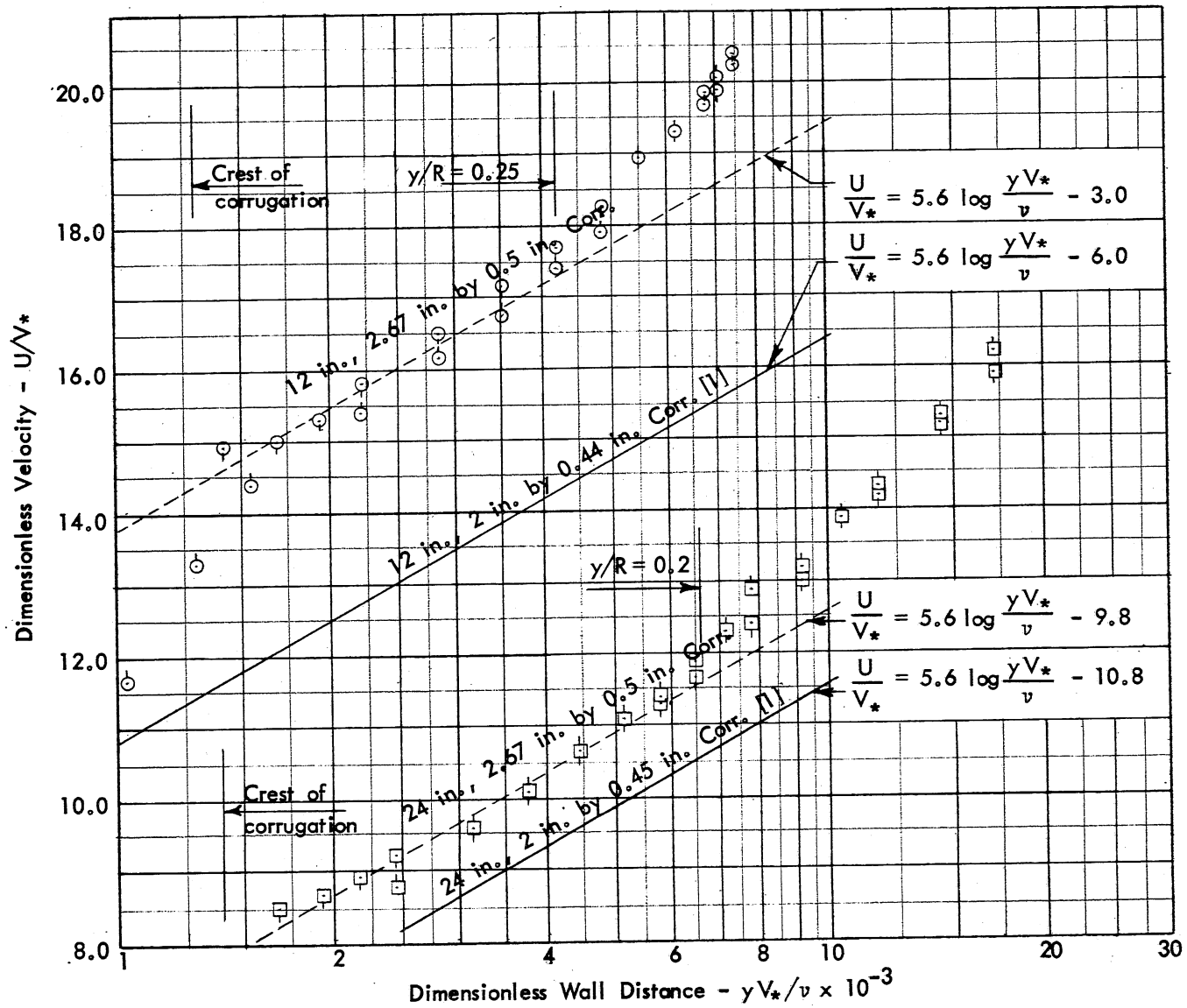


Fig. B-6 - Velocity Profiles in Law-of-the-Wall Form

